ADAPTIVE CONTROL OF GUIDED MISSILES

A THESIS SUBMITTED TO
THE GRADUATE SCHOOL OF NATURAL AND APPLIED SCIENCES
OF
MIDDLE EAST TECHNICAL UNIVERSITY

BY

KADRİYE TİRYAKİ KUTLUAY

IN PARTIAL FULFILLMENT OF THE REQUIREMENTS
FOR
THE DEGREE OF DOCTOR OF PHILOSOPHY
IN
AEROSPACE ENGINEERING

FEBRUARY 2010

Approval of the thesis

ADAPTIVE CONTROL OF GUIDED MISSILES

submitted by **KADRİYE TİRYAKİ KUTLUAY** in partial fulfillment of the requirements for the degree of **Doctor of Philosophy in Aerospace Engineering Department, Middle East Technical University** by,

Prof. Dr. Canan Özgen
Dean, Graduate School of **Natural and Applied Sciences** ____________

Prof. Dr. Ozan Tekinalp
Head of Department, **Aerospace Engineering** ____________

Asst. Prof. Dr. İlkay Yavrucuk
Supervisor, **Aerospace Engineering Dept., METU** ____________

Examining Committee Members:

Prof. Dr. Serkan Özgen
Aerospace Engineering Dept., METU ____________

Asst. Prof. Dr. İlkay Yavrucuk
Aerospace Engineering Dept., METU ____________

Prof. Dr. M. Kemal Özgören
Mechanical Engineering Dept., METU ____________

Prof. Dr. Ozan Tekinalp
Aerospace Engineering Dept., METU ____________

Asst. Prof. Dr. Yakup Özkazanç
Electrical and Electronics Engineering Dept., Hacettepe University ____________

Date: 10.02.2011

I hereby declare that all information in this document has been obtained and presented in accordance with academic rules and ethical conduct. I also declare that, as required by these rules and conduct, I have fully cited and referenced all material and results that are not original to this work.

Name, Last Name	:Kadriye TİRYAKİ KUTLUAY
Signature	:

ABSTRACT

ADAPTIVE CONTROL OF GUIDED MISSILES

Tiryaki Kutluay, Kadriye

Ph.D., Department of Aerospace Engineering

Supervisor: Asst. Prof. Dr. İlkay Yavrucuk

February 2011, 147 Pages

This thesis presents applications and an analysis of various adaptive control augmentation schemes to various baseline flight control systems of an air to ground guided missile. The missile model used in this research has aerodynamic control surfaces on its tail section. The missile is desired to make skid to turn maneuvers by following acceleration commands in the pitch and yaw axis, and by keeping zero roll attitude.

First, a linear quadratic regulator baseline autopilot is designed for the control of the missile acceleration in pitch axis at a single point in the flight envelope. This baseline autopilot is then augmented with a Direct Model Reference Adaptive Control (D-MRAC) scheme using Neural Networks for parameter estimation, and an L1 Adaptive Control scheme. Using the linearized longitudinal model of the missile at the design point, simulations are performed to analyze and demonstrate the performance of the two adaptive augmentation schemes. By injecting uncertainties to the plant model, the effects of adaptive augmentations on the linear baseline autopilot are examined.

Secondly, a high fidelity simulation software of the missile is used in order to analyze the performance of the adaptive augmentations in 6 DoF nonlinear flight simulations. For the control of the missile in three axis, baseline autopilots are designed using dynamic inversion at a single point in the flight envelope. A linearizing transformation is employed during the inversion process. These coarsely designed baseline autopilots are augmented with L1 adaptive control elements. The performance of the adaptive control augmentation system is tested in the presence of perturbations in the aerodynamic model and increase in input gain, and the simulation results are presented.

Keywords: L1 Adaptive Control, Model Reference Adaptive Control, Adaptive Control Augmentation, Dynamic Inversion, Control of Guided Missiles.

ÖZ

GÜDÜMLÜ FÜZELERİN ADAPTİF KONTROLÜ

Tiryaki Kutluay, Kadriye
Doktora, Havacılık ve Uzay Mühendisliği Bölümü
Tez Yöneticisi : Yrd. Doç. Dr. İlkay Yavrucuk

Şubat 2011, 147 Sayfa

Bu tez havadan karaya güdümlü bir füzenin ana uçuş kontrol sistemine çeşitli adaptif kontrol destek yapılarının uygulanmalarını ve analizini sunmaktadır. Bu araştırmada kullanılan füze modeli, kuyruk kısmında aerodinamik kontrol yüzeylerine sahiptir. Füzenin yunuslama ve yana dönme eksenlerinde ivme komutları izleyerek ve yuvarlanma yönelimini sıfırda tutarak kayarak-dönme manevraları yapması istenmektedir.

İlk olarak, füzenin yunuslama eksenindeki kontrolü için, uçuş zarfındaki tek bir noktada, doğrusal kuadratik düzenleyici yöntemi ile bir ana otopilot tasarlanmıştır. Daha sonra bu ana otopilot, parametre kestiriminde Yapay Sinir Ağları kullanan Doğrudan Modele Dayalı Uyarlamalı Kontrol yapısı ve L1 Uyarlamalı Kontrol yapısı ile desteklenmiştir. Füzenin tasarım noktasındaki doğrusallaştırılmış boyuna modeli kullanılarak, bu iki adaptif destek yapısının performansını analiz etmek için benzetimler yapılmıştır. Füze modeline belirsizlikler verilerek uyarlamalı destek yapılarının ana otopilot üzerindeki etkileri incelenmiştir.

İkinci olarak, adaptif desteklerin 6 serbestlik dereceli doğrusal olmayan uçuş benzetimlerindeki performansını analiz etmek için, füzenin yüksek güvenilirlik seviyesindeki bir benzetim yazılımı kullanılmıştır. Füzenin üç eksendeki kontrolü için uçuş zarfındaki tek bir noktada dinamik tersine çevrim yöntemi ile ana otopilotlar tasarlanmıştır. Tersine çevrim işleminde doğrusallaştırma dönüşümü uygulanmıştır. Daha sonra kabaca tasarlanmış olan bu ana otopilotlar L1 uyarlamalı kontrol elemanları ile desteklenmiştir. Uyarlamalı kontrol destek sisteminin performansı aerodinamik modelde hatalar olması ve girdi kazancının artması durumunda test edilmiş ve benzetim sonuçları sunulmuştur.

Anahtar Kelimeler: L1 Uyarlamalı Kontrol, Modele Dayalı Uyarlamalı Kontrol, Uyarlamalı Kontrol Desteği, Dinamik Tersine Çevrim, Güdümlü Füze Kontrolü.

To my father İbrahim Tiryaki with aspiration and gratitude

ACKNOWLEDGEMENTS

This research was supported by TUBITAK SAGE. TUBITAK SAGE is greatly acknowledged for providing the necessary substructure of this research.

I would like to express my deepest acknowledgements to my supervisor Asst. Prof. Dr. İlkay Yavrucuk. His precious guidance was invaluable and his endless belief in me throughout this study was the biggest motivation.

I would like to extend my acknowledgements to thesis committee members Prof Dr. M. Kemal Özgören, Prof. Dr. Ozan Tekinalp and Prof. Dr. Serkan Özgen for their invaluable comments and guidance they provided at the thesis progress meetings.

I would like to present my acknowledgements to my coordinator Dr. A. Pınar Koyaz for her valuable support and her trust in women in science.

My deepest gratitudes go to my dearest husband Ümit Kutluay for his endless support, love and invaluable patience. I am forever grateful to him for standing by me through all the forcible experiences of this period and still being able to make me smile.

My special gratitudes go to Ümran, Kamil and Emir Kutluay for their precious support, love and understanding throughout this study.

I would like to extend my thanks to my family members. Each of my aunts, uncles and cousins has always shown an endless support and love to me.

I would like express my acknowledgements to my dear friends Özge and Ersin Özçıtak. Taking a break at their side was a big pleasure, and talking to Özge has been an invaluable relief for me.

I would like to express my thanks to my dear friend Ebru Ortakaya. She was there to encourage me to accomplish my study.

I would like to thank to my dear friends, Belgin Bumin, Biter Boğa, Didem Asil, Ezgi Kiper, Gökçen Aydemir, Güzin Kurnaz and Havva Özsaraç,Tülay Adıgüzel for our motivating, and joyful chats and meetings.

I would like to thank to all of my colleagues in TUBITAK SAGE for their support and motivation.

Finally, I am thankful to my dear mother and father, Fatma and İbrahim Tiryaki. This work has been possible as a result of my beloved father's will.

.

TABLE OF CONTENTS

LIST OF FIGURES

FIGURES

NOMENCLATURE

a_y	Body acceleration in y axis
a_z	Body acceleration in z axis
a_{yc}	Body acceleration command in y axis
a_{zc}	Body acceleration command in z axis
A	System matrix
b	Input vector
c	Output vector
A_m	System matrix for desired dynamics
b_m	Input vector for desired dynamics
c_m	Output vector for desired dynamics
A_{ref}	System matrix for reference dynamics
b_{ref}	Input vector for reference dynamics
c_{ref}	Output vector for reference dynamics
B_m, B_{um}	Input matrix for matched and unmatched disturbances
$f(x), g(x)$	Arbitrary nonlinear functions
$f_1(.,.,.), f_2(.,.,.)$	Arbitrary nonlinear functions
K_x, K_z	Feedback gains of baseline autopilot
$\hat{k}_x, \hat{k}_z$	Incremental adaptive feedback gains
M	Mach number
P	Solution of algebraic Ricatti equation
Q	Symmetric positive definite matrix

r	Reference input
p, q, r	Body rates in roll, pitch and yaw axis
p_c, q_c, r_c	Body rate commands in roll, pitch and yaw axis
x	State vector
y	Output vector
z	State vector
$\hat{x}$	Estimated state vector
$\hat{y}$	Estimated output vector
u_{bl}	Baseline control signal
u_{ad}	Adaptive control signal
V	Lyapunov function
α	Angle of attack
β	Angle of sideslip
$\delta_e, \delta_r, \delta_a$	Effective control surface deflections in pitch, yaw, roll axis
θ	Adaptive parameter vector
σ	Unknown disturbance vector
ω	Unknown input gain
$\hat{\theta}$	Estimated adaptive parameter vector
$\hat{\sigma}$	Estimated disturbance vector
$\hat{\omega}$	Estimated input gain
$\hat{\sigma}_m, \hat{\sigma}_{um}$	Estimated matched and unmatched nonlinear functions
Θ	Unknown parameter set
ξ	Damping of control actuation system
$\kappa(.)$	Unknown nonlinear function
$\Gamma_\theta, \Gamma_\sigma, \Gamma_\omega$	Adaptation rates

ϕ	Roll angle
$\phi(.)$	Radial basis function vector
$\omega_{n_{CAS}}$	Bandwidth of control actuation system
ν	Pseudo control vector

LIST OF ABREVIATIONS

CAS	Control Augmentation System
DMI	Dynamic Model Inversion
DoF	Degrees of Freedom
IMU	Inertial Measurement Unit
JDAM	Joint Direct Attack Munition
LA	Lever Arm
LQR	Linear Quadratic Regulator
MIMO	Multi Input Multi Output
MRAC	Model Reference Adaptive Control
NASA	National Aeronautics and Space Administration
NN	Neural Networks
RSLQR	Robust Servomechanism Linear Quadratic Regulator
SISO	Single Input Single Output
UAV	Unmanned Aerial Vehicle
UCAV	Unmanned Combat Aerial Vehicle

CHAPTER 1

INTRODUCTION

1.1 Motivation

Flight control of guided munitions has been a challenging area for control engineers. As the agility, speed and skills of guided munitions increase, related control problems became more challenging. However, besides its challenges, guided missiles serve as perfect platforms for testing novel control architectures. Most of the guided missiles are cheaper than other flying platforms such as aircraft, spacecraft or Unmanned Aerial Vehicles (UAV). Moreover, because of their unmanned nature, guided munitions provide more flexibility to test novel control architectures for the first time. As the maturity of knowledge about adaptive control methods increase, more of them started to be applied and flight tested on guided missiles. With the help of adaptive control algorithms, a very common problem in flight control, the dependency of controller performance on aerodynamic parameters, is desired to be solved. Very successful results have been obtained for various systems.

This research takes its motivation to find adaptive controller solutions for guided missiles. The research consists of a detailed survey on state of the art in adaptive control methods. Applications of these methods on missile systems and robustness issues of these controllers are studied.

1.2 Dynamic Model Inversion Control

Flight control systems have to cope with the nonlinear and time varying nature of flight vehicles, as well as the uncertainties and un-modeled dynamics in the system and physical environment around them.

Gain scheduling has been a popular flight control methodology for guided missiles. This method is composed of designing linear controllers at pre-specified trim conditions inside the flight envelope, scheduling the pre-calculated gains in a table, and interpolating between these gains for the corresponding flight condition during the flight. Although gain scheduling has served to flight control community with success for long years, the design process can be very time consuming. Also the aerodynamic data should be accurate and cover the whole flight envelope. This increases time and cost in the controller design phase.

Feedback linearization has emerged as a nonlinear control method that can eliminate the need for extensive gain scheduling and simplify the controller design process. By dynamically recasting the nonlinear system into a linear form, this method allows the calculation of the nonlinear control signal from an inverse transformation. In [1] autopilot design of an air to air missile with dynamic model inversion method is given. [2], [3], [4] and [5] presents various applications of dynamic model inversion method for flight control of missiles. [6] and [7] deals with stability and robustness issues of missile autopilots designed with dynamic inversion.

A problem dealt with in literature is the fact that dynamic inversion cannot be applied to non-minimum phase systems. In [1] and [4] different approaches to deal with this problem is presented.

Another complication of dynamic model inversion is that the stability and performance of the controller depends on an accurate plant model. Since, most of the time, the system parameters are not exactly known and the plant inversion is not perfect, dynamic inversion controllers may possess performance degradation. In literature, in order to overcome the potential performance degradations of a dynamic inversion controller due to imperfect inversion or non-accurate aerodynamics, the control loop is augmented with adaptive elements.

1.3 Adaptive Control Augmentation

There has been an increasing interest in the adaptive control of flight vehicles. Throughout the years the experience and progress has grown rapidly. Recently, in addition to stand alone adaptive controller schemes [8], adaptive elements are also used as augmentations to roughly designed baseline controllers.

Neural networks, known for their capability of modeling highly nonlinear functions, are a powerful tool for the estimation of modeling errors, uncertainties, etc. Hence, neural networks are frequently used for parameter estimation purposes in adaptive control. [9]-[12] present pioneering research on the application of neural network augmentation to baseline dynamic inversion controllers for air to air missiles, aircraft, tilt-rotor and helicopter. In [13] and [14] an implementation and application of an online learning neural network augmentation to a dynamic inversion based acceleration autopilot of a family of guided munition is given. Flight test results showed that the adaptive augmentation eliminate the inversion errors of an approximate plant model.

In [15], the back-stepping design approach is used to improve the transient performance of a dynamic inversion missile autopilot. Adaptive control augmentation examples were concentrated on the application to dynamic inversion based autopilots. In [16], Sharma et.al., proposed a new method of augmenting existing linear controllers, including several classical and modern forms and MIMO dynamic compensators, with neural networks.

On the other hand, Model Reference Adaptive Control (MRAC) is an architecture used to control linear systems with unknown coefficients [17]. Here, a reference model with the desired closed loop response is used to shape the control signal and consequently the closed loop response of the plant. The objective is to take the error between the outputs of the reference system and the plant go asymptotically zero.

In 2005 Boeing Company has implemented a direct adaptive model reference control to a modified version of the MK82 JDAM flight control system. The baseline controller was a gain scheduled controller designed with linear quadratic regulator approach. In this work, the controller is augmented with an adaptive element in order to compensate for the changes due to modifications made on the external configuration. The flight tests carried out in 2006, using adaptive augmentation were successful.

Yet, some drawbacks are present in the adaptive controller application. In [18] some problems about the application of direct adaptive model reference control to aircraft and weapon systems are stated.

It is rather hard to show stability margins in adaptive control schemes analytically. The behavior of adaptive controllers during transient phases like gust, turbulence, or in the face of perturbed aerodynamics, is prone to produce large or high frequency control signals. The solutions to these problems like dead-zone or adaptive learning rates are conservative most of the times.

In [19] and [20], Hovakimyan et.al., applied a low pass filter to the adaptive signal, which allows the arbitrary increase of the adaptation gain. This L1 adaptive controller scheme enabled controlled adaptive signals while eliminating high frequency adaptive signal output during transients. In [19] and [20], the weaknesses of present adaptive control architectures during the transient phase compared to the L1 controller is presented. The L1 controller is shown to have guaranteed robustness in the tracking errors during the transient phase. In addition to the asymptotic stability characteristics of the controller, this new architecture guarantees that the control signal is in a low-frequency range. This new architecture produces an adaptive control signal which makes the input and output of an uncertain linear system track the input and output of a desired linear system during the transient phase, in addition to asymptotic tracking.

1.4 L1 Adaptive Control

The control architecture proposed for L1 adaptive control is a cascaded system which is composed of a desired closed loop reference system, a low pass filter, an adaptation law and the plant itself. The desired closed loop reference system, which is actually a passive identifier allows for the incorporation of a low pass filter in the feedback loop. The adaptive control signal is passed through the low pass filter, which gives the freedom to increase the adaptation gain arbitrarily to enforce the desired transient response within the limits of the bandwidth of the control channel, without causing any high frequency in the control signal

A systematic design procedure is presented for the L1 adaptive control architecture. The elements of L1 adaptive controller are expressed below:

State Predictor: The state predictor defines the desired closed loop system which will serve as a reference system for the plant.

Adaptation Law: Adaptive law defines the formulation for the calculation of the unknown parameters used in the system equation.

Control Law: Control law defines the formulation of the adaptive control signal. The adaptive control signal formulation involves the adaptive elements calculated by the adaptation law, the low pass filter and the reference signal.

In [19] and [20], L1 adaptive control architecture formulation is given for systems with bounded, matched system uncertainties. In [21] and [22] the formulation is extended to systems with unknown time varying parameters and bounded disturbances. In [23] the L1 adaptive controller methodology for parametric strict feedback systems is presented. The output feedback formulation of L1 adaptive controller is presented in [24] for systems with time-varying unknown parameters and bounded disturbances. In [25] and [26] an L1 based neural network adaptive control architecture is proposed. In 2008, L1 adaptive controller formulation is extended for MIMO systems in the presence of unmatched disturbances in [27], and for a class of systems with unknown nonlinearities in [28].

L1 adaptive control has been studied for various platforms, and some of them are flight tested. In [29] L1 adaptive controller is designed for the pitch channel control of miniature air vehicles. Other design examples were missile longitudinal autopilot design in [30], [31], L1 adaptive output feedback controller for aerospace vehicles in [32], flexible space launch vehicle control in [33], simulator testing of longitudinal flying qualities of a fighter with L1 adaptive control in [34], application to UCAV and Aerial Refueling problem in [35], application to NASA AirSTAR Flight Test Vehicle in [8]. In these examples, the L1 adaptive controller was serving as the baseline control architecture for the flight vehicle. L1 adaptive control is also reformulated to be an adaptive augmentation element on top of a baseline autopilot to serve as an aiding and correcting control element. In [36] commercial autopilots are augmented by L1 adaptive control for 3D path following for small UAVs. In [37] the dynamic inversion based autopilots of X-48B aircraft is augmented with L1 adaptive control augmentation system.

The L1 adaptive controllers are also verified through flight tests. Some results are presented in [8], [33], [35], [38].

This thesis work includes applications of L1 adaptive control theory. Implementations of this theory on flight control of a guided missile are studied.

1.5 Contributions of This Thesis Work

This thesis work involves an analysis and applications of adaptive control augmentation systems to a guided missile.

The contributions of this thesis work can be stated as follows:

Design of a linear quadratic regulator based autopilot for the control of a missile in longitudinal axis. Augmentation of this baseline autopilot with direct MRAC and L1 adaptive control. Demonstration of performance of these two adaptive control schemes on a linear missile model.

Design of a Dynamic Model Inversion (DMI) controller with two time-scale separation method for the control a missile in 6DoF. Augmentation of this DMI controller with novel L1 adaptive Control Augmentation System (CAS). Demonstration of the performance of augmented DMI controller on a missile model with nonlinear 6 DoF flight simulations. L1 adaptive CAS was tested through nonlinear simulations for the first time.

Desing of a Dynamic Model Inversion (DMI) controller with output redefinition for the control of a missile in 6DoF with L1 adaptive CAS. Demonstration of the performance of this controller with nonlinear 6 DoF flight simulations. L1 adaptive CAS was tested through nonlinear simulations.

1.6 Thesis Outline

In Chapter 1 the motivation of the thesis study is stated. A literature survey about the dynamic inversion control, adaptive control methods concentrating on guided missiles, and the evolution and state of the art of the novel L1 adaptive control method is presented.

In Chapter 2, the design methodology of a dynamic inversion controller is presented. The design steps of a cascade two time-scale separation dynamic inversion controller for the acceleration control of a missile are explained. Then the non-minimum phase behavior of tail controlled missiles is discussed and the "Output Redefinition" methodology is presented. The design of a cascade dynamic inversion controller with output redefinition for the acceleration control of a missile is expressed.

In Chapter 3, the theory of Model Reference Adaptive Control and novel L1 adaptive control is explained. L1 adaptive controller design methods for different class of systems are presented.

In Chapter 4, design of a linear quadratic regulator based autopilot for the longitudinal control of a missile is presented. Augmentation of this baseline autopilot with direct MRAC and L1 adaptive control is demonstrated. Linear simulation results of these augmentation schemes are presented.

In Chapter 5, design of dynamic model inversion controllers for the control of a missile in longitudinal, directional and lateral axes is presented. Two time scale separation and output redefinition design options are applied. Augmentation of these baseline autopilots with L1 adaptive control augmentation system is demonstrated. Nonlinear, 6 DoF flight simulation results of these augmentation schemes are presented.

In Chapter 6, conclusions and recommendations for future work is given.

CHAPTER 2

DYNAMIC MODEL INVERSION CONTROL

The most widely studied approach of nonlinear control design is feedback linearization. This technique involves the use of a nonlinear coordinate transformation to recast the nonlinear system into a linear time invariant form. Linear tools can then be applied for the control synthesis. A specific case of feedback linearizing control is known as "dynamic inversion". Since the 1980's dynamic model inversion is applied in flight control problems. Comprehensive investigations of dynamic inversion in flight control applications are provided in [39], [40].

In this chapter, firstly the generalized methodology of dynamic inversion based control is given. Then, in the following sections, the design process of a dynamic inversion based acceleration autopilot of a missile with two time scale separation and output redefinition methods will be explained. Lastly, the design process of a dynamic inversion based roll attitude autopilot is described.

2.1 Problem Formulation

The nonlinear system dynamics can be expressed by using a set of nonlinear differential equations. A MIMO nonlinear dynamic system can be written in such a form as follows [4]:

$$\dot{x} = f(x) + g(x)u \tag{1}$$

where $x \in \mathbb{R}^n$ is the state vector, $u \in \mathbb{R}^m$ is the control, $f(x)$ and $g(x)$ denote nonlinear functions. It is assumed that $g(x)$ is invertible and x is perfectly known.

For the missile control problem, u is the control signal, which denotes the effective control surface deflections in three axes. For the missile under consideration, this includes the elevator, rudder and aileron deflections. y is the selected control variable. For the missile under consideration the control variables are the body accelerations in pitch and yaw axes, and the roll attitude in roll axis.

The system in (1) can be transformed into a linear system as follows:

$$\dot{x} = v \tag{2}$$

Then, the control u can be computed as :

$$u = g(x)^{-1}[v - f(x)] \tag{3}$$

The variable v is a new control for the transformed system. v is called as pseudo control in some references [13], [14]. The real control u is computed by (3), hence the linearizing transformation technique can be used if the dynamics are known, all the states are measured, and $g(x)^{-1}$ is invertable for all values of x. It is assumed that $g(x)$ is square where $g(x) \in \mathbb{R}^{n\times n}$ and the number of controls are equal to the number of states, i.e. $n = m$. Figure 1 shows the block diagram of the linearizing transformation.

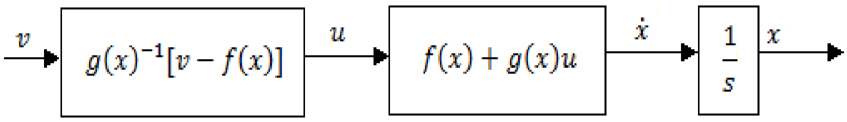

Figure 1 Dynamic Inversion Architecture

2.2 Application to Missile Autopilot Design

Dynamic inversion technique explained in the previous section is applied to the autopilot design of a guided missile. The missile under consideration is a tail controlled, skid-to-turn missile with axis-symmetric external geometry. During the flight, roll attitude of the missile is kept at 0 deg, and the body accelerations are controlled in the pitch and yaw axis.

One drawback of dynamic model inversion is that it cannot be applied to non-minimum phase systems due to the inversion process employed during the calculation of the control signal. For tail-controlled missiles the transfer function from control surface deflection to acceleration is inherently non-minimum phase. Hence, it is not possible to directly design a dynamic inversion controller for the acceleration control. In this thesis, two different methods are used to overcome this problem. One way to control the missile acceleration with dynamic model inversion is to first design a dynamic inversion controller for the inner loop by using a state variable which has minimum phase transfer function. The state variables like pitch rate, q and yaw rate, r or the angle-of-attack, α, and sideslip, β which have minimum-phase transfer functions with control surface deflection are trivial candidates for the inner loop control. Then an outer loop controller can be designed with classical methods for the acceleration control. This methodology is called as two timescale separation design in the literature [1], [4]. However, state variables may have undesirable zero dynamics, which may degrade the performance of dynamic inversion controller due to inversion process employed.

Another method offered in literature to deal with the non-minimum phase characteristics of acceleration control with dynamic inversion is "Output Redefinition". In this method a new inner loop variable with favorable zero dynamics is formed and inversion is applied to this variable. Then a classically designed outer acceleration loop is closed around this inner loop controller.

Since the missile under consideration has an axis symmetric geometry, and skid-to-turn maneuver is used, the autopilot design for the directional axis is essentially identical in form to the autopilot design for the longitudinal axis. Hence, for simplicity only the longitudinal axis design is considered in the following sections.

2.2.1 Missile Dynamics

The linearized rigid body equations of motion in the missile body axis are used to design the dynamic inversion autopilots. Aerodynamic, inertial and kinematic cross couplings are neglected and small angle assumptions are made whenever applicable. The resulting linear dynamics of the open loop plant used to design the baseline controllers are as follows:

Longitudinal Dynamics:

$$\dot{\alpha} = Z_{\alpha}\alpha + Z_{\delta_e}\delta_e + q \tag{4}$$

$$\dot{q} = M_\alpha \alpha + M_q q + M_{\delta_e} \delta_e \tag{5}$$

$$a_z = U_0(\dot{\alpha} - q) \tag{6}$$

Lateral Dynamics:

$$\dot{\beta} = Y_\beta \beta + Y_{\delta_r} \delta_r - r \tag{7}$$

$$\dot{r} = N_\beta \beta + N_r r + N_{\delta_r} \delta_r \tag{8}$$

$$a_y = U_0(\dot{\beta} + r) \tag{9}$$

Roll Dynamics:

$$\dot{p} = L_p p + L_{\delta_a} \delta_a \tag{10}$$

$$\dot{\phi} = p \tag{11}$$

where Z_α, Z_{δ_e}, M_α, M_{δ_e}, M_q, Y_β, Y_{δ_r}, N_β, N_{δ_r}, N_r, L_p, L_{δ_a} are the dimensional aerodynamic derivatives which are formulated as given in Appendix A, α is the angle of attack, β is the sideslip angle, ϕ is the roll attitude, p, q, r are the roll, pitch and yaw rates and δ_a, δ_e, δ_r are the control surface deflections effective in roll, pitch and yaw axes respectively.

The nonlinear aerodynamic coefficients of the missile are taken to be functions of Mach number, M, angle of attack, α and sideslip angle, β as $C(M, \alpha, \beta)$.

2.2.2 DMI Based Control of Lateral and Longitudinal Accelerations

2.2.2.1 Dynamic Inversion Based Acceleration Autopilot Design with Two Timescale Separation

It is noted in [1] and [4] that in the two timescale separation approach the inner loop and outer loops are separated into fast and slow dynamics. In the design approach of this thesis the pitch rate q and the yaw rate r corresponds to the fast states. The fast states are controlled through three equivalent control surface deflections known as elevator, rudder and aileron deflections. After designing a fast state inversion controller for the rates, an outer loop inversion controller is designed for the slow states which are the angle of attack, α, and sideslip, β. The slow states are controlled by using the commands for q and r as control inputs. The effect of control surface deflections on the slow states is assumed to be negligible. Then a classically designed acceleration loop is closed around these two inner loops as shown in Figure 2.

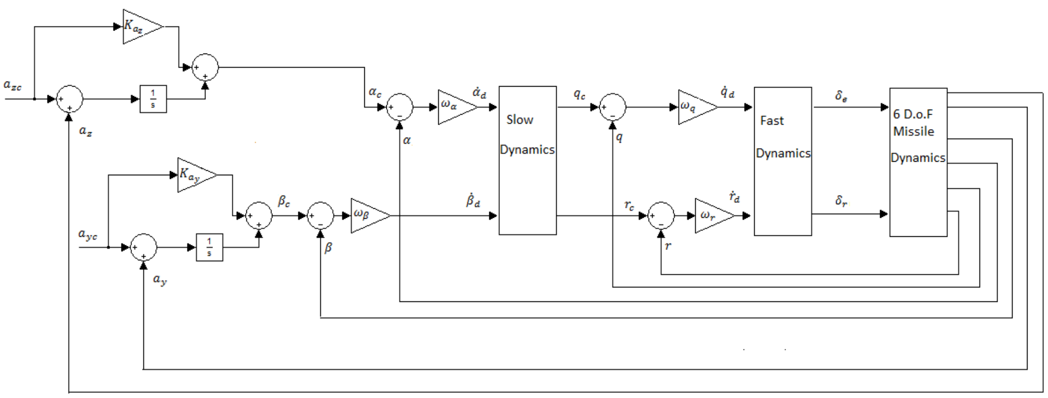

Figure 2 Dynamic Inversion Based Acceleration Control with Two Timescale Separation

In Figure 2, it is seen that there are two dynamic inversion controllers in this architecture. One is from slow states to fast states (α to q and β to r) and the other one is from fast states to control (q to δ_e and r to δ_r).

In different phases of flight of a guided munition, different control variables may be required to be commanded. For example, after safe separation phase, rate autopilots can be used to damp the high rates caused by the separation effects. Then, during the guided flight angle of attack and sideslip autopilots, or acceleration autopilots can be used to realize the desired maneuvers. This selected architecture allows the use of the inner rate loops, the outer α and β loops, and the acceleration loops independently, which allows for the control of different variables in a single architecture.

Here the methods stated in [1], [3], [4] and [13] is followed for the controller design.

Dynamic Model Inversion for Pitch Rate Control

In order to be able to make the linearizing transformation explained in Section 2.1 , a desired linear system dynamics should be selected. Since in the following sections, dynamic inversion controller will serve as a baseline control which will be augmented with adaptive control elements, desired dynamics is selected to be first order in order to make the dynamic inversion controller design process as simple and straightforward as possible.

The desired closed loop dynamics for the pitch rate is modeled to be a first order system as:

$$\frac{q(s)}{q_c(s)} = \frac{\omega_q}{s + \omega_q} \tag{12}$$

which results in the following differential equation:

$$\dot{q}_d = \omega_q(q_c - q) \tag{13}$$

Here $\dot{q}_d$ is the desired pitch acceleration, ω_q is the desired closed loop bandwidth of the q loop, q_c is the commanded pitch rate calculated from the outer angle of attack loop. The longitudinal linearized dynamics for q was given as:

$$\dot{q} = M_\alpha \alpha + M_q q + M_{\delta_e}\delta_e \tag{14}$$

Hence, given the desired pitch acceleration $\dot{q}_d$, the elevator deflection is calculated from (13) and (14) as:

$$\delta_e = \omega_q q_c - \left(\omega_q - M_q\right)q - M_\alpha \alpha / M_{\delta_e} \tag{15}$$

Dynamic Model Inversion for Angle of Attack Control

Following a similar way of design as the pitch rate loop, the desired closed loop dynamics for the angle of attack is modeled to be a first order system as:

$$\dot{\alpha}_d = \omega_\alpha(\alpha_c - \alpha) \tag{16}$$

Here $\dot{\alpha}_d$ is the desired angle of attack rate, ω_α is the desired closed loop bandwidth of the α loop, α_c is the commanded angle of attack calculated from the acceleration loop.

The linearized dynamics for α was given as:

$$\dot{\alpha} = Z_\alpha \alpha + Z_{\delta_e} \delta_e + q \tag{17}$$

In the two time scale approach, the fast states dynamics is assumed to perfectly track their commanded values. Hence the effect of control surface deflection on the slow states is assumed to be negligible. For the missile model under consideration, Z_{δ_e} is inherently small and $\frac{Z_\alpha}{Z_{\delta_e}} \gg 1$. Hence this derivative will be safely neglected and regarded as a disturbance that will be reduced by the feedback loop of angle of attack. Given the desired angle of attack rate $\dot{\alpha}_d$, the pitch rate command q_c for the inner pitch rate control loop can be calculated from (16) and (17) as:

$$q_c = \omega_\alpha \alpha_c - (\omega_\alpha + Z_\alpha)\alpha \tag{18}$$

Acceleration Control

For the acceleration loop, the acceleration commands should be transformed to angle of attack commands. Hence, a proper transformation is needed.

At steady-state $\dot{\alpha} = \dot{q} = 0$. Hence, from (6), the steady-state expression of pitch rate can be written as:

$$q = -\frac{a_z}{U_0} \tag{19}$$

Eliminating the term δ_e in (4) and (5), and substituting (19), the normal acceleration and angle of attack can be related through the following equation:

$$\left(1 - \frac{Z_{\delta_e} M_q}{M_{\delta_e}}\right)\frac{a_z}{U_0} = \left(Z_\alpha - \frac{Z_{\delta_e} M_\alpha}{M_{\delta_e}}\right)\alpha \tag{20}$$

Since Z_{δ_e} term is small compared to M_{δ_e}, (20) can be rewritten for the angle of attack as:

$$\alpha = \frac{a_z}{U_0 Z_\alpha} = K a_z \tag{21}$$

Hence, given an acceleration command, the commanded angle of attack can be directly computed from (21). To reduce the steady-state error possibly caused by the uncertainty in K, in the closed loop controller, an integral controller is added. The open loop acceleration control is given in Figure 3.

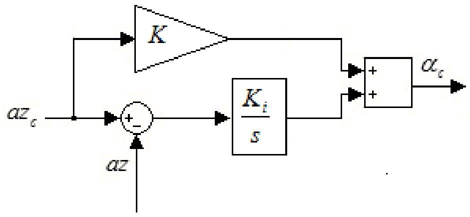

Figure 3 Open Loop Acceleration Control

This ends the dynamic inversion based acceleration autopilot design for the pitch axis. The same methodology is followed for the yaw axis control design.

2.2.2.2 Dynamic Inversion Based Acceleration Autopilot Design with Output Redefinition

As explained in the previous section, dynamic inversion method inverts the open loop transfer function from the control to the output being controlled to calculate the desired control signal. Therefore, non-minimum phase plants cannot be inverted because of the destabilizing right half plane zero dynamics in the numerator.

State variables are the trivial candidates to be used as the inner loop control variables. However, the zero dynamics of the transfer functions of tail controlled guided missiles from control surface deflection to inner loop variables, like q and r or α and β have zero dynamics which has undesirable characteristics for the inversion process. The transfer functions from control surface deflection to aerodynamic angles have a zero, which is far in the left half plane. It is stated in [13] that if the inversion is not exact, this zero results in undesirable transient response and increases the sensitivity to time delays. On the other hand, the transfer function from control surface deflections to body rates has a zero, which is very close to the origin. This results in a slow mode and threatens the stability of the controller in front of parameter errors. A solution to overcome the disadvantages of this undesirable zero dynamics is offered in [3], which is called “Output Redefinition”. Output redefinition offers an alternative inner loop control variable with desirable zero dynamics. Here, this alternative approach from [3] and [13] will be explained and used for the longitudinal control of a missile. In this approach, the inner loop variable is defined as a linear combination of the state variables. This allows the designer to place the zero of the associated transfer function at a desirable location. Thus, for example a combination of both angle of attack and pitch rate could be used to define the commanded inner loop variable.

Here, the redefined output for the longitudinal axis given in [13] is used and taken as follows:

$$y \triangleq \alpha + C_q q \tag{22}$$

The proof of the derivation of the redefined control variable is given in [3]:

From (4) and (5) the following transfer functions can be derived as follows:

$$\frac{q(s)}{\delta_e(s)} = \frac{M_{\delta_e}\left(s + \left(\frac{M_\alpha Z_{\delta_e}}{M_{\delta_e}} - Z_\alpha\right)\right)}{D(s)} \tag{23}$$

$$\frac{\alpha(s)}{\delta_e(s)} = \frac{Z_{\delta_e}\left(s + \frac{M_{\delta_e}}{Z_{\delta_e}}\right)}{D(s)} \tag{24}$$

where $D(s) = s^2 - (Z_\alpha + M_q)s - M_\alpha + Z_\alpha M_q$.

Substituting (23) and (24) into (22), the transfer function for the newly defined output variable y is obtained as follows:

$$\frac{y(s)}{\delta_e(s)} = \frac{K_y(s + z_y)}{D(s)} \tag{25}$$

where

$$K_y = M_{\delta_e} + C_q Z_{\delta_e} \tag{26}$$

$$z_y = \frac{Z_{\delta_e} a_\alpha + C_q M_{\delta_e} a_q}{K_y} \tag{27}$$

$$a_\alpha = \left(\frac{M_\alpha Z_{\delta_e}}{M_{\delta_e}} - Z_\alpha\right) \tag{28}$$

$$a_q = \frac{M_{\delta_e}}{Z_{\delta_e}} \tag{29}$$

Using the output y, it is aimed to select C_q so that the zero of the transfer function of the new output, z_y has an order of one, $O(1)$. From (26) and (27), C_q can be calculated as:

$$C_q = \frac{Z_{\delta_e}(a_\alpha - z_y)}{Z_{\delta_e}(z_y - a_q)} \tag{30}$$

Dynamic Inversion with Output Redefinition

The block diagram of pitch axis acceleration autopilot with the newly defined inner loop variable y is given in Figure 4.

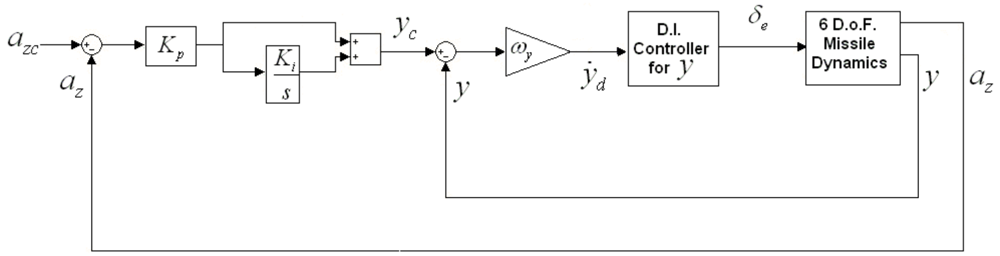

Figure 4 Dynamic Inversion Based Acceleration Control

The desired dynamics for the redefined output variable y is taken to be of first order as follows:

$$\dot{y}_d = \omega_y(y_c - y) = u_y \tag{31}$$

Here ω_y is the desired bandwidth of the inner loop, y_c is the commended inner loop variable produced by the outer acceleration loop.

From (22) $\dot{y}$ can be written as:

$$\dot{y} = \dot{\alpha} + C_q\dot{q} \tag{32}$$

For a given y_c command, the control surface deflection command δ_e can be calculated by substituting (4), (5), and (31) into (32) as follows:

$$\delta_e = \frac{u_y - q - C_q\left(M_\alpha \alpha + M_q q\right) - Z_\alpha \alpha}{(Z_{\delta_e} + U_0 C_q M_{\delta_e})} \tag{33}$$

where u_y is the corresponding *pseudocontrol* (desired rate of change of y)

2.2.3 Dynamic Inversion Based Roll Attitude Autopilot

For the roll attitude control, first an inner loop controller is designed with dynamic inversion method for the roll rate control. Then a proportional outer loop controller is designed for the roll attitude, which produces the roll rate commands for the inner loop.

The block diagram of the roll attitude control is given in Figure 5.

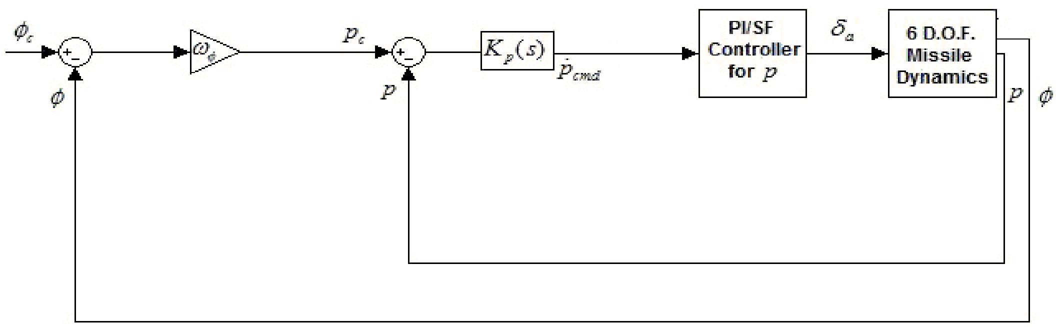

Figure 5 Dynamic Inversion Based Roll Attitude Control

The desired dynamics for the roll rate is taken to be of first order as follows:

$$\dot{p}_d = k_p(p_c - p) \tag{34}$$

Here $\dot{p}_d$ is the desired roll acceleration, p_c is the commanded roll rate calculated from the outer roll attitude loop. Substituting (34) into (10), for a given desired roll rate, δ_a can be calculated as follows:

$$\delta_a = \frac{\dot{p}_d - L_p p}{L_{\delta_a}} \tag{35}$$

Neglecting all aerodynamic, kinematic and inertial cross couplings, the linearised roll angle dynamics is as follows:

$$\dot{\phi} = p \tag{36}$$

Let the desired dynamics for the roll angle be:

$$\dot{\phi}_d = \omega_\phi(\phi_c - \phi) \tag{37}$$

Hence the commanded roll rate for the inner loop can be calculated as:

$$p_c = \dot{\phi}_d = \omega_\phi(\phi_c - \phi) \tag{38}$$

The methodology followed in dynamic inversion based acceleration and roll attitude autopilots are explained. In Chapter 5, this methodology will be applied to the missile model under consideration. Then L1 adaptive control augmentation will be applied to the dynamic inversion based autopilots to increase the robustness of these autopilots to uncertainties. Numerical simulation results will be given.

CHAPTER 3

L1 ADAPTIVE CONTROL

Adaptive controllers are desired to adapt to uncertainties in the system by producing a realizable control signal. Most adaptive control architectures are shown to be asymptotically stable by Lyapunov stability theory. Various improvements have been suggested for robustness and enhanced performance properties of these architectures. However, in practical applications, these architectures suffered from poor robustness characteristics especially during transient dynamics. The fast nature of transients requires fast and robust adaptation. Hovakimyan et.al. addressed this problem and enabled fast adaptation without sacrificing robustness [18], [19], [20], [21], [24]. This novel architecture ensures uniformly bounded transient response for both the input and output signals. The architecture employs a low pass filter in the feedback loop, which provides control designer the ability to calibrate between performance and robustness, within the bandwidth of the control loop. The name "L1 Adaptive Control" stems from the stability criteria of this novel control architecture which uses Small Gain Theorem [42], written for L1 gain. The stability criteria is given in (69).

In this part of the thesis, an introductory theory of the L1 adaptive control is explained. Then the problem formulation, stability and convergence results of the initial form of the L1 adaptive controller are presented. Similarly, the design issues of the L1 adaptive controllers are mentioned. During the evolution of L1 Adaptive Control, the controller design formulation was presented for several different classes of systems. In this chapter, L1 adaptive Controller for SISO systems in the presence of matched uncertainties and disturbances will be explained. Then, L1 Adaptive Controller for multi-input multi-output systems in the presence of nonlinear unmatched uncertainties will be described according to [43]. This architecture is later used in the augmentation of a baseline controller of a missile in Chapter 4 and Chapter 5.

3.1 Model Reference Adaptive Controller (MRAC)

The objective of Model Reference Adaptive Control is to define an adaptive control signal for the control of a closed loop system, the output of which tracks the output of a desirable reference system, even in the presence of uncertainties or variations in plant parameters.

Here, the system dynamics considered is single input single output and linear time invariant as follows [43]:

$$\dot{x}(t) = Ax(t) + bu(t), \;\; y(t) = c^T x(t), \;\; x(0) = x_0 \tag{39}$$

where $x(t) \in \mathbb{R}^n$ is the system state vector (measurable), $u(t) \in \mathbb{R}$ is the control signal, $b, c \in \mathbb{R}^n$ are known constant vectors, A is an unknown $n \times n$ matrix, $y(t) \in \mathbb{R}$ is the regulated output.

During the formulation of MRAC design, the following assumptions will be in effect:

Assumption 1: There exist a Hurwitz matrix $A_m \in \mathbb{R}^{n\times n}$ and a vector of ideal parameters $\theta \in \mathbb{R}^n$ such that (A_m, b) is controllable and $A_m - A = b\theta^T$. A_m defines the desired reference dynamics for the closed loop system.

Assumption 2: The unknown parameter θ belongs to a given compact convex set Θ, i.e. $\theta \in \Theta$.

Assumption 3: The reference input $r(.)$ is piecewise continuous and bounded in $\mathbb{R}$.

According to *Assumption 1*, the system dynamics can be rewritten as follows:

$$\dot{x}(t) = Ax(t) + bu(t) - b\theta^T x(t), \qquad y(t) = c^T x(t), \;\; x(0) = x_0 \tag{40}$$

The ideal controller for this system dynamics that will eliminate the uncertainties and provide tracking of the reference input is:

$$u^*(t) = \theta^T x(t) + k_g r(t) \tag{41}$$

where $k_g = -\frac{1}{c^T A_m^{-1} b}$ can be used to have zero steady state error to step reference inputs. Here, it is assumed that the desired reference dynamics A_m is selected such that $c^T A_m^{-1} b \neq 0$.

The ideal controller reduces the system dynamics to the reference model dynamics as follows:

$$\dot{x}_m(t) = A_m x_m(t) + bk_g r(t), \qquad y_m(t) = c^T x_m(t) \tag{42}$$

where $x_m(t) \in \mathbb{R}^n$ is the state of the reference model and $y_m(t) \in \mathbb{R}^n$ is the output vector.

The model reference adaptive controller is defined as:

$$u(t) = \hat{\theta}^T(t)x(t) + k_g r(t) \tag{43}$$

where $\hat{\theta}(t) \in \mathbb{R}^n$ are the adaptive parameters, which are the estimates of the ideal parameters $\theta(t)$. And the corresponding adaptive law is given as:

$$\dot{\hat{\theta}}(t) = \Gamma Proj\big(\hat{\theta}(t), x(t)e^T(t)Pb\big), \qquad \hat{\theta}(0) = \hat{\theta}_0 \tag{44}$$

Here, $\Gamma = \Gamma_\mathrm{c}\mathrm{I}_{\mathrm{n}\times\mathrm{n}}, \Gamma_\mathrm{c} > 0$ is the adaptation gain, $P = P^T > 0$ is the solution of the algebraic Lyapunov equation $A_m^T P + PA_m = -Q$ for arbitrary $Q > 0$, $e(t) = x_m(t) - x(t)$ is the tracking error between the reference dynamics in (42) and the system dynamics in (40).$Proj$ is a projection based mathematical operator used to keep the adaptive parameters bounded [46]. The projection operator is explained in detail in Appendix B. Hence, to achieve the control objective, a control architecture as shown in Figure 6 is used [43].

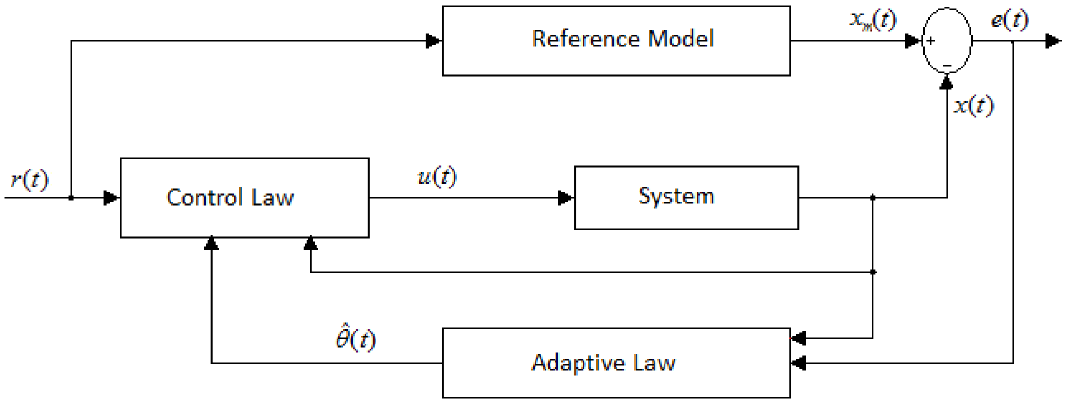

Figure 6 Model Reference Adaptive Controller Architecture

The closed loop tracking error dynamics of the MRAC can be written as follows:

$$\dot{e}(t) = A_m e(t) - b\left(\hat{\theta}(t) - \theta(t)\right)^T x(t) \tag{45}$$

Considering the Lyapunov function candidate:

$$V\left(e(t), \tilde{\theta}(t)\right) = e^T(t)Pe(t) + \tilde{\theta}^T(t)\Gamma^{-1}\tilde{\theta}(t) \tag{46}$$

where $\tilde{\theta}(t) = \hat{\theta}(t) - \theta(t)$

It can be verified that:

$$\dot{V}(t) = -e^T(t)Qe(t) + 2e^T(t)Pb\tilde{\theta}^T(t)x(t) + \frac{2}{\Gamma}\tilde{\theta}^T(t)\dot{\tilde{\theta}}(t)$$

$$= -e^T(t)Qe(t) + 2\tilde{\theta}^T(t)\left(\frac{1}{\Gamma}\dot{\hat{\theta}}(t) + x(t)e^T(t)Pb\right)$$

$$= -e^T(t)Qe(t) \leq 0$$

$$\dot{V}(t) = -e^T(t)Qe(t) \leq 0 \tag{47}$$

This result implies that the signals $e(t)$ and $\tilde{\theta}(t)$ are bounded. In order to verify asymptotic stability of the error dynamics, second derivative of the Lyapunov function is computed as follows:

$$\ddot{V}(t) = -2e^T(t)Q\dot{e}(t) \tag{48}$$

Since $e(t) = x_m(t) - x(t)$ is found to be bounded and the state of the closed loop reference dynamics in (42), $x_m(t)$, is also bounded, then it can be concluded that $x(t)$ is bounded. Hence, from (47), $\dot{e}(t)$ is bounded. From (48) $\ddot{V}(t)$ is also bounded, which implies that $\dot{V}(t)$ is uniformly continuous.

From Barbalat's Lemma it follows that:

$$\lim_{t\to\infty} \dot{V}(t) = 0$$

which implies that:

$$\lim_{t\to\infty} e(t) = 0$$

Hence the tracking error goes to zero asymptotically as $t \to \infty$ which means that the output of the closed loop system will asymptotically converge to the output of the reference system. This completes the stability proof of model reference adaptive control architecture.

Although MRAC provides asymptotic stability for the tracking error dynamics, asymptotic stability of the parameters is not guaranteed. It is hard to talk about the behaviour of the closed loop system during the transient phase in case of system uncertainties. Large transient errors can cause, large adaptive gains, which in turn causes high frequency control signal. MRAC can cause unpredictable/undesirable situations involving control signals of high frequency or large amplitudes, large transient errors or slow convergence rate of tracking errors during transient phase.

3.2 Model Reference Adaptive Controller with State Predictor

In this section a control architecture which is equivalent to Model Reference Adaptive Control (MRAC) architecture is presented. Then this architecture is used to explain the novel L1 adaptive controller architecture.

Given the system in (40), a state predictor model which can be thought as an identifier to the system in (40) is defined as follows:

$$\begin{aligned} \dot{\hat{x}}(t) &= A_m\hat{x}(t) + bu(t) - b\hat{\theta}^T x(t), \\ \hat{y}(t) &= c^T\hat{x}(t), \;\; \hat{x}(0) = x_0 \end{aligned} \tag{49}$$

where $\hat{x}(t) \in \mathbb{R}^n$ is the state of the predictor, and $\hat{\theta}(t)$ is the estimated value of the unknown parameter $\theta(t)$.

Compared to the MRAC architecture, this companion system can be thought as equivalent to the reference model dynamics in MRAC. The MRAC with state predictor is given in Figure 7 [43].

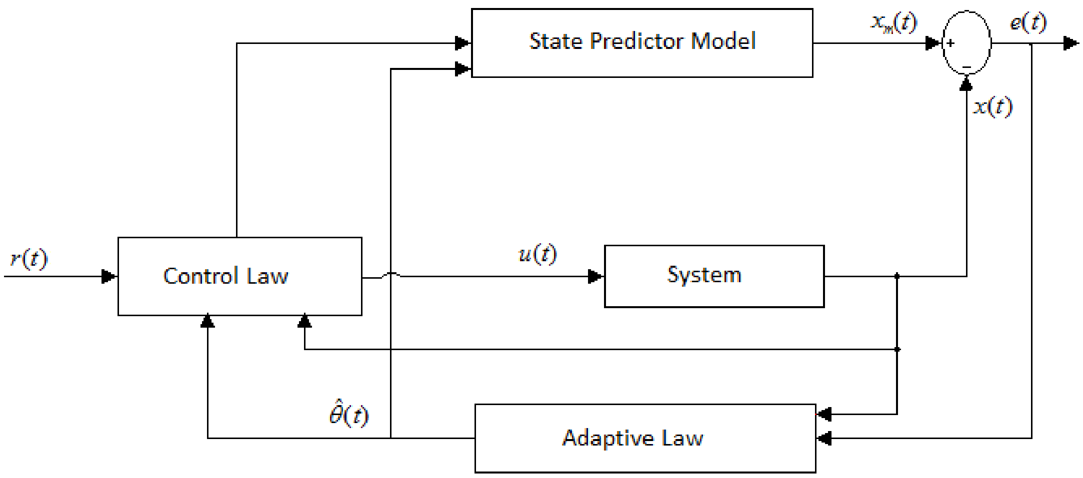

Figure 7 MRAC with State Predictor Architecture

The error dynamics between (40) and (42) can be written as:

$$\dot{\tilde{x}}(t) = A_m \tilde{x}(t) + b\tilde{\theta}^T(t)x(t), \;\; \tilde{x}(0) = 0 \tag{50}$$

where $\tilde{x}(t) \triangleq \hat{x}(t) - x(t)$ and $\tilde{\theta}(t) \triangleq \hat{\theta}(t) - \theta(t)$. It is seen that the error dynamics in (50) is in the same structure with the error dynamics in (45).

Given a bounded reference input signal $r(t)$ of interest to track, the following direct adaptive controller is used:

$$u(t) = \hat{\theta}^T(t)x(t) + k_g r(t) \tag{51}$$

with the following update law for the parameter estimates:

$$\dot{\hat{\theta}}(t) = \Gamma Proj\big(\hat{\theta}(t), x(t)\tilde{x}^T(t)Pb\big), \qquad \hat{\theta}(0) = \hat{\theta}_0 \tag{52}$$

where $\hat{\theta}(t) \in \mathbb{R}^n$ are the adaptive parameters, $\Gamma = \Gamma_c \mathrm{I}_{n\times n}, \Gamma_c >$ is the adaptation gain, $P = P^T > 0$ is the solution of the algebraic Lyapunov equation $A_m^T P + PA_m = -Q$ for arbitrary $Q > 0$, $\tilde{x}(t) = \hat{x}(t) - x(t)$ is the tracking error between the state predictor dynamics and the system dynamics in (40). With the following choice of Lyapunov function candidate:

$$V\left(\tilde{x}(t), \tilde{\theta}(t)\right) = \tilde{x}^T(t)P\tilde{x}(t) + \tilde{\theta}^T(t)\Gamma^{-1}\tilde{\theta}(t) \tag{53}$$

it is ensured that $\lim_{t\to\infty} \tilde{x}(t) = 0$. Thus, the model reference adaptive control architecture with state predictor leads to the same tracking error dynamics with MRAC, if they start from the same initial condition.

3.3 Error Bound for MRAC and MRAC with State Predictor

From equations (46), (53), and the asymptotic stability results, the following inequality can be obtained for the error states:

$$\|\tilde{x}(t)\| \leq \sqrt{\frac{\bar{\theta}_{max}}{\lambda_{min}(P)\Gamma}} \text{ for } t \geq 0 \tag{54}$$

Here $\bar{\theta}_{max} = \max_{\theta\in\Theta} \sum_{i=1}^{n} 4\theta_i^2$, and $\lambda_{min}(P)$ is the minimum eigenvalue of P.

From (54) it is seen that as the adaptation gain is increased, the error state can be decreased arbitrarily. However the increase in Γ results in high frequency control signals according to (43), (44), (51) and (52).

3.4 L1 Adaptive Controller

The L1 adaptive controller introduces a filtering technique for MRAC with state predictor architecture, which enables to prove fast adaptation and robustness at the same time. L1 adaptive control not only deals with the magnitude and frequency characteristics of the output tracking error, but also with these characteristics of the input signal to the system [18], [19], [20], [43]. The architecture of L1 adaptive controller is given in Figure 8 [43].

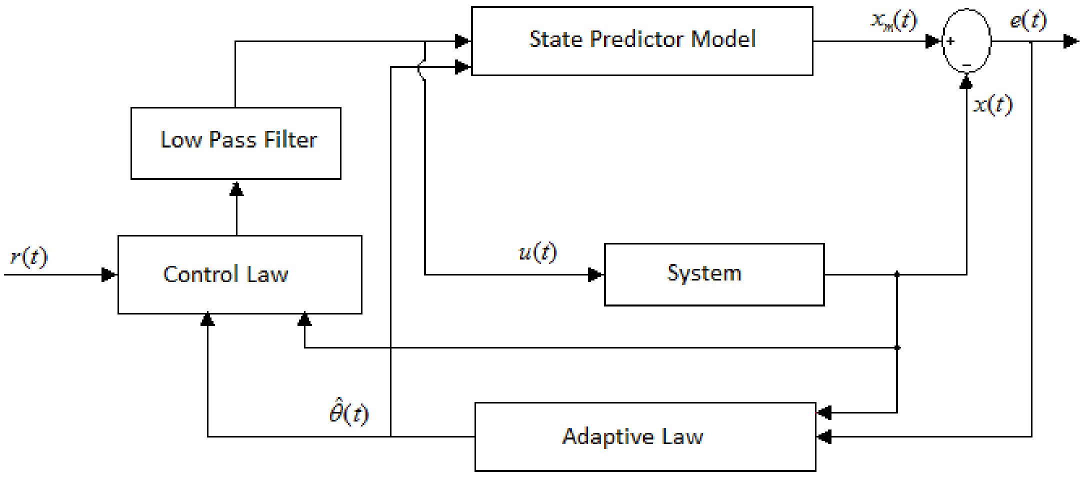

Figure 8 L1 Adaptive Controller Architecture

Instead of (51), L1 adaptive control theory offers the following control design for (40) and (49):

$$u(s) = C(s)(\bar{r}(s) + k_g r(s)) \tag{55}$$

where $\bar{r}(t) = \hat{\theta}^T(t)x(t)$, and $\bar{r}(s)$, $r(s)$, $u(s)$, $\hat{x}(s)$ are the Laplace transformations of $\bar{r}(t)$, $r(t)$, $u(t)$, $\hat{x}(t)$, k_g is a pre-specified design gain and $C(s)$ is a low pass filter with low pass gain 1. With this control law, the adaptive control signal is filtered by a low pass filter before it is introduced to the system dynamics.

3.5 L1 Gain Requirement

In the derivation of L1 adaptive control theory L1 Small Gain Theorem is used to define the limits for the filter design.

The closed loop MRAC model with state predictor in (49) can be written as an LTI system with two inputs $r(t)$ and $\bar{r}(t)$ as follows:

$$\hat{x}(s) = \bar{G}(s)\bar{r}(s) + G(s)r(s) \tag{56}$$

Where $\bar{G}(s) = H_0(s)(C(s) - 1)$, $G(s) = k_g H_0(s)C(s)$, $H_0(s) = (s\mathrm{I} - A_m)^{-1}b$.

For the stability of the MRAC with state predictor dynamics small gain theorem is used to define the following L1 gain requirement [45]:

$$||\bar{G}(s)||_{\mathcal{L}_1}\theta_{max} < 1 \tag{57}$$

where $||\bar{G}(s)||_{\mathcal{L}_1}$ is the $\mathcal{L}_1$ gain of $\bar{G}(s)$. The $\mathcal{L}_1$ gain of a stable proper SISO system $\bar{G}(s)$ is defined in [50] as :

$$||\bar{G}(s)||_{\mathcal{L}_1} = \int_0^\infty |\bar{g}(t)|dt \tag{58}$$

where $\bar{g}(t)$ is the impulse response of $\bar{G}(s)$. The $\mathcal{L}_1$ gain of a stable proper m input n output system $\bar{G}(s)$ is defined as:

$$\|\bar{G}(s)\|_{\mathcal{L}_1} = \max_{i=1,\ldots,n}\left(\sum_{j=1}^{m}\left\|\bar{G}_{ij}(s)\right\|_{\mathcal{L}_1}\right) \tag{59}$$

θ_{max} is defined as follows:

$$\theta_{max} \triangleq \max_{\theta\in\Theta}\sum_{i=1}^{n}|\theta_i| \tag{60}$$

Where θ_i is the i^{th} element of θ, Θ is the compact unknown parameter set.

The block diagram of L1 gain requirement is given in Figure 9.

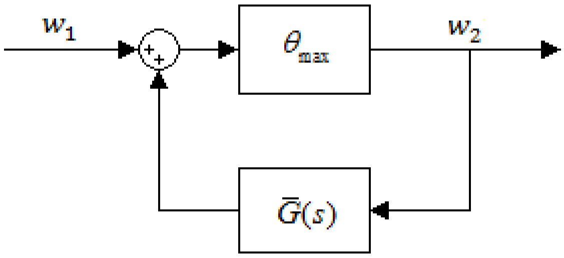

Figure 9 Block diagram for L1 gain requirement

The requirement in (57) is used to determine the bandwidth of the low-pass filter $C(s)$.

Now that, all the components of L1 Adaptive Controller are defined. The following theorem concludes the basic form of L1 Adaptive Controller according to [19], [20].

Theorem:

Given the system in (40) and the L1 adaptive controller defined by, (49), (52) and (55) subject to (57), the tracking error converges to zero asymptotically $\lim_{t\to\infty} \tilde{x}(t) = 0$.

3.6 L1 Adaptive Controller for SISO Systems in the Presence of Matched Time Varying Uncertainties and Disturbances with Uncertain System Input Gain

In this section, a theoretical extension of the L1 adaptive control theory for SISO systems in the presence of matched time varying uncertainties and disturbances with uncertain system input gain is explained [43]. In Chapter 4, this architecture is referenced for the adaptive control augmentation of a missile autopilot.

The system dynamics of a SISO system with unmatched nonlinear uncertainties can be modeled as follows:

$$\begin{gathered} \dot{x}(t) = A_m x(t) + b\big(\omega u(t) + \theta(t)^T x(t) + \sigma(t)\big) \\ y(t) = c^T x(t) \end{gathered} \tag{61}$$

where $x \in \mathbb{R}^n$ is the state vector, $u \in \mathbb{R}$ is the control input, $y \in \mathbb{R}$ is the output. A_m is a known, Hurwitz $n \times n$ matrix which represents the desired closed loop dynamics. ω models the unknown input gain, $\theta(t) \in \mathbb{R}^n$ is a vector of time varying unknown parameters and $\sigma(t)$ models the unknown disturbances in the missile dynamics.

For the adaptive control design the following assumptions are done on the uncertainties:

$\theta(t) \in \Theta$, $\sigma(t) < \Delta_0$ for $\forall\, t \geq 0$ and $\omega \in \Omega_0 \triangleq [\omega_{l0} \quad \omega_{u0}]$ where $0 < \omega_{l0} < \omega_{u0}$.

Also $\theta(t)$ and $\sigma(t)$ are assumed to be continuously differentiable with uniformly bounded derivatives:

$\left\|\dot{\theta}(t)\right\| \leq d_\theta < \infty$, $\|\dot{\sigma}(t)\| \leq d_\sigma < \infty$, for $\forall\, t \geq 0$.

For the systems that can be modeled as in (61) , the following adaptive controller is offered.

State Predictor:

$$\begin{aligned} \dot{\hat{x}}(t) &= A_m \hat{x}(t) + b\left(\hat{\omega} u(t) + \hat{\theta}(t)^T x(t) + \hat{\sigma}(t)\right) \\ \hat{y}(t) &= c^T \hat{x}(t) \end{aligned} \tag{62}$$

Adaptive Laws:

$$\dot{\hat{\theta}}(t) = \Gamma_\theta \mathrm{Proj}(\hat{\theta}(t), -\tilde{x}^T(t) P b x(t)) \tag{63}$$

$$\dot{\hat{\sigma}}(t) = \Gamma_\sigma \mathrm{Proj}(\hat{\sigma}(t), -\tilde{x}^T(t) P b) \tag{64}$$

$$\dot{\hat{\omega}}(t) = \Gamma_\omega \mathrm{Proj}(\hat{\omega}, -\tilde{x}^T(t) P b u(t)) \tag{65}$$

where Γ_θ, Γ_σ, Γ_ω are the positive definite adaptation rates, $\tilde{x} = \hat{x} - x$ is the error between the states of the state predictor and reference dynamics. P is the positive definite solution of the algebraic Lyapunov equation:

$$P A_m + A_m^T P = -Q \tag{66}$$

Q is symmetric positive definite matrix. $Proj(.,.)$ is the "Projection Operator" which is a mathematical operator used to keep the adaptive parameters bounded. [46] The projection operator is explained in detail in Appendix B.

Control Law:

$$u(s) = -kD(s)(\hat{\eta}(s) - k_g r(s)) \tag{67}$$

where $\hat{\eta}(t) \triangleq \hat{\omega}u(t) + \hat{\theta}(t)^T x(t) + \hat{\sigma}(t)$, $k_g = -\frac{1}{c^T A_m^{-1} b}$, $k > 0$ is a feedback gain

and $D(s)$ is a strictly proper transfer function leading to the following strictly proper stable transfer function for the low pass filter

$$C(s) \triangleq \frac{\omega k D(s)}{1 + \omega k D(s)} \tag{68}$$

Simplest choice for $D(s) = \frac{1}{s}$. Here, it is assumed that A_m is selected that $c^T A_m^{-1} b \neq 0$

The L1 controller defined by (62)-(67) is subject to the following condition:

$$\|G(s)\|_{\mathcal{L}_1} L < 1 \tag{69}$$

where $G(s) = H(s)(1 - C(s))$, $H(s) = (sI - A_m)^{-1} b$ and $L \triangleq \max_{\theta \in \Theta} \|\theta\|_1$

3.7 L1 Adaptive Controller for Multi-Input Multi-Output Systems in the Presence of Nonlinear Unmatched Uncertainties

In this section, a theoretical extension of the L1 adaptive control theory for multi-input multi-output systems in the presence of nonlinear unmatched uncertainties is explained [26], [43]. In Chapter 5, this architecture is referenced for the adaptive control augmentation of a missile autopilot.

The system dynamics of a MIMO system with unmatched nonlinear uncertainties can be modeled as follows:

$$\begin{aligned}\dot{x}(t) = A_m x(t) + B_m\big(\omega u(t) + f_1(x(t), z(t), t)\big)\\ + B_{um} f_2(x(t), z(t), t),\ \ x(0) = x_0\end{aligned} \tag{70}$$

$$z(t) = g_0(x_z(t), t)$$

$$\dot{x}_z(t) = g(x_z(t), x(t), t), \qquad x_z(0) = x_{z0}$$

$$y(t) = Cx(t)$$

where $x(t) \in \mathbb{R}^n$ is the measured system state vector, $u(t) \in \mathbb{R}^m$ is the control signal, $y(t) \in \mathbb{R}^m$ is the regulated output, A_m is a known, Hurwitz, $n \times n$ matrix that defines the desired dynamics for the closed loop system, $B_m \in \mathbb{R}^{n\times m}$ is a known constant matrix,(A_m, B_m) controllable, $B_{um} \in \mathbb{R}^{n\times(n-m)}$ is a constant matrix such that $B_m^T B_{um} = 0$ and $rank(B_m, B_{um}) = n$, $C \in \mathbb{R}^{n\times m}$ is a known full-rank constant matrix, (A_m, C) observable, ω is the system input gain matrix,$z(t)$ and $x_z(t)$ are the output and the state vector of the internal un-modeled dynamics $f_1(.), f_2(.), g_0(.)$ and $g(.)$ are unknown nonlinear functions. In this problem formulation $f_1(.)$ represents the matched part of the uncertainties, whereas the term $B_{um}\, f_2(.)$ represents the unmatched part of the uncertainty dynamics.

For the L1 adaptive controller architecture to be valid for this kind of system dynamics, the assumptions that the system in (70) should satisfy are listed below:

Assumption 1: The z dynamics are bounded input bounded output stable, i.e. there exist $L_{z1} > 0$ and $L_{z2} > 0$ such that for all $t \geq 0$

$$\|z_t\|_{\mathcal{L}_\infty} \leq L_{z1}\|x_t\|_{\mathcal{L}_\infty} + L_{z2}$$

Assumption 2: Let $X(t) \triangleq [x^T(t)\ z^T(t)\ ]^T$. For arbitrary $\delta > 0$, there exist positive $K_{1\delta}$, $K_{2\delta}$ and B_i such that

$\|f_i(X_1, t) - f_i(X_2, t)\| \leq K_\delta \|X_1(t) - X_2(t)\|_\infty$,

$|f_i(0, t)| \leq B_i \qquad i = 1,2$

For all $\|X_i(t)\|_\infty \leq \delta$, $i = 1,2$, uniformly in t.

Assumption 3: The system input gain matrix ω is assumed to be an unknown (non-singular) strictly row diagonally dominant matrix with $sgn(\omega_{ii})$ known. Also, it is assumed that there exists a known compact convex set Ω, such that $\omega \in \Omega \subset \mathbb{R}^{m\times m}$, and that a nominal system input gain $\omega_0 \in \Omega$ is known.

Assumption 4: The transmission zeros of the transfer matrix

$H_m(s) = C(s\mathrm{I} - A_m)^{-1}B_m$ lie on the open left half plane.

3.7.1 L1 Adaptive Controller Architecture

L1 adaptive controller for MIMO systems in the presence of unmatched nonlinear uncertainties consists of the following components [26]:

State Predictor:

$$\dot{\hat{x}}(t) = A_m\hat{x}(t) + B_m K_g r(t) + B_m\big(u_{ad}(t) + \hat{\sigma}_m(t)\big) + B_{um}\hat{\sigma}_{um}(t), \;\; \hat{x}(0) = x_0 \tag{71}$$

$$\hat{y}(t) = C\hat{x}(t)$$

where $\hat{\sigma}_m(t) \in \mathbb{R}^m$ and $\hat{\sigma}_{um}(t) \in \mathbb{R}^{n-m}$ are the adaptive estimates of the nonlinear functions defined in (70).

Adaptive Laws:

The adaptive parameters are calculated by the following piecewise constant adaptive law:

$\hat{\sigma}_m(t) = \hat{\sigma}_m(kT_s)$, $\hat{\sigma}_{um}(t) = \hat{\sigma}_{um}(kT_s)$, $t \in [kT_s, (k+1)T_s]$

$$\begin{bmatrix} \hat{\sigma}_m(kT_s) \\ \hat{\sigma}_{um}(kT_s) \end{bmatrix} = -[B_m \quad B_{um}]^{-1}\phi^{-1}(T_s)e^{A_m T_s}\tilde{x}(kT_s), k = 0,1,2,\ldots \tag{72}$$

where T_s is the sampling rate of the model, $\phi(T_s) = A_m^{-1}(e^{A_m T_s} - \mathrm{I})$ and $\tilde{x}(t) = \hat{x}(t) - x(t)$ is updated every T_s.

Control Law:

$$u_{ad} = -C_1(s)\hat{\sigma}_m(s) - C_2(s)H_1^{-1}(s)H_2(s)\hat{\sigma}_{um}(s) \tag{73}$$

where

$$H_1(s) = C(s\mathrm{I} - A_m)^{-1}B_m$$

$$H_2(s) = C(s\mathrm{I} - A_m)^{-1}B_{um}$$

$C_1(s)$ is a strictly proper stable transfer function and $C_2(s)$ is selected to ensure that $C_2(s)H_1^{-1}(s)H_2(s)$ is also proper and stable. Furthermore the transmission zeros of $H_1(s)$ sholuld lie on the open left half plane. $C_1(s)$ and $C_2(s)$ are filtering out the high frequencies from the adaptive control signal. Therefore they serve as a trade-off between robustness and performance. As the bandwidth of these filters is increased the performance of the adaptive controller will increase but the time delay margin will eventually decrease. On the other hand, if the bandwidth of the filters is decreased the robustness of the adaptive controller will increase with an increase in time delay, but the performance of the controller will eventually degrade.

The stability proof for this architecture is given in [26].

CHAPTER 4

ADAPTIVE CONTROL AUGMENTATION TO A LINEAR MISSILE LONGITUDINAL AUTOPILOT WITH NEURAL NETWORKS AND L1 ADAPTIVE CONTROL

In this chapter, adaptation characteristics of a neural network based adaptive control augmentation design, and L1 adaptive control augmentation design will be demonstrated on the same baseline linear autopilot of a missile in longitudinal axis. Firstly, the baseline linear autopilot design method will be explained. Model Reference Adaptive Control augmentation design of the baseline linear autopilot will be presented. Then, L1 adaptive control augmentation design of the same baseline linear autopilot will be explained. Finally linear simulation results of these two augmentation schemes will be presented.

4.1 Baseline Linear Autopilot Design: Robust Servomechanism Linear Quadratic Regulator with Projective Control

In this section, the elements of the baseline linear autopilot architecture used for the adaptive control augmentation are presented. The closed loop dynamics with the baseline autopilot will serve as the reference model in the adaptive model following augmentation design. Hence the formulation of closed loop baseline dynamics will be given in order to be used later in the adaptive augmentation design.

The aim of the baseline autopilot is to control the missile acceleration in longitudinal direction, i.e. a_z. The acceleration control is achieved by a cascade architecture, which allows for the control of the pitch rate, q , in the inner loop, and the normal acceleration,a_z in the outer loop. A block diagram of this architecture is given in Figure 10.

The inner loop design is performed by “Robust Servomechanism Linear Quadratic Regulator Methodology” with “Projective Control”.[41], [47].

Robust servomechanism linear quadratic regulator architecture employs an optimal full state feedback gain matrix. And an integral control action is added to the plant dynamics for zero steady state error.

Projective control is used to retain the dominant eigen-structure of a linear quadratic regulator with state feedback by using the states that are available for feedback. Namely, projective control transforms the full state feedback architecture into output feedback architecture by preserving the dominant performance and robustness characteristics of the full state feedback control.

These two methods, i.e. RSLQR and Projective Control forms a robust control architecture that uses the available outputs for feedback while providing a performance that approximates the performance of the full state feedback design.

After designing the inner loop, the outer loop gain is found by Root Locus method.

4.1.1 Inner Loop Design Method: Robust Servomechanism Linear Quadratic Regulator Design

An open-loop linear plant can be described as follows [41]:

$$\begin{cases} \dot{x}(t) = Ax(t) + Bu(t) + E\omega(t) \\ y(t) = Cx(t) + Du(t) + F\omega(t) \\ \qquad z(t) = Fy(t) \end{cases} \tag{74}$$

where $x(t) \in \mathbb{R}^n$ is the state vector, $u(t) \in \mathbb{R}^m$ is the control vector, $C = [I \quad 0]$, $y(t) \in \mathbb{R}^r$ is the output vector , $\omega(t)$ is an unmeasurable disturbance, $z(t) \in \mathbb{R}^t$ is the vector of controlled outputs, (A, B) controllable and (A, C) observable. The command input vector $r(t) \in \mathbb{R}^q$ has dimension less than the outputs, and it is assumed that k^{th} differential equation for $r(t)$ is known.

For the derivation of RSLQR, an error signal between the controlled outputs and the inputs is defined as follows:

$$e(t) = y_c(t) - r(t) \tag{75}$$

where $y_c(t)$ is a subset of the output vector $y(t)$. The output vector is divided into $y_c(t)$, i.e the controlled outputs and, $y_{nc}(t)$,i.e. the non-controlled outputs.

$$y(t) = \begin{bmatrix} y_c(t) \\ y_{nc}(t) \end{bmatrix} = \begin{bmatrix} C_c \\ C_{nc} \end{bmatrix} x(t) \tag{76}$$

The objective in RSLQR is to make the error $e(t) \to 0$ as $t \to \infty$, in the presence of unmeasurable disturbances ω.

In RSLQR methodology a new state vector is defined as follows:

$$z = \begin{bmatrix} e \\ \dot{e} \\ \vdots \\ e^{(k-1)} \\ \dot{x} \end{bmatrix} \tag{77}$$

Hence z dynamics becomes:

$$\dot{z} = \tilde{A}z + \tilde{B}\mu \tag{78}$$

where

$$\tilde{A} = \begin{bmatrix} 0 & I & \cdots & 0 & 0 \\ 0 & 0 & & 0 & 0 \\ \vdots & & \ddots & \vdots & \\ \alpha_k I & \alpha_{k-1} I & \cdots & \alpha_1 I & C_c \\ 0 & 0 & & 0 & A \end{bmatrix}, \quad \tilde{B} = \begin{bmatrix} 0 \\ 0 \\ \vdots \\ D_c \\ B \end{bmatrix} \tag{79}$$

$$\mu(t) = \frac{du(t)}{dt} \tag{80}$$

RSLQR is obtained by applying linear quadratic regulator theory to (78). By this formulation, q outputs in $y(t)$, i.e. $y_c(t)$, is forced to follow $r(t)$, while integral control action is applied to the error signal.

The performance index used to apply the LQR theory is as follows:

$$J = \int_0^\infty (z^T Q z + \mu^T R \mu) \tag{81}$$

By solving the Algebraic Ricatti Equation using Q and R, the optimal control $u(t)$ is found as follows:

$$u(t) = \int \mu(t)dt = -K_c \int z(t)dt = -K_i \int e(t)\,dt - K_x x(t) \tag{82}$$

The basic design steps of an LQR controller with full state feedback and integral action on error signal is given. A detailed derivation of RSLQR is given in [41]. To be able to use the formulation in (82), all of the states must be available for feedback. But usually this is not possible for the missile systems. Hence, in the next section a design methodology to employ output feedback is given.

4.1.2 RSLQR with Projective Control

For the system defined in (74), an LQR state feedback control can be written as follows:

$$u(t) = -R^{-1}B^T Sx(t) = -Kx(t) \tag{83}$$

$$A^T S + SA - SBR^{-1}B^T S + Q = 0 \tag{84}$$

where $Q \geq 0$, $R > 0$, and the pair $(A, Q^{1/2})$ observable and S is the solution of(84). Substituting (83) into (74), the closed loop system can be described by:

$$\dot{x}(t) = (A - BRBS)x(t) = (A - BK)x(t) \tag{85}$$

If the number of available outputs for feedback is r, ($y \in \mathbb{R}^r$), Projective Control Theory states that, r eigenvalues (λ_r) and their associated eigenvectors (V_r) can be retained by applying the following transformation on the full state feedback gain matrix K:

$$K_{proj} = KV_r(CV_r)^{-1} \tag{86}$$

where

$$\left(A - BK_{proj}C\right)V_r = V_r\lambda_r, \quad V_r \in \mathbb{R}^{n\times r} \tag{87}$$

Now that the full state feedback gains are transformed into output feedback gains which contain the dominant performance and robustness properties of the full state feedback design. Similarly, projective control can be applied to the robust servomechanism linear quadratic regulator control signal given in (82).

If the number of states available for feedback or the resulting output feedback design is not adequate to retain the desired performance and robustness properties, then a dynamic observer can be designed. However, for the missile under consideration, the states available for feedback were adequate to obtain the desired performance and robustness characteristics according to (86). Hence, dynamic observer design will not be dealt within the scope of this section.

4.1.3 Baseline Closed Loop Dynamics

In order to be used in the adaptive augmentation design, the closed loop dynamics of the baseline autopilot will be presented.

The plant dynamics can be written as follows:

$$\begin{cases} \dot{x}_p = A_p x_p + B_p u \\ y = C_p x_p + D_p u \\ z_p = F y \end{cases} \tag{88}$$

where x_p is the plant state dynamics, u is the input signal, y is the sensor measurements, and z_p is the subset of plant outputs that are to be controlled.

The controller dynamics of the cascaded inner and outer loop can be written as follows:

$$\begin{cases} \dot{x}_c = A_c x_c + B_{1c}^z z_c + B_{2c}^z z_p \\ u = C_c x_c + D_{1c}^z z_c + D_{2c}^z z_p \end{cases} \tag{89}$$

where x_c is the controller state vector, z_c is the outer loop commands and z_p is the system controlled output.

Substituting the open loop plant dynamics into controller dynamics, and solving for the control signal u, the following expression is obtained for the nominal controller:

$$u = \left(I - D_{2c}^{z} F D_p\right)^{-1} \left(C_c x_c + D_{1c}^{z} z_c + D_{2c}^{z} F C_p x_p\right) \tag{90}$$

The extended system dynamics containing both the controller and plant dynamics is given by:

$$\begin{gathered}
\begin{pmatrix} \dot{x}_p \\ \dot{x}_c \end{pmatrix} = \underbrace{\begin{pmatrix} A_p & 0 \\ B_{2c}^{z} F C_p & A_c \end{pmatrix}}_{A} \underbrace{\begin{pmatrix} x_p \\ x_c \end{pmatrix}}_{x} + \underbrace{\begin{pmatrix} B_p \\ B_{2c}^{z} F D_p \end{pmatrix}}_{B_1} u + \underbrace{\begin{pmatrix} 0 \\ B_{1c}^{z} z_c \end{pmatrix}}_{B_2} z_c \\
y = \underbrace{\begin{pmatrix} C_p & 0 \end{pmatrix}}_{C} x + D_p u \\
u = K_x^T x + K_z^T z_c
\end{gathered} \tag{91}$$

Hence the closed loop reference dynamics can be represented as follows:

$$\begin{gathered}
x = \underbrace{\left(A + B_1 K_x^T\right)}_{A_{ref}} x + \underbrace{\left(B_1 K_z^T + B_2\right)}_{B_{ref}} z_c \\
y = \underbrace{\left(C + D_p K_x^T\right)}_{C_{ref}} x + \underbrace{D_p K_z^T}_{D_{ref}} z_c
\end{gathered} \tag{92}$$

4.2 Neural Network Augmentation Design of Baseline Linear Autopilot

The adaptive augmentation scheme used to augment the baseline autopilot designed in the previous section is a direct model-reference adaptive control architecture given in [47]. In the baseline architecture the actuator dynamics is removed and system matched uncertainties are introduced to the baseline architecture. The resulting open loop system can be interpreted as:

$$\dot{x} = Ax + B_1\Lambda\left(u + \kappa(x_p)\right) + B_2 z_c \tag{93}$$

Here Λ is a diagonal matrix that models the uncertainties in control effectiveness or control surface failure, and $\kappa(x_p)$ is a function, which can be nonlinear, that models the system matched uncertainties. If the uncertainties are omitted, i.e. if $\Lambda = \mathrm{I}$, and $\kappa(x_p) = 0$, (93) coincides with the reference model.

The aim of the adaptive augmentation is to cancel the effects of the uncertainties Λ and $\kappa(x_p)$ by making proper augmentations to the control signal u, and restore the reference dynamics performance in the presence of these uncertainties.

4.2.1 Adaptive Control Input, Function Approximation and Update Law

The adaptive control input is formulated as follows:

$$u = u_{bl} + u_{ad} = K_x^T x + K_z^T z_c + \hat{k}_x^T x + \hat{k}_z^T z_c - \hat{\kappa}(x_p) \tag{94}$$

Here $\hat{k}_x^T$ are the incremental feedback gains, $\hat{k}_z^T$ are the incremental feedforward gains, and $\hat{\kappa}(x_p)$ is the online approximation of the matched system uncertainties. A multilayer Neural Network (NN) is used for the approximation of $\hat{\kappa}(x_p)$. The neural network structure used in this study is a feedforward neural network that uses Radial Basis Functions (RBF) in its hidden inner layer which is formulated as follows:

$$K(x_p) = \Theta^{\mathrm{T}}\phi(\mathrm{x_p}) + \varepsilon_0(\mathrm{x_p}) \tag{95}$$

Here Θ is the ideal outer layer NN weights matrix, $\phi(x_p)$ is the radial basis function vector, $\varepsilon_0(x_p)$ is the approximation tolerance. For a sufficient number of RBF neurons, there exits an ideal Θ matrix that allows $K(x_p)$ to be approximated within the tolerance $\varepsilon_0(x_p)$. [49]

Since the ideal weights matrix,Θ, is not known an estimation of this matrix, $\widehat{\Theta}$ will be used. The function approximation for $K(x_p)$ becomes:

$$\widehat{K}(x_p) = \widehat{\Theta}^T \phi(x_p) \tag{96}$$

Similarly the incremental feedback and feedforward gains are not known. The update law used for the estimation of the unknown parameters is as follows:

$$\dot{\hat{k}}_x = \Gamma_x \mathrm{Proj}(\hat{k}_x, -x e^T P B_1) \tag{97}$$

$$\dot{\hat{k}}_z = \Gamma_z \mathrm{Proj}(\hat{k}_z, -z_c e^T P B_1) \tag{98}$$

$$\dot{\widehat{\Theta}} = \Gamma_\Theta \mathrm{Proj}(\widehat{\Theta}, \phi(x_p) e^T P B_1) \tag{99}$$

In (3)-(4) Γ_x, Γ_z, Γ_Θ are the positive definite adaptation rate matrices, $e = x - x_{ref}$ is the error between the states of the closed loop dynamics and reference dynamics. P is the positive definite solution of the algebraic Lyapunov equation:

$$PA_{ref} + A_{ref}^{T}P = -Q \tag{100}$$

Q is symmetric positive definite matrix. $Proj(.,.)$ is the “Projection Operator” which is a mathematical operator used to keep the adaptive parameters bounded [46]. The projection operator is explained in detail in Appendix B. The baseline controller is designed with the nominal plant information. Hence, as long as the uncertainties in the missile model are small, and the error dynamics is kept small, there is no need for the adaptive elements to augment the control signal of the baseline controller. Moreover the adaptive elements may produce unwanted augmentation signal due to noise in the signals. Therefore in order to prevent the adaptive elements to make unnecessary and undesired augmentation “Dead-Zone Modification” is used. Dead-zone modification is simply to freeze the adaptation process when the magnitude of tracking error is less than a pre-specified value.

4.3 L1 Adaptive Augmentation of Baseline Linear Autopilot

In order to augment the baseline linear controller with L1 adaptive control, the L1 adaptive controller formulation explained in Chapter 3, Section 3.6 will be used. The aim is to formulate an adaptive control signal, which will be added to the baseline control signal, that can be calculated by the formulation given in (67).

This section presents the design steps to convert the stand alone L1 adaptive controller into an adaptive augmentation element to the baseline autopilot given in Section 4.1. The method given in [48] is adopted for the adaptive augmentation design of the particular baseline autopilot used in this study.

Consider the SISO plant dynamics:

$$\begin{gathered} \dot{x}(t) = Ax(t) + b\big(\omega u(t) + \theta(t)^{T}x(t) + \sigma(t)\big) \\ y(t) = c^{T}x(t) \end{gathered} \tag{101}$$

where $x \in \mathbb{R}^n$ is the state vector, $u \in \mathbb{R}$ is the control input, $y \in \mathbb{R}$ is the output vector. The states are assumed to be available for feedback. A is a known $n \times n$ matrix which represents the plant dynamics. ω models the unknown input gain, $\theta(t)$ is a vector of time varying unknown parameters and $\sigma(t)$ models the unknown disturbances in the missile dynamics.

When the uncertainties and disturbances are omitted, i.e. $\omega = 1$, $\theta = 0$, $\sigma = 0$ the baseline closed loop system is obtained by applying the baseline control signal $u_{bl}(t)$ as follows:

$$\dot{x}(t) = Ax(t) + bu_{bl}(t) \tag{102}$$

The aim of the adaptive augmentation is to produce the control signal that will make the system converge to baseline closed loop dynamics, the ideal controller for (101) can be written as:

$$u(t) = \frac{1}{\omega}(u_{bl}(t) - \theta(t)^T x(t) - \sigma(t)) \tag{103}$$

Subtracting the baseline control signal $u_{bl}(t)$ from $u(t)$, the portion of the ideal control signal that should be produced by the adaptive augmentation can be calculated as follows:

$$u_{ad,ideal}(t) = \frac{1}{\omega}((1 - \omega)u_{bl}(t) - \theta(t)^T x(t) - \sigma(t)) \tag{104}$$

Hence

$$u(t) = u_{bl}(t) + u_{ad,ideal}(t) \tag{105}$$

The next step in the augmentation design is to split the baseline control signal as follows:

$$u_{bl}(t) = \bar{u}_{bl}(t) - Kx(t) \tag{106}$$

K can be selected to make $A - bK$ has poles close to the baseline closed loop dynamics.

Substituting (105) and (106) into (101), and making the necessary modifications to be able to use L1 adaptive controller formulation, the system dynamics becomes:

$$\begin{aligned}\dot{x}(t) = Ax(t) + b(\omega \left(\bar{u}_{bl}(t) - Kx(t) + u_{ad,ideal}(t)\right) \\ \mp \bar{u}_{bl}(t) \mp Kx(t) + \theta(t)^T x(t) \\ + \sigma(t)\end{aligned} \tag{107}$$

(107) can be written as :

$$\begin{aligned}\dot{x}(t) = A_{ref}x(t) + b\bar{u}_{bl}(t) + b(\omega u_{ad,ideal}(t) + \bar{\theta}(t)^T x(t) \\ + \bar{\sigma}(t))\end{aligned} \tag{108}$$

where

$$A_{ref} = A - bK$$

$$\bar{\theta}(t) = \theta(t) + (1-\omega)K^T$$

$$\bar{\sigma}(t) = \sigma(t) + (\omega - 1)\bar{u}_{bl}(t)$$

The system dynamics and the control signal for which the L1 adaptive control design formulation given in Chapter 3, Section 3.6 is rewritten here to setup the analogy:

$$\begin{aligned} \dot{x}(t) &= A_{ref}x(t) + b(\omega u_{ad}(t) + \theta(t)^T x(t) + \sigma(t)) \\ y(t) &= c^T x(t) \end{aligned} \tag{109}$$

$$u(t) = kD(p)(k_g r(t) - \hat{\omega}(t)u(t) - \hat{\theta}(t)^T x(t) - \hat{\sigma}(t)) \tag{110}$$

The system given in (108) has the same system structure with the system given in (109) , except for the term $b\bar{u}_{bl}(t)$. This term can be regarded as doing the effect of $k_g r$ in (110) and the effect of this term can be compensated by defining the adaptive control signal augmentation term as follows:

$$u_{ad}(t) = -kD(p)(\hat{\omega}u_{ad}(t) + \hat{\theta}(t)^T x(t) + \hat{\sigma}(t) \tag{111}$$

Hence the adaptive control signal that can be used to augment a baseline linear controller is derived to be used in the missile longitudinal autopilot design.

4.4 Application to Missile Longitudinal Autopilot

In this section, the application of the baseline autopilot design method described in Section 4.1 to a missile longitudinal autopilot is presented. Then, application of the adaptive augmentation designs presented in Section 4.2 and 4.3 to the baseline missile autopilot is explained. The baseline autopilot design is performed with the nominal data of the missile at a single point in the flight envelope. The performance of the baseline controller and the effect of the adaptive augmentation designs is demonstrated with linear simulations. Aerodynamic model uncertainties are introduced to the simulation model. The performance of the two adaptive augmentation schemes is compared.

4.4.1 Baseline Autopilot Design

Baseline autopilot architecture is given in Figure 10.[44]

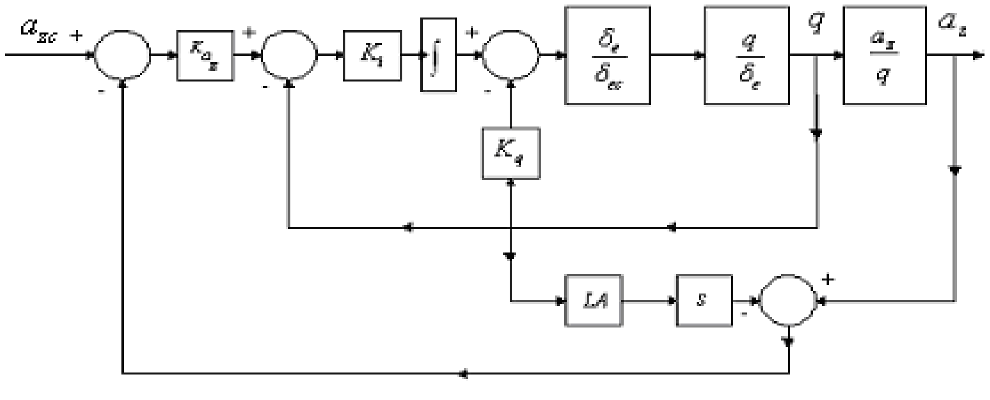

Figure 10 Baseline RSLQR Autopilot Architecture

Pitch rate is controlled in the inner loop of this architecture. Robust servomechanism linear quadratic regulator combined with projective control is used to design the inner loop. The outer acceleration loop is designed with Root Locus method. In the outer feedback loop pitch rate is combined with normal acceleration to obtain the normal acceleration at center of percussion. This treatment changes the zeros of the acceleration transfer function and improves the stability margins. A detailed information about this treatment is given in [44]. LA gain in Figure 10 stands for the lever arm between the center of gravity and IMU location. $LA = 0.5$ is used for the missile under consideration.

4.4.1.1 Inner Loop Design

The baseline missile autopilot design is performed with the aerodynamic data of the missile at a single flight condition of $Mach = 0.9$, $\alpha = 0\ deg$, $h = 5000m$.

The linearized missile dynamic equations in the longitudinal channel are used for the design:

$$\dot{\alpha} = Z_{\alpha}\alpha + Z_{\delta_e}\delta_e + q \tag{112}$$

$$\dot{q} = M_{\alpha}\alpha + M_q q + M_{\delta_e}\delta_e \tag{113}$$

The control actuator system of the missile is modeled with a second order transfer function having a natural frequency of $\omega n_{CAS} = 75\ rad/s$, and damping of $\xi = 0.707$ as follows:

$$\frac{\delta_e}{\delta_{ec}} = \frac{(\omega_{n_{CAS}})^2}{s^2 + 2\xi\omega_{n_{CAS}}s + (\omega_{n_{CAS}})^2} \tag{114}$$

The state vector used in RSLQR design is:

$$x = \left[\int e_q dt \quad \alpha \quad q \quad \delta_e \quad \dot{\delta}_e \right] \tag{115}$$

where $e_q = q_c - q$.

The performance index used in the LQR state feedback design is:

$$J = \int_0^\infty (q_i (\int e_q dt)^2 + u^T u) \tag{116}$$

Here, q_i is selected to be the only design parameter to be adjusted for the performance and robustness requirements.

The stability, performance and robustness criteria for the selection of q_i is to make the closed loop system stable, satisfy a minimum of 0.2 seconds for 63% risetime, satisfy a maximum of 300 deg/s $\dot{\delta}_e$ for 1 radians of pitch rate command, and satisfy a minimum of 6 dB gain margin, 30 deg phase margin for the open loop transfer function.

q_i, satisfying these criterias is selected and the corresponding full state feedback gains are calculated. For the missile under consideration, the pitch rate q and the pitch acceleration a_z are the measured variables. Hence in (115), 2 of the 5 state variables, q and $\int e_q dt$, are available for feedback. Using projective control, and selecting the 2 most dominant poles to be retained the inner loop design is completed. for the design condition the gains are found as $K_q = -0.1837$, and $K_i = 1.235$.

4.4.1.2 Outer Loop Design

The outer loop gain is designed by the well known Root Locus method. For the design condition $K_{az} = -0.0187$ gives a desired step response and provides a gain margin greater than 6 dB, and a phase margin of 30 deg.

4.4.2 MRAC Adaptive Augmentation

The longitudinal dynamics of the missile will be modeled according to (93) for the NN augmentation design:

$$\begin{pmatrix} \dot{\alpha} \\ \dot{q} \\ \dot{q}_i \end{pmatrix} = A \begin{pmatrix} \alpha \\ q \\ q_i \end{pmatrix} + B_1 \Lambda\big(\delta_e + \kappa(\alpha, q)\big) + B_2 \begin{pmatrix} a_{zc} \\ q_c \end{pmatrix} \tag{117}$$

The control signal with the adaptive augmentation becomes:

$$\begin{aligned} \delta_e = \delta_e)_{bl} + \delta_e)_{ad} \\ &= K_i q_i - K_q q + \hat{k}_\alpha \alpha + \hat{k}_q q + \hat{k}_i q_i \\ &- \kappa(\alpha, q) \end{aligned} \tag{118}$$

where $\kappa(\alpha, q) = \widehat{\Theta}^{\mathrm{T}} \phi(\alpha, q)$.

The adaptive elements in (118), $\hat{k}_x$ and $\widehat{\Theta}$ are calculated by the adaptation laws given in (97) and (99). No feedforward gains are used, hence $\hat{k}_z = 0$.

$$\begin{pmatrix} \dot{\hat{k}}_\alpha \\ \dot{\hat{k}}_q \\ \dot{\hat{k}}_i \end{pmatrix} = \Gamma_x Proj\left(\begin{pmatrix} \hat{k}_\alpha \\ \hat{k}_q \\ \hat{k}_{q_i} \end{pmatrix}, -\begin{pmatrix} \alpha \\ q \\ q_i \end{pmatrix}(\alpha - \alpha_{ref} \quad q - q_{ref} \quad q_i - q_{iref})P\begin{pmatrix} \frac{Z_{\delta_e}}{V} \\ M_{\delta_e} \\ 0 \end{pmatrix}\right) \tag{119}$$

$$\dot{\widehat{\Theta}} = \Gamma_\Theta Proj\left(\widehat{\Theta}, \phi(\alpha, q)(\alpha - \alpha_{ref} \quad q - q_{ref} \quad q_i - q_{iref})P\begin{pmatrix} \frac{Z_{\delta_e}}{V} \\ M_{\delta_e} \\ 0 \end{pmatrix}\right) \tag{120}$$

The design parameters to be determined for the simulations are the adaptation rates Γ_x, Γ_Θ and the positive definite symmetric matrix Q. For the simulations $Q = I_{3\times3}$ is used, and the adaptive parameters are determined by trial and error as:

$$\Gamma_x = 100 I_{3\times3}$$

$$\Gamma_\Theta = [0.001 \quad 0.002 \quad 0.003 \quad 0.004 \quad 0.005]\, I_{5\times5}$$

4.4.3 L1 Adaptive Control Augmentation

The longitudinal missile dynamics will be modeled according to (101) for L1 adaptive augmentation design.

$$\begin{pmatrix}\dot{\alpha}\\ \dot{q}\end{pmatrix} = A\begin{pmatrix}\alpha\\ q\end{pmatrix} + b\big(\omega\delta_e + \theta(t)^T x(t) + \sigma(t)\big) \tag{121}$$

$$y(t) = c^T x(t)$$

where

$$\begin{aligned}\delta_e &= \delta_e)_{bl} + \delta_e)_{ad}\\ &= K_i q_i - K_q q - \frac{kD(p)(\hat{\theta}(t)^T x(t) + \hat{\sigma}(t))}{(1 + kD(p)\widehat{\omega})}\end{aligned} \tag{122}$$

For the adaptive augmentation design, the baseline controller is divided into two portions

$$\delta_e)_{bl} = \overline{\delta_e)}_{bl} - Kx(t)$$

The reference closed loop dynamics for the baseline autopilot architecture presented in Figure 10 can be derived and adopted to the system definitions in Section 4.3 as follows:

$$\begin{pmatrix}\dot{\alpha}\\ \dot{q}\end{pmatrix} = A\begin{pmatrix}\alpha\\ q\end{pmatrix} + b\delta_e)_{bl} \tag{123}$$

$$\delta_e)_{bl} = K_i q_i - K_q q \tag{124}$$

For the given control architecture q_i can be written as follows:

$$q_i = \int K_{az}\big(a_{zc} - (a_z - \dot{q}LA)\big) - q \;\; dt \tag{125}$$

a_z should be replaced with its definition formed by the state variables α and q.

$$a_z = U_0(\dot{\alpha} - q) \tag{126}$$

where U_0 is the freestream velocity.

Substituting (126) into (125) and taking the Laplace transform of this new q_i equation, the baseline control input takes the following form:

$$\begin{aligned} \delta_e)_{bl} = {} & \underbrace{\left[-K_{az}K_iU_0 \quad K_{az}\frac{K_i}{s}(U_0 + LAs) - \frac{K_i}{s} - K_q\right]}_{K_1}\begin{bmatrix}\alpha \\ q\end{bmatrix} \\ & + \underbrace{K_{az}\frac{K_i}{s}}_{K_2}a_{zc} \end{aligned} \tag{127}$$

Substituting (127) into (123) the closed loop system equation for the baseline controller takes the form

$$\begin{pmatrix} \dot{\alpha} \\ \dot{q} \end{pmatrix} = (A + bK_1) \begin{pmatrix} \alpha \\ q \end{pmatrix} + K_2 a_{zc} \tag{128}$$

The output y can be written as:

$$y = [U_0 s \quad -1] \begin{pmatrix} \alpha \\ q \end{pmatrix} \tag{129}$$

In order to select the feedback vector K, the closed loop eigenvalues of the system given in (128) and (129) should be found. These eigen-values are found as:

$$\lambda_{1,2,3,4} = [0 \quad -5.3828 + 8.4463\mathrm{i} \quad -5.3828 - 8.4463\mathrm{i} \quad -4.8369]$$

for the missile model at the given design condition.

The feedback vector K can be selected, in order $A - bK$ to have poles at the same locations with the baseline closed loop dynamics. The baseline closed loop characteristics is dominated by the poles at $\lambda_1 = -4.8369$ and $\lambda_{2,3} = -5.3828 \mp 8.4463\mathrm{i}$. In this application, K is designed to have a reference dynamics which has two poles at $\lambda_{1,2} = -4.8369$. By this selection, the effects of the complex eigenvalues are disregarded and a reference dynamics which has better performance characteristics than the reference baseline closed is preferred. Pole placement is done using Ackermann's method and the following feedback vector is obtained at the design point $K = [-0.3149 \quad 0.1024]$.For this application $k = 35$ and $D(s) = \frac{1}{s}$ is selected which forms a low pass filter of $C(s) = \frac{35}{s+35}$ for the adaptive control signal. A bandwidth of 35 rad/s is selected for the low pass filter in order not to interfere with and be realizable by the control actuation system bandwidth which has a bandwidth of 75 rad/s.

Adaptation gains are selected as $\Gamma_{\theta} = \begin{bmatrix} 10 & 0 \\ 0 & 10 \end{bmatrix}$ and $\Gamma_{\omega} = \Gamma_{\sigma} = 10$. These gains are determined by trial and error.

4.5 Simulation Results

In this section, the acceleration tracking performance of the missile longitudinal autopilot with and without adaptive augmentation designs is presented. The simulations are performed using the linearized models of the missile at specified flight conditions. For a given commanded acceleration signal, the performance of the autopilots with nominal and perturbed aerodynamic data cases will be presented.

4.5.1 Input Data

A pulse type normal acceleration input is used for the simulations. The input signal has an amplitude of $10\ m/s^2$ and a period of 5 seconds. Both the Model Reference Adaptive Control augmentation and L1 adaptive augmentation designs are performed by using the baseline closed loop dynamics as their reference dynamics. Hence the adaptive augmentation autopilots are desired to retain the tracking performance of baseline autopilot to the given input signal. In Figure 12-Figure 20 the tracking performance of these autopilots are presented.

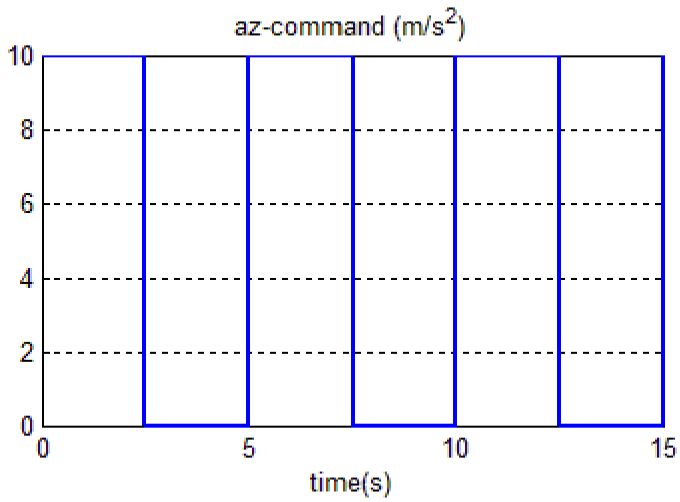

Figure 11 Variation of Normal acceleration Command

The control effectiveness of the missile is decreased by 75 %, and the stability derivative and damping derivative are multiplied by zero. Hence the open loop system is made marginally stable.

The baseline controller becomes unstable and loses control in front of these severe uncertainties given to the aerodynamic coefficients of the missile. These perturbations in the aerodynamic coefficients cause highly nonlinear effects on the response of the missile. Under these circumstances, the performance of the adaptive control augmentation schemes is tested. Below, the simulation results are given for direct MRAC and L1 adaptive control augmentations.

4.5.2 Simulation Results for Direct MRAC Augmented Design

In Figure 12-Figure 16 the response of the pitch acceleration autopilot to the input signal given in Figure 11 is presented. The autopilot is designed with RSLQR and augmented with direct MRAC.

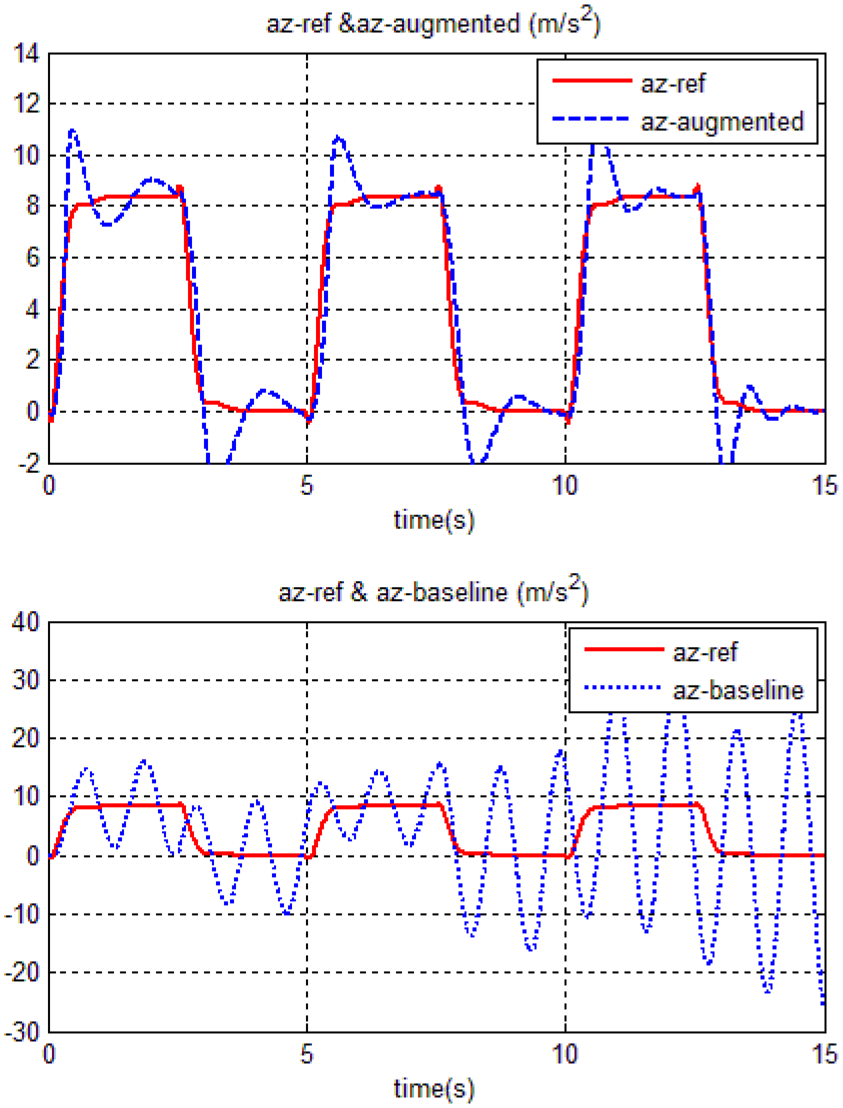

Figure 12 Variation of Normal Acceleration for MRAC Adaptive Augmentation

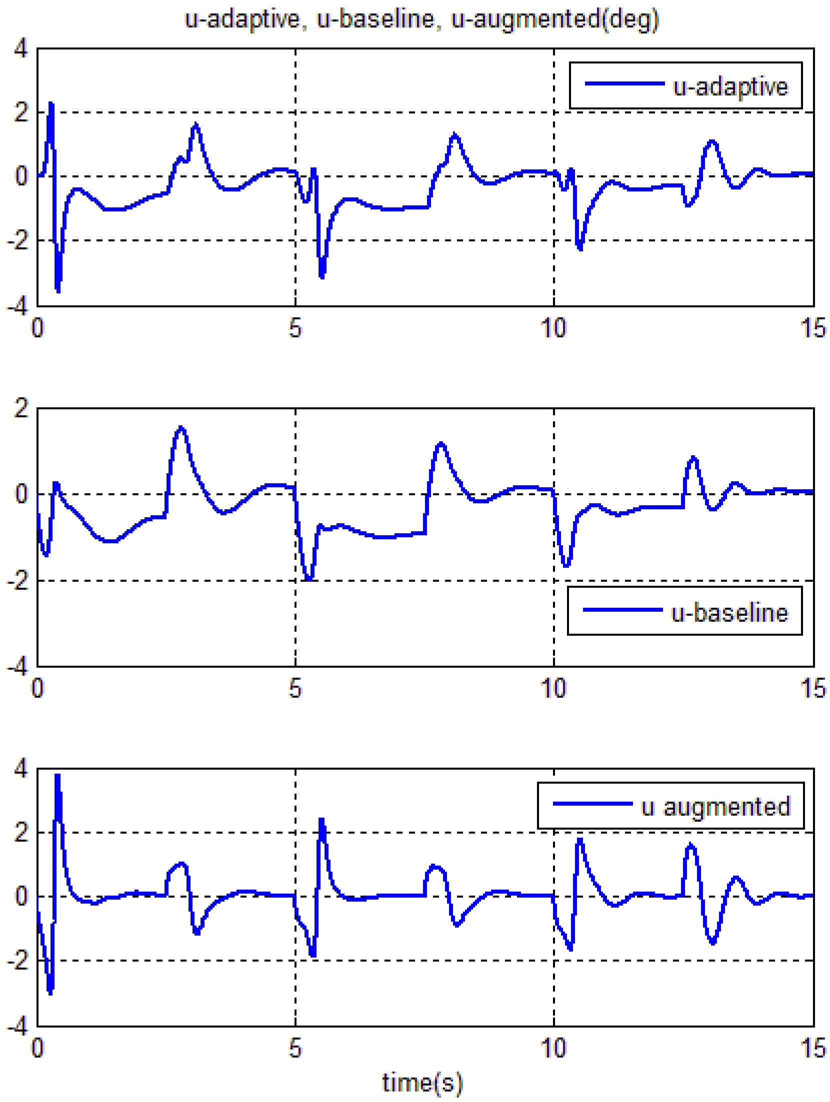

Figure 13 Variation of Control Signals for MRAC Augmentation

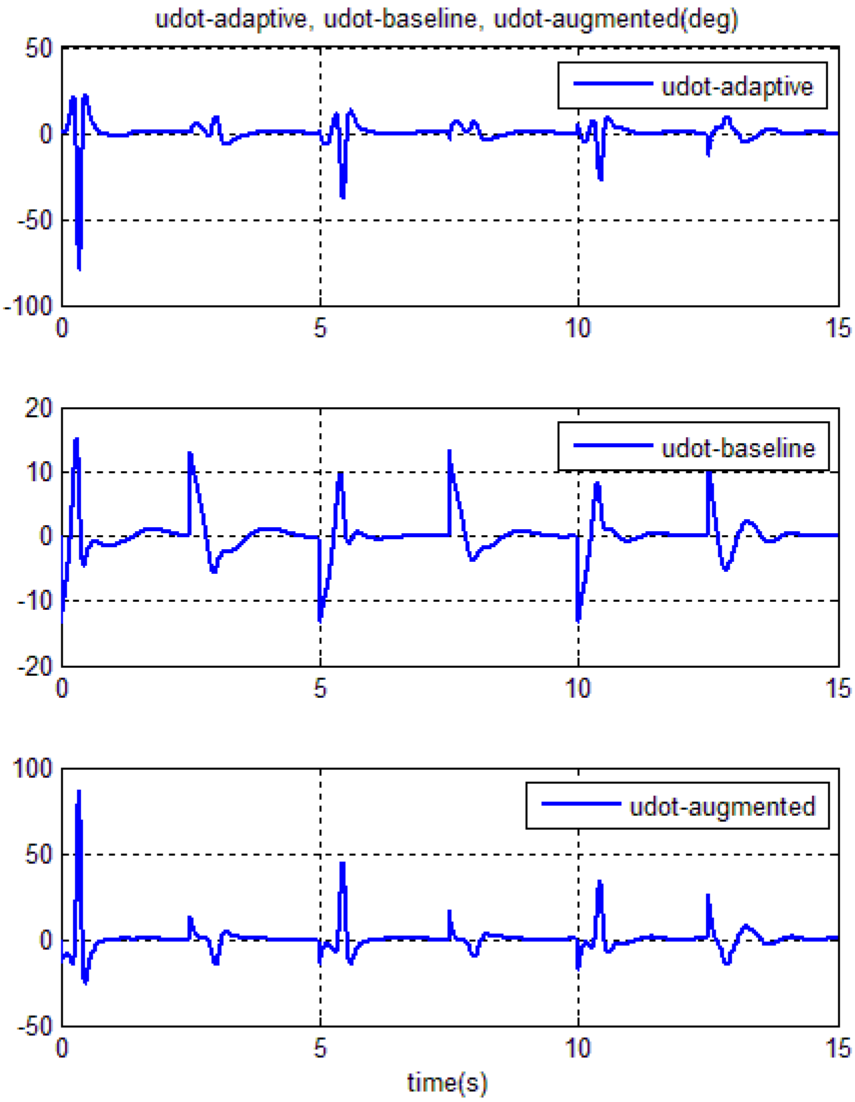

Figure 14 Variation of Control Signal Rates for MRAC Augmentation

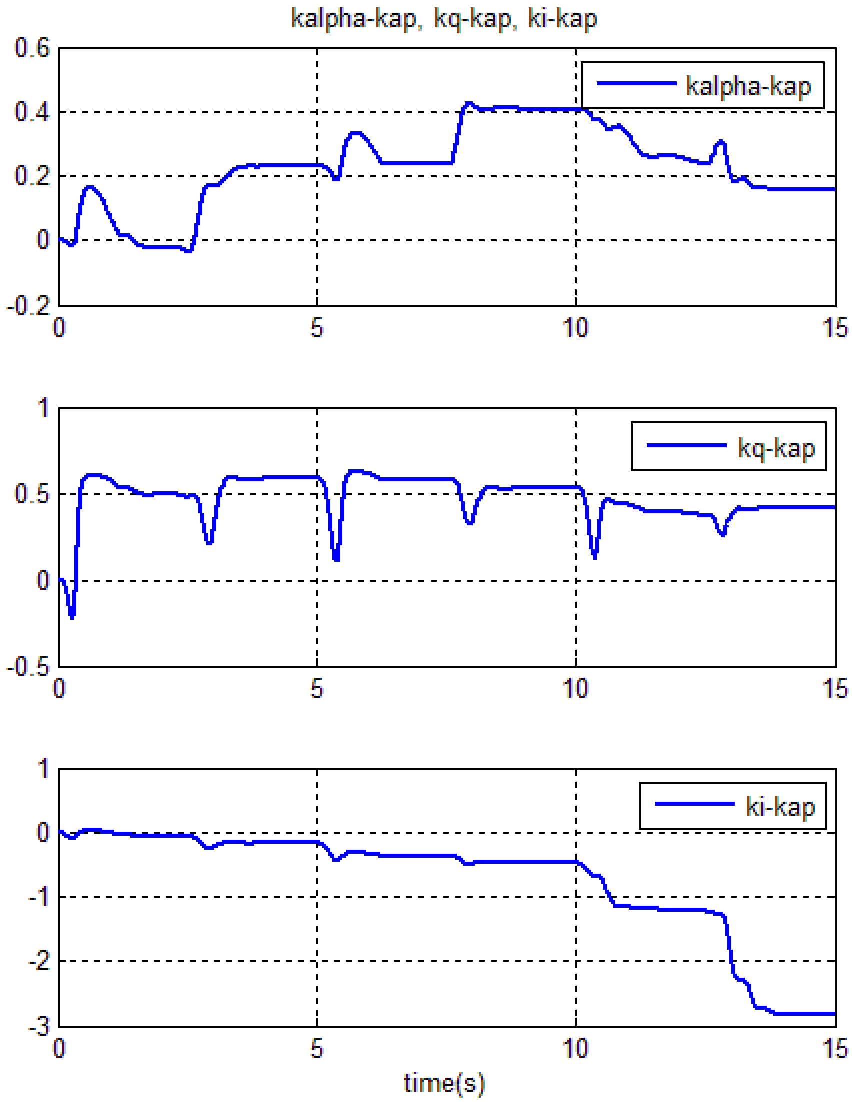

Figure 15 Variation of Incremental Adaptive Feedback Gains for MRAC Augmentation

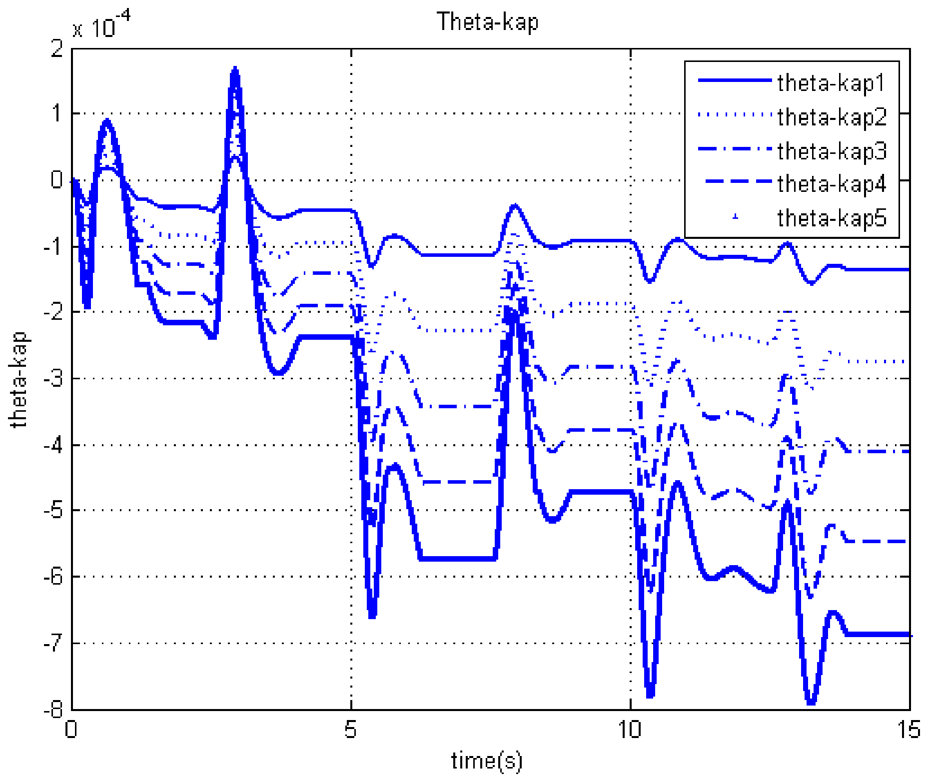

Figure 16 Variation of Adaptive Parameters for MRAC Augmentation

4.5.3 Simulation Results for L1 Augmented Design

In Figure 17-Figure 20 the response of the pitch acceleration autopilot to the input signal given in Figure 11 is presented. The autopilot is designed with RSLQR and augmented with L1 Adaptive Control.

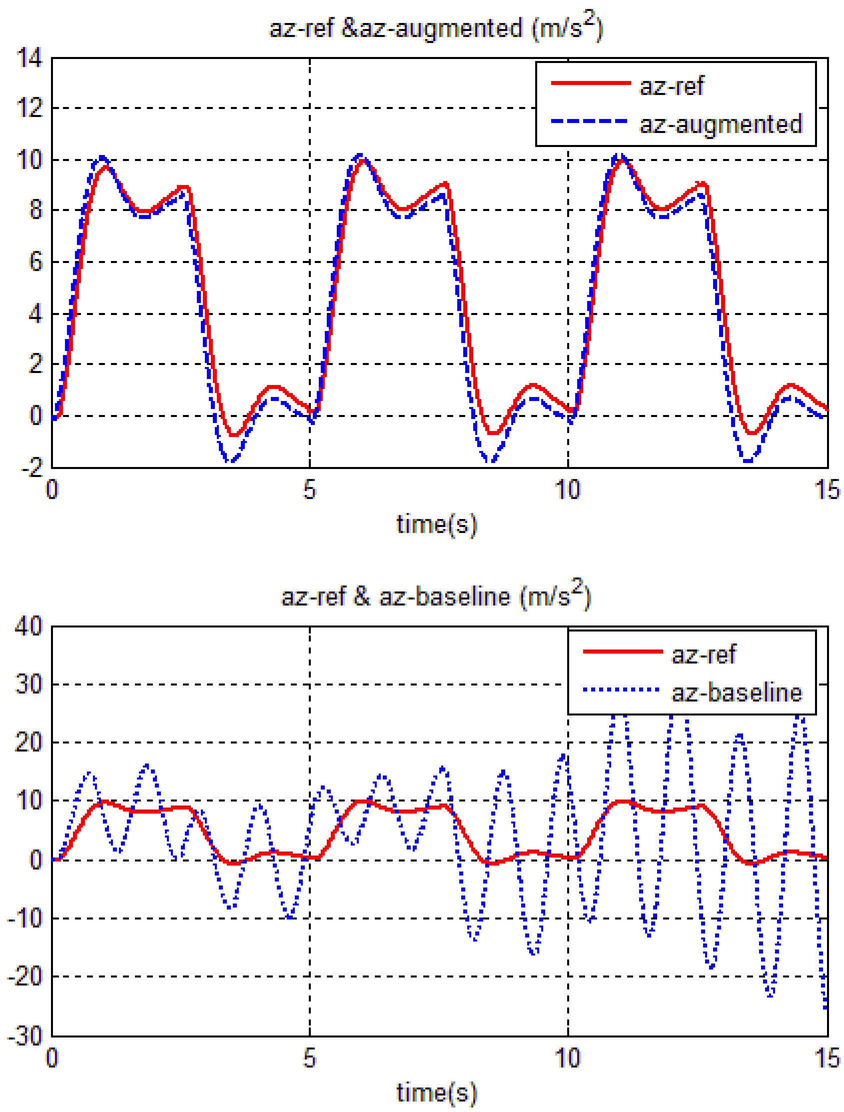

Figure 17 Variation of Normal Acceleration for L1 Adaptive Augmentation

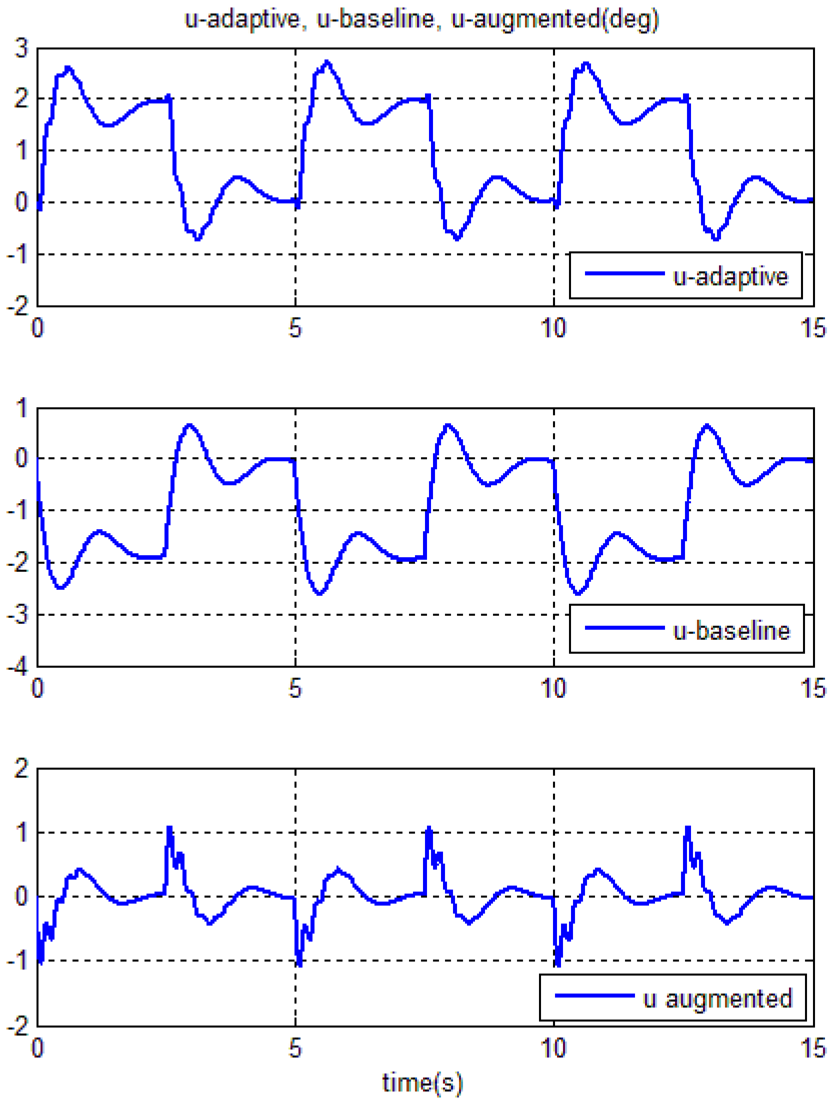

Figure 18 Variation of Control Signals for L1 Adaptive Augmentation

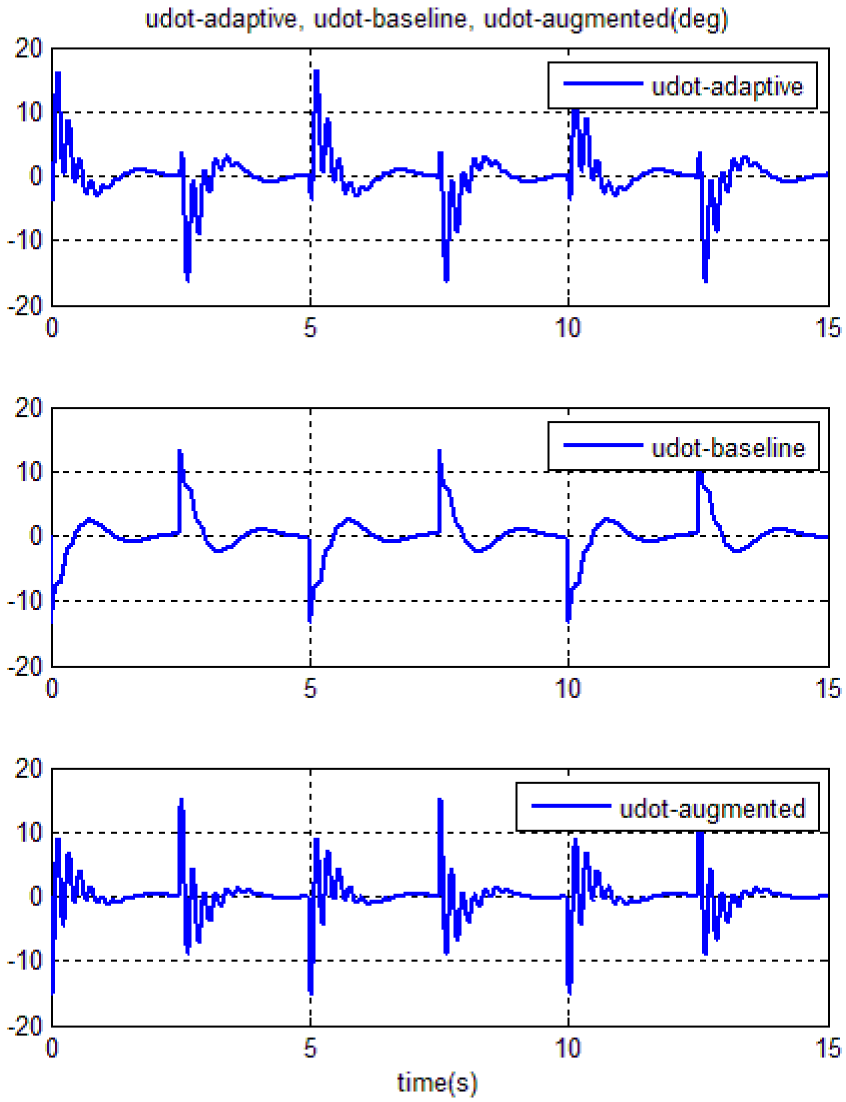

Figure 19 Variation of Control Signal Rates for L1 Adaptive Augmentation

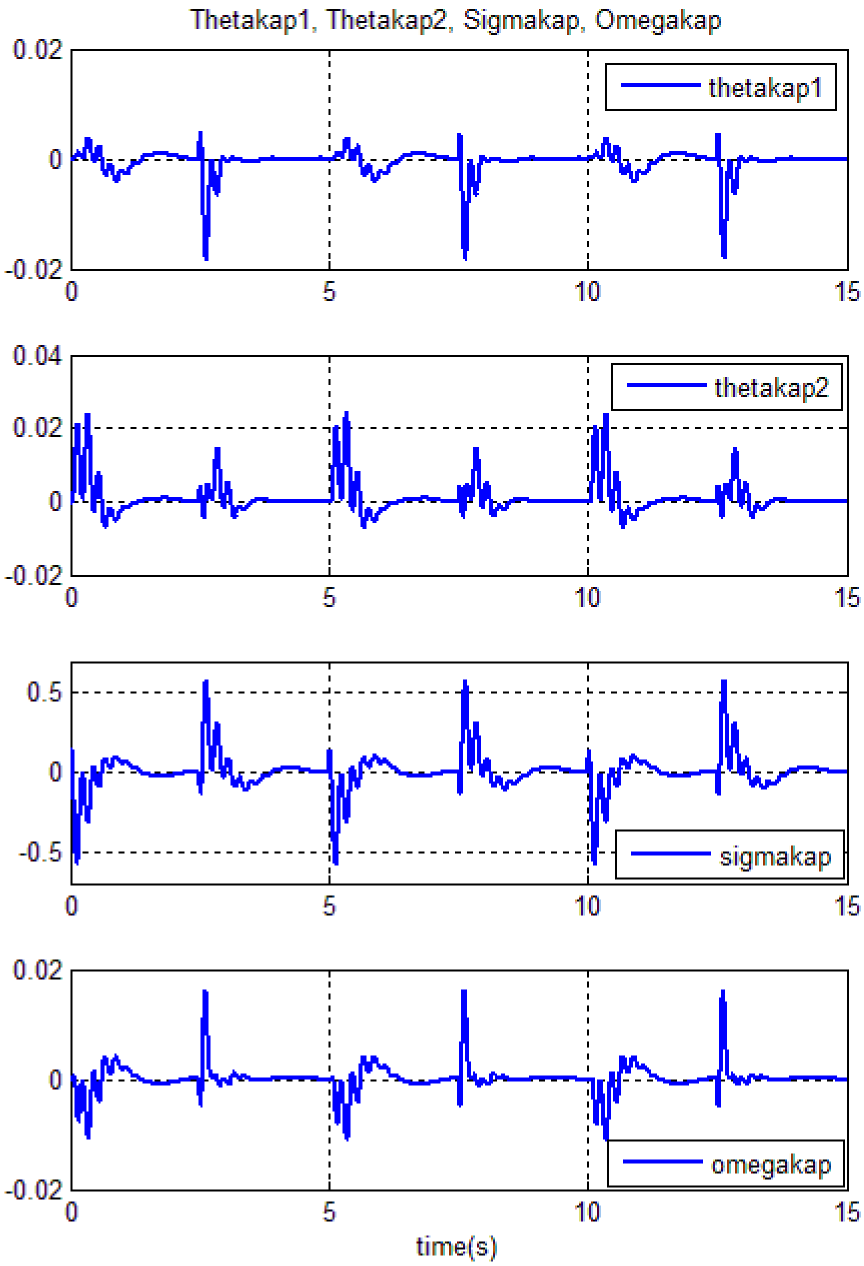

Figure 20 Variation of Adaptive Parameters for L1 Adaptive Augmentation

4.6 Remarks on Simulation Results

Simulation results show that, for the given uncertainties on the plant model, the baseline autopilot loses stability and control. On the other hand, both of the adaptive augmentations are successful in stabilizing the missile and satisfy a good tracking performance in front of severe perturbations in the missile model.

For the MRAC design closed loop dynamics with the baseline autopilots serves as the reference dynamics for the adaptive augmentation. It is seen from the simulation results with MRAC that the missile acceleration successfully tracks the reference dynamics acceleration. The overshoots in the transients are caused by the tuning of the adaptation rates. Fast adaptation can be obtained by increasing the adaptation rates, however the transient response characteristics of MRAC adaptive augmentation degrades as the adaptation rate is increased. MRAC adaptive control has well defined asymptotic stability proof. However there are no well defined guidelines for the transient behaviour of this adaptation scheme. Hence a trial and error methodology is followed for tuning the design parameters of this scheme.

For L1 Adaptive Augmentation design, it is seen in Figure 17 that, the tracking performance is very good both in transient and steady state. This graph proves the fast and robust adaptation features of L1 adaptive control scheme for this example problem.

It is seen Figure 13 and Figure 18 that the magnitude characteristics of the adaptive control signal that is produced by both of the adaptive schemes is realizable and small. However, comparing the control surface deflection rates given in Figure 14 and Figure 19, it is seen that L1 adaptive augmentation produced lower control surface deflection rates than MRAC augmentation. Especially at the beginning of the simulation, when the magnitude of the error signal is high, MRAC augmentation causes a faster control surface deflection rate, which caused the initial oscillatory behaviour seen in Figure 12.

CHAPTER 5

L1 ADAPTIVE CONTROL AUGMENTATION TO DYNAMIC INVERSION BASED AUTOPILOTS

In this chapter, an application of the L1 adaptive control augmentation to a missile autopilot that was designed with dynamic inversion method will be presented. Firstly, the missile model used for the autopilot design is explained and the flight simulation environment is described. Then, the design of a dynamic inversion autopilot for the control of this missile in longitudinal, directional and lateral axes is presented. The design will be done with the aerodynamic data of a single point in the flight envelope. Hence, the dynamic inversion autopilot will only serve as a nominal controller with limited operation envelope. Then, augmentation of these dynamic inversion baseline autopilots with the L1 adaptive control will be shown. The performance and robustness characteristics of the autopilots are tested by high fidelity, 6 DoF, nonlinear flight simulation of the missile. The simulation scenarios and the resulting variation of the flight variables will be presented.

5.1 Missile Model

The missile model used for the implementation of controller designs is a generic, air to ground, guided missile with axis-symmetric geometry and aerodynamic controls on tail section. With this moment producing control surfaces on tail, the missile is designed to follow acceleration commands by making skid to turn maneuvers in the pitch and yaw axis. The roll attitude of the missile is aimed to be kept at 0 deg by the lateral autopilot. Hence, for the control of missile in longitudinal and directional axes acceleration autopilots will be designed. And for the control of missile in lateral axis, a roll attitude autopilot will be designed.

5.2 Simulation Environment

In order to perform the flight simulations of the missile, a high fidelity, nonlinear, 6 degrees of freedom flight simulation environment established in Matlab/ Simulink is used.

The aerodynamic coefficients of the missile are stored in a 3-D look-up tables as a nonlinear function of Mach number,M, angle of attack, α, and sideslip β. The aerodynamic forces and moments acting on the missile are also calculated in this block.

The aerodynamic data of the missile is valid in $\pm$30 deg. angle of attack and sideslip range. This range covers the assumed nominal flight envelope of the missile. Hence, if the angle of attack or sideslip of the missile exceeded 30 degrees during a simulation it would stop.

The 6 DoF nonlinear equations of motion and navigation equations, environmental models of atmosphere and wind disturbance, guidance and autopilot algorithms, a second order nonlinear control actuation system are also modeled.

5.3 Dynamic Inversion Based Autopilot Design Application

5.3.1 Design Point

The purpose of this study is to demonstrate the effects of L1 adaptive control augmentation on a coarsely designed baseline autopilot. It is desired to see the effectiveness of adaptive augmentation in front of minimum model information, perturbation on aerodynamic coefficients and input gain alteration. The baseline autopilot is designed at a single point in the flight envelope. This design point is selected as:

$$M = 0.9, \alpha = 0\ deg, \beta = 0\ deg$$

The baseline autopilot design method used in this thesis is dynamic inversion. Hence, dynamic inversion based autopilot design applications explained in the following sections are performed by using the aerodynamic data of this single design point.

5.3.2 Dynamic Inversion Based Roll Attitude Autopilot Design

For the roll attitude control, first an inner loop controller is designed with dynamic inversion for the roll rate control. Then a proportional outer loop controller is designed for the roll attitude, which produces the roll rate commands for the inner loop.

The block diagram of the roll attitude control is given in Figure 21.

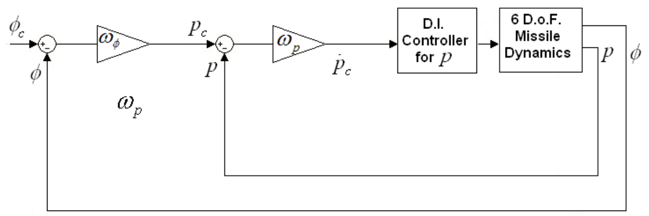

Figure 21 Dynamic Inversion Based Roll Attitude Control

5.3.2.1 Desired Bandwidth Selection for Roll Channel

The desired dynamics for the roll rate is taken to be of first order as follows:

$$\dot{p}_d = \omega_p (p_c - p) \tag{130}$$

Here $\dot{p}_d$ is the desired roll acceleration, p_c is the commanded roll rate calculated from the outer roll attitude loop, p is the roll rate, ω_p is the desired bandwidth of the roll rate loop.

The missile is desired to make skid to turn maneuvers. Hence the roll autopilot will be designed to keep the roll attitude of the missile at 0 degrees at all times. This brings the requirement that the roll loop should be faster than the pitch and yaw loops, so that pitch and yaw maneuvers will be realized in the correct plane. Keeping this requirement in mind, the desired closed loop bandwidth for roll rate channel is selected to be the maximum bandwidth that will not interfere with the control actuation system bandwidth and the structural modes. The control actuation system used in flight simulations is selected to have a bandwidth of $\omega_{CAS} = 75\,rad/s$. The structural modes of the missile model under consideration are much higher than $75\,rad/s$. Hence the desired bandwidth of the roll rate loop is selected to be $\omega_p = 16\,rad/s$, which is nearly 5 times slower than the control actuation system bandwidth. This selection of the roll rate loop bandwidth is low enough to allow effective operation of the control actuation system.

5.3.2.2 Roll Attitude Control Design

The desired dynamics for the roll attitude is defined as follows:

$$\dot{\phi}_d = \omega_\phi(\phi_c - \phi) \tag{131}$$

Desired bandwidth of the roll attitude loop is selected to be $\omega_\phi = 8\,rad/s$, which is sufficiently lower than the desired bandwidth of the roll rate loop.

5.3.3 Dynamic Inversion Based Acceleration Autopilot Design: Two Time Scale Separation Approach

As mentioned before in Chapter 2, in the two timescale approach the inner loop and outer loops are separated into fast and slow dynamics. Here, the pitch rate q and the yaw rate r correspond to the fast states. The fast states in pitch and yaw axes are controlled through two equivalent control surface deflections known as elevator and rudder deflections respectively. The slow states are the angle of attack and sideslip. The slow states are controlled by the using the commands for q and r as control inputs. Then a classically designed acceleration loop is closed around the angle of attack loop as shown in Figure 22.

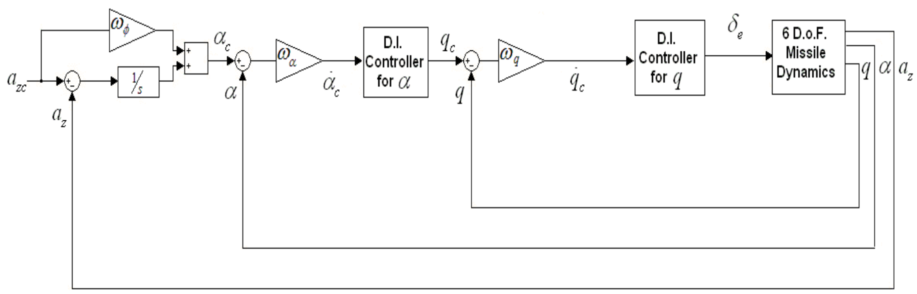

Figure 22 Acceleration Control with Dynamic Inversion, Two Time Scale Approach

5.3.3.1 Desired Bandwidth Selection for Pitch and Yaw Rate Control

The desired closed loop dynamics for the pitch rate and yaw rate are modeled to be first order as follows:

$$\dot{q}_d = \omega_q(q_c - q) \tag{132}$$

$$\dot{r}_d = \omega_r(r_c - r) \tag{133}$$

Here $\dot{q}_d$ and $\dot{r}_d$are the desired pitch and yaw acceleration, ω_q and ω_r are the desired closed loop bandwidth of these control loops, q_c and r_c are the commanded pitch and yaw rate calculated from the slow dynamics control law as shown in Figure 22.

Since the missile makes skid to turn maneuvers, the roll autopilot is designed to keep the roll attitude of the missile at 0 degrees. Therefore the roll loop should be faster than the pitch and yaw loops, so that pitch and yaw maneuvers will be realized in the correct plane. According to this requirement, the desired closed loop bandwidth for pitch and yaw rate channels are selected to be the maximum bandwidth that will not interfere with the roll rate loop, the control actuation system bandwidth and the structural modes. In Section 5.3.2.1 the bandwidth of the roll rate loop is selected as $\omega_p = 16\,rad/s$, and it is mentioned that the bandwidth of the control actuation system and structural modes are much higher than roll rate loop bandwidth Hence desired bandwidth of the pitch and yaw rate loops is selected to be $\omega_q = \omega_r = 8\,rad/s$, which is slow enough not to interfere with the roll rate loop, or the control actuation system and structural modes.

5.3.3.2 Desired Bandwidth Selection for Angle of Attack and Sideslip Control

The desired closed loop dynamics for the angle of attack and sideslip are modeled as a first order system as follows:

$$\dot{\alpha}_d = \omega_\alpha(\alpha_c - \alpha) \tag{134}$$

$$\dot{\beta}_d = \omega_\beta(\beta_c - \beta) \tag{135}$$

Here $\dot{\alpha}_d$ and $\dot{\beta}_d$ are the desired angle of attack and sideslip rate, ω_α and ω_β are the desired closed loop bandwidth of the system, α_c and β_c are the commanded angle of attack and sideslip calculated from the acceleration loop control law.

Desired bandwidth of the angle of attack and sideslip loops are selected to be $\omega_\alpha = \omega_\beta = 4\ rad/s$, so that these two loops will not interfere with the faster inner pitch rate and yaw rate loops.

5.3.3.3 Acceleration Loop Control Design

The acceleration loop is desired to produce angle of attack and side-slip commands for the inner slow dynamics loop. The derivation of the angle of attack command from the acceleration loop is explained in Chapter 2. According to this derivation, acceleration and angle of attack can be related through the following expression:

$$\left(1 - \frac{Z_{\delta_e} M_q}{M_{\delta_e}}\right)\frac{a_z}{U_0} = \left(Z_\alpha - \frac{Z_{\delta_e} M_\alpha}{M_{\delta_e}}\right)\alpha \tag{136}$$

At the design point, $M = 0.9, \alpha = 0\ deg, \beta = 0\ deg$, the missile has a $Z_{\delta_e} = 0.033$, and $M_{\delta_e} = 27.5$. Since Z_{δ_e} term is very small compared to M_{δ_e}, (136) can be safely decreased to the following expression for the angle of attack as:

$$\alpha = \frac{a_z}{U_0 Z_\alpha} = K a_z \tag{137}$$

The numerical value of K for the design point is found to be $K = -0.07$.

Hence, given an acceleration command, the commanded angle of attack can be directly computed from (137). To reduce the steady-state error possibly caused by the uncertainty in K, an integral controller is added to the control loop. The open loop acceleration control architecture is given in Figure 23.

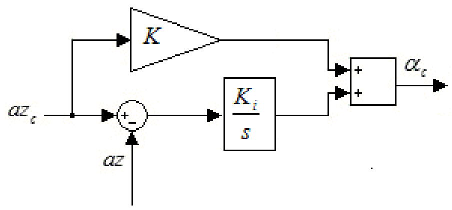

Figure 23 Open Loop Acceleration Control Architecture

The integral gain K_i is designed with classical control methods.

If the inversion is exact in pitch rate and angle of attack loops, the dynamic inversion controller simply reduces to an integral action. Hence, assuming perfect inversion of dynamics, at the design point, $M = 0.9, \alpha = 0\ deg, \beta = 0\ deg$, the root locus of the outer acceleration loop given in Figure 22 is as follows:

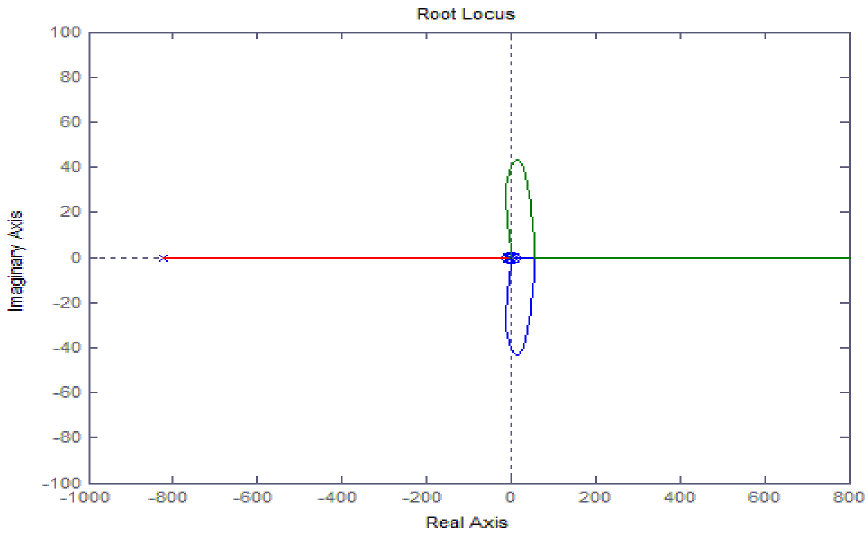

Figure 24 Root Locus Plot of Acceleration Loop

Zooming in the root locus plot for gain selection, Figure 25 is obtained.

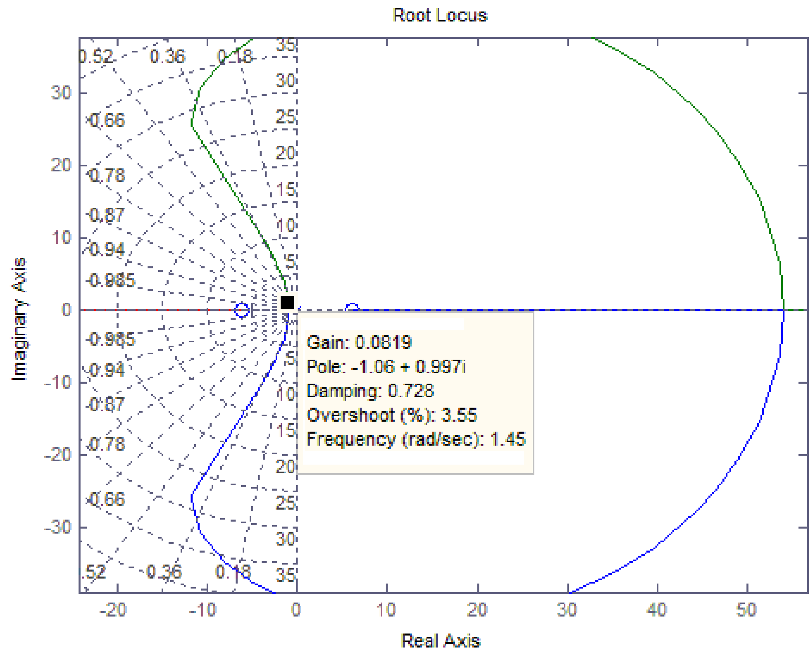

Figure 25 Zoomed Root Locus Plot of Acceleration Loop

A selection of $K_i = 0.0819$ provides a frequency of 1.45 rad/s and damping of 0.728.

5.3.4 Dynamic Inversion Based Acceleration Autopilot Design: Output Redefinition Approach

In Chapter 2, the motivation and use of output redefinition methodology has been explained. Here numerical examples for the output redefinition design will be shown.

At the design point, $M = 0.9, \alpha = 0\ deg, \beta = 0\ deg$, the zeros of the pitch rate and angle of attack transfer functions are calculated by the following transfer functions as follows:

$$\frac{q(s)}{\delta_e(s)} = \frac{M_{\delta_e}\left(s + \left(\frac{M_\alpha Z_{\delta_e}}{M_{\delta_e}} - Z_\alpha\right)\right)}{D(s)} \tag{138}$$

$$\frac{\alpha(s)}{\delta_e(s)} = \frac{Z_{\delta_e}\left(s + \frac{M_{\delta_e}}{Z_{\delta_e}}\right)}{D(s)} \tag{139}$$

where $D(s) = s^2 - (Z_\alpha + M_q)s - M_\alpha + Z_\alpha M_q$.

the numerical evaluation of the zero of $\frac{q(s)}{\delta_e(s)}$ transfer function is:

$$a_q = \left(\frac{M_\alpha Z_{\delta_e}}{M_{\delta_e}} - Z_\alpha\right) = 0.0456$$

Hence it is seen that the zero of the transfer function from pitch rate to control surface deflection is very small. Upon inversion of this transfer function for the calculation of the control signal, this zero will be moved to the denominator of the transfer function. Since the inversion is performed after a linearization process, it is not exact. Also, due to the inexactness of the model parameters, the small zero value appearing at the denominator of the control input formulation may cause an overly slow mode, and threaten stability.

At the design point, $(M = 0.9, \alpha = 0, \beta = 0)$, the numerical evaluation of the zero of $\frac{\alpha(s)}{\delta_e(s)}$ transfer function is:

$$a_\alpha = \frac{M_{\delta_e}}{Z_{\delta_e}} = 821.9$$

The zero of the transfer function from angle of attack to control surface deflection is large. Because of the same reasons mentioned for the inversion of pitch rate transfer function, this zero appearing at the denominator of control input formulation may cause high frequency transients in control signal, sensitivity to time delay etc.

Therefore, in order to get rid of the possible undesired effects of the zero locations of pitch rate and angle of attack transfer functions in the dynamic inversion process, a new output variable is defined according to the output redefinition methodology. This new output variable is formulated as a linear combination of the angle of attack and pitch rate as follows:

$$y \triangleq \alpha + C_q q$$

A desirable zero of the transfer function from this new variable to control input is order of one. Such a zero location will prevent the undesirable effects due to inversion. Hence the design variable C_q should be selected to ensure a desired value for the zero of this transfer function. As derived in Chapter 2, C_q can be calculated by the following equation:

$$C_q = \frac{Z_{\delta_e}(a_\alpha - z_y)}{M_{\delta_e}(z_y - a_q)} \tag{140}$$

Here Z_{δ_e} and M_{δ_e} are the dimensional derivatives, a_α and a_q are the zeros of the angle of attack and pitch rate transfer functions respectively, and z_y is the desired location of the zero of the transfer function for the new output variable y.

Since $a_\alpha = 821.9 \gg z_y$, and $a_q = 0.045 \ll z_y$, C_q will be approximated as:

$$C_q \approx \frac{Z_{\delta_e} a_\alpha}{M_{\delta_e} z_y} \approx \frac{1}{z_y}$$

The objective of output redefinition is to make the designer be able to attain a desired zero location for the inner loop transfer function which is order of one. In this design, the following values are attained for the zero location z_y and C_q:

$$z_y = 4$$

$$C_q = \frac{1}{z_y} = 0.25$$

5.3.4.1 Desired dynamics for the new output variable y

The block diagram of pitch axis autopilot with the newly defined inner loop variable y is given in Figure 26.

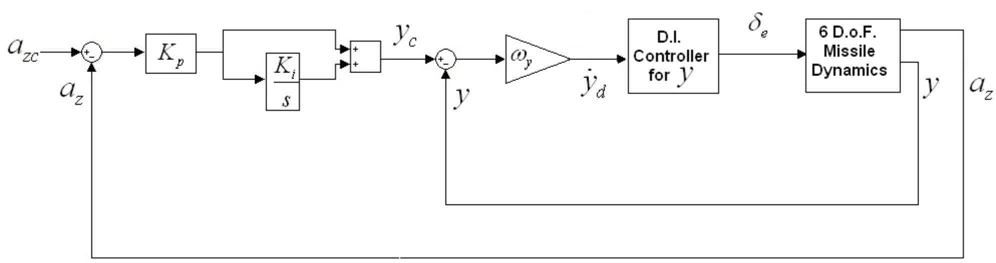

Figure 26 Dynamic Inversion Based Acceleration Control with Output Redefinition

The desired dynamics for the redefined output variable y is taken to be of first order:

$$\dot{y}_d = \omega_y(y_c - y) = u_y \tag{141}$$

The desired bandwidth ω_y of the inner loop is selected to be smaller than the bandwidth of the roll rate loop, control actuation system bandwidth, and structural modes bandwidth. In Section 5.3.2.1, the bandwidth of the roll rate channel is selected as $\omega_p = 16\, rad/s$. Hence $\omega_y = 5\, rad/s$ is selected, so that this loop will not to interfere with the roll rate loop, or the control actuation system and structural modes

5.3.4.2 Acceleration Loop Control Design

The inner control loop, which is designed with dynamic inversion method provides fast tracking of the commanded new output variable y_c. The outer acceleration loop can be designed with classical control methods. For the control design of the outer loop, the inner loop will be assumed to provide perfect tracking of the commanded variable. Namely, the dynamic inversion block in Figure 26 will serve as an integral action and $\dot{y}_d = \dot{y}$.

In order to be able to plot the root locus of the control architecture in Figure 26, the transfer function $\frac{a_z(s)}{y(s)}$ should be found.

The pitch axis acceleration can be expressed as follows:

$$a_z = U_0(\dot{\alpha} - q) \tag{142}$$

Hence:

$$a_z(s) = U_0(s\alpha(s) - q(s)) \tag{143}$$

The linearized equation for angle of attack is:

$$\dot{\alpha} = Z_\alpha \alpha + Z_{\delta_e}\delta_e + q \tag{144}$$

As mentioned before, Z_{δ_e} is very small and will be neglected. Hence (144) can be written as:

$$q(s) = (s - Z_\alpha)\alpha(s) \tag{145}$$

Substituting (145) into the new output variable y , it takes the following form:

$$y(s) = \left(1 + C_q s - C_q Z_\alpha\right)\alpha(s) \tag{146}$$

Substituting (145) and (146) into (143), the transfer function $\frac{a_z(s)}{y(s)}$ can be found as follows:

$$\frac{a_z(s)}{y(s)} = \frac{U_0 Z_\alpha}{(1 + C_q s - C_q Z_\alpha)} \tag{147}$$

Hence, the loop transfer function for the architecture in Figure 26 becomes:

$$G(s) = \frac{-K_p U_0 Z_\alpha \omega_y (s + K_i)}{s(s + \omega_y)(1 + C_q s - C_q Z_\alpha)} \tag{148}$$

A choice of $K_i = \frac{1 - C_q Z_\alpha}{C_q}$, will result in a pole zero cancellation in the loop transfer function, and will simplify the analysis. Now a desired second order transfer function can be used to make pole placement, and calculate the rest of the unknown parameters.

$$\omega_y = 2\xi\omega_n \tag{149}$$

$$K_p = -\frac{C_q \omega_n}{2\xi U_0 Z_\alpha} \tag{150}$$

Since the desired bandwidth of the inner y loop was decided to be $\omega_y = 5\, rad/s$, the desired natural frequency of the outer loop ω_n can be calculated from (149), by selecting a damping ratio. For $\xi = 0.707$, $\omega_n = 3.54\, rad/s$ is calculated. From (150), $K_p = 0.044$ is found.

5.4 L1 Adaptive Control Augmentation of a Dynamic Inversion Based Autopilot

In this section, the implementation of the novel L1 adaptive control augmentation system to a dynamic inversion based missile autopilots is presented. In Section 5.3, autopilots were designed with dynamic inversion method for the control of a missile in roll, pitch and yaw axes. These autopilots were designed at a single point in the flight envelope to simplify the baseline autopilot design phase, hence they are not expected to poses desired performance throughout the flight. The L1 adaptive control augmentation system will serve to generate an aiding control signal that will fulfill the deficient control signal generated by the baseline dynamic inversion autopilot.

The deficiency of the baseline dynamic inversion autopilots can be summarized in two points: One is the inexactness of the inversion process carried out by making linearization assumptions. The other is the single point design implementation. In addition to these forcing conditions, matched and unmatched perturbations are given to the aerodynamic model of the missile. L1 adaptive control augmentation is expected to augment the control signal so as to discard these effects.

5.4.1 Problem Formulation

The inner loop dynamics of the autopilot architectures given in Figure 21, Figure 22 and Figure 26 will be augmented with L1 adaptive control.

5.4.2 L1 Adaptive Control Augmentation of Dynamic Inversion Based Roll Attitude Autopilot

In the inner loop of the dynamic inversion based roll attitude autopilot, the roll rate is controlled. Hence, the inner loop dynamics given in (70) can be applied to roll rate channel as follows:

$x(t) = p(t), r(t) = p_c(t)$

The desired dynamics that should be defined for the L1 adaptive control augmentation is taken from the desired dynamics defined for the dynamic inversion autopilot. The desired dynamics for the roll rate channel was given as follows:

$$\dot{p}_d = \omega_p(p_c - p)$$

Which results in $A_m = -\omega_p$, $B_m = \omega_p$, $C = 1$.

Hence, (70) can be written for the roll rate channel as follows:

$$\begin{aligned} \dot{p}(t) = -\omega_p p(t) + \omega_p K_g p_c(t) & \\ + \omega_p\big(u_{ad}(t) + f_1(x(t), z(t), t)\big) & \\ + B_{um} f_2(x(t), z(t), t), \;\; p(0) = p_0 & \end{aligned} \tag{151}$$

With (151) and the equations given in (71), (72) and (73) L1 adaptive control augmentation is implemented to roll rate channel. The control architecture is shown in Figure 27.

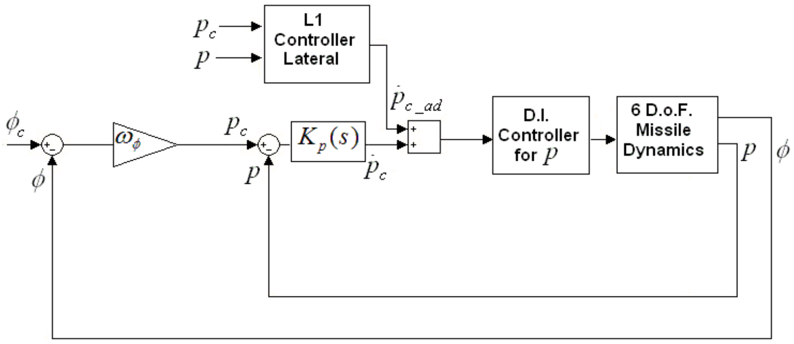

Figure 27 Roll Attitude Control with L1 Adaptive Control Augmentation

The low pass filters $C_1(s)$ and $C_2(s)$ used in L1 adaptive control are chosen to be of first order for simplicity. The bandwidth of the filters is selected to be as high as the control actuation system can handle. The control actuation system bandwidth is $\omega_{CAS} = 75\, rad/s$. Hence $\omega_{filter} = 35\, rad/s$ is selected so that the adaptive control augmentation will generate control signal frequency that is high enough to handle high frequency transient dynamics and low enough to be carried out by the existing control actuation system.

$$C_1(s) = C_2(s) = \frac{35}{s + 35}$$

With L1 adaptive control, the bandwidth of the filters can be changed according to the system dynamics, and performance/ robustness requirements.

5.4.3 L1 Adaptive Control Augmentation of a Dynamic Inversion Based Acceleration Autopilot

5.4.3.1 Two Timescale Separation Method

The inner loop dynamics given in (70) can be applied to pitch rate channel as follows:

Pitch channel:

The inner loop dynamics of the pitch channel

$x(t) = \begin{bmatrix} \alpha(t) \\ q(t) \end{bmatrix}, r(t) = \alpha_c(t)$

The desired dynamics for the pitch rate and angle of attack was given as:

$$\dot{q}_d = \omega_q(q_c - q) \tag{152}$$

$$\dot{\alpha}_d = \omega_\alpha(\alpha_c - \alpha) \tag{153}$$

$$A_m = \begin{bmatrix} 0 & -\omega_\alpha \\ -\omega_q(\omega_\alpha + Z_\alpha) & -\omega_q \end{bmatrix}, B_m = \begin{bmatrix} 1 \\ \omega_q \end{bmatrix}, C = \begin{bmatrix} 1 & 0 \end{bmatrix}$$

Hence, (70) can be written for the pitch rate channel as follows:

$$
\begin{aligned}
\begin{bmatrix} \dot{q}(t) \\ \dot{\alpha}(t) \end{bmatrix} = \begin{bmatrix} 0 & -\omega_\alpha \\ -\omega_q(\omega_\alpha + Z_\alpha) & -\omega_q \end{bmatrix} \begin{bmatrix} q(t) \\ \alpha(t) \end{bmatrix} \\
+ \begin{bmatrix} 1 \\ \omega_q \end{bmatrix} K_g \begin{bmatrix} q_c(t) \\ \alpha_c(t) \end{bmatrix} \\
+ \omega_p\big(u_{ad}(t) + f_1(x(t), z(t), t)\big) \\
+ B_{um} f_2(x(t), z(t), t), \quad q(0) = q_0, \alpha(0) \\
= \alpha_0
\end{aligned} \tag{154}
$$

With the L1 adaptive control augmentation, the control architecture takes the form shown in Figure 28.

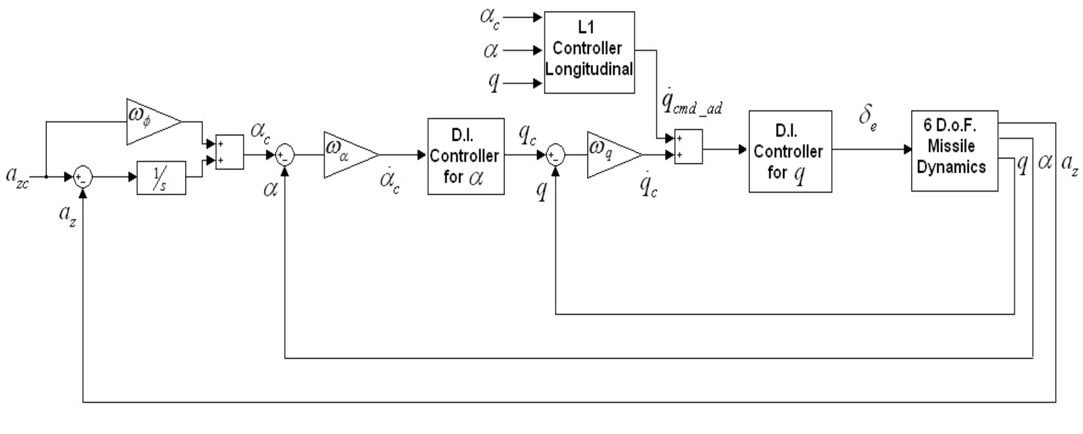

Figure 28 Acceleration Control with L1 Adaptive Control Augmentation

The low pass filters used in L1 adaptive control are selected as follows:

$$
C_1(s) = C_2(s) = \frac{35}{s + 35}
$$

5.4.3.2 Output Redefinition Method

In the inner loop of the dynamic inversion based acceleration autopilot with output redefinition, the newly defined output is controlled. Hence, the inner loop dynamics given in (70) can be applied to new inner loop channel as follows:

$x(t) = y(t), r(t) = y_c(t)$

The desired dynamics that should be defined for the L1 adaptive control augmentation is taken from the desired dynamics defined for the dynamic inversion autopilot. The desired dynamics for the newly defined output was given as follows:

$$\dot{y}_d = \omega_y(y_c - y)$$

Which results in $A_m = -\omega_y$, $B_m = \omega_y$, $C = 1$.

Hence, the inner loop channel with redefined output as follows:

$$\begin{aligned}\dot{y}(t) = -\omega_y y(t) + \omega_y K_g y_c(t) \\ + \omega_y\big(u_{ad}(t) + f_1(x(t), z(t), t)\big) \\ + B_{um} f_2(x(t), z(t), t), \quad y(0) = y_0\end{aligned} \tag{155}$$

5.5 Simulation Results

In order to examine the performance of dynamic inversion based autopilot designs in three axes, and the effect of the L1 adaptive control augmentation on the baseline control, 6 DoF nonlinear guided flight simulations of the missile are performed. A guidance algorithm is designed to produce proportional navigation based acceleration commands. The missile is desired to follow these guidance acceleration commands by making skid to turn maneuvers in the pitch and yaw axis. The roll attitude of the missile is aimed to be kept at 0 deg by the lateral autopilot. Since the missile under consideration is an air to ground missile, the simulation scenario starts with release of the missile from an altitude with given initial conditions. After the release, the missile is controlled with aerodynamic control surfaces at the tail section. Finally the missile is desired to reach a pre-specified target location. At the final phase the acceleration autopilots are closed, and the inner loop autopilots are taken into action in order to make the angle of attack and sideslip of the missile zero.

The aerodynamic data of the missile is valid in ± 30 deg. angle of attack and sideslip range. This range covers the assumed nominal flight envelope of the missile. Hence, if the angle of attack or sideslip of the missile exceeded 30 degrees during a simulation it would stop.

In this section results of example simulations are presented.

The simulation results will consist of the time variation plots of horizontal and vertical trajectories, flight parameters such as pitch and yaw axis accelerations, angle of attack, angle of sideslip, roll axis body rate and attitude, control surface deflections, baseline and adaptive input signals.

Release conditions and target location are given for each simulation.

5.5.1 Simulation I: Nominal Aerodynamics

In this scenario the nominal aerodynamic model is used. Hence, the aerodynamic model used for the simulation is the same as the aerodynamic model used for the design of baseline autopilot. In this simulation, performance of the baseline autopilot designed with output redefinition method is presented.

Release Position:(0, 0, -10660) m, Release Mach: 0.9, Target: (12200, 2300, -1000) m.

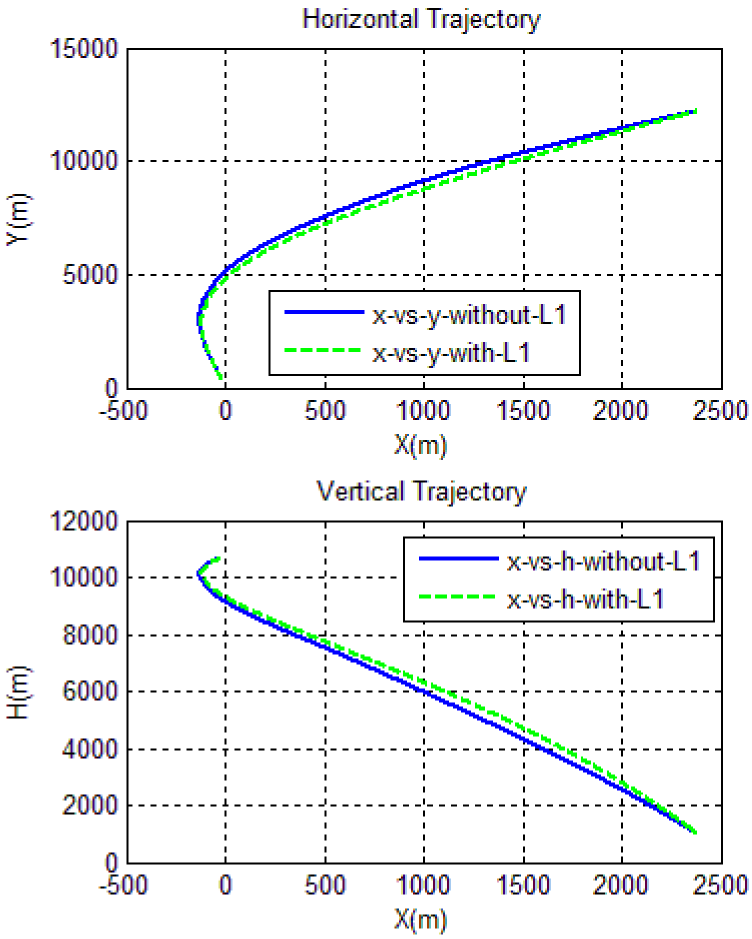

Figure 29 Variation of Trajectory

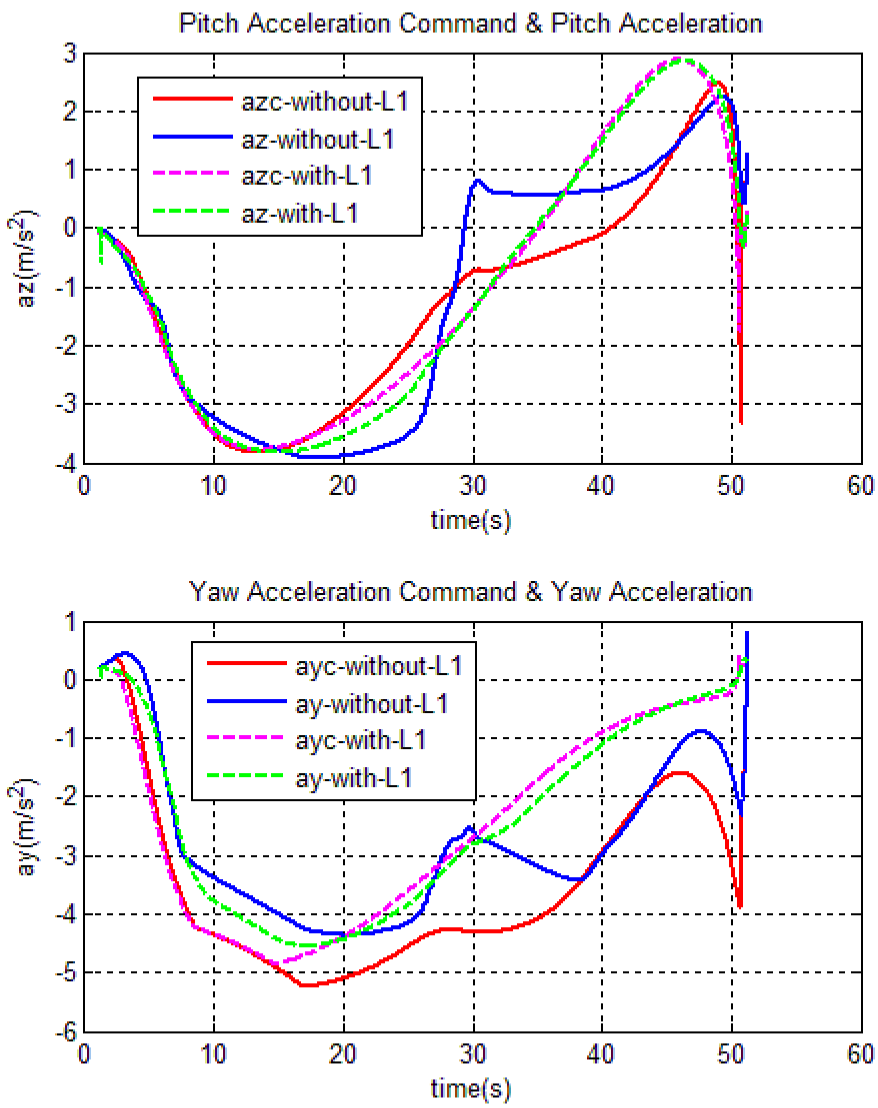

Figure 30 Variation of Pitch and Yaw Acceleration with Time

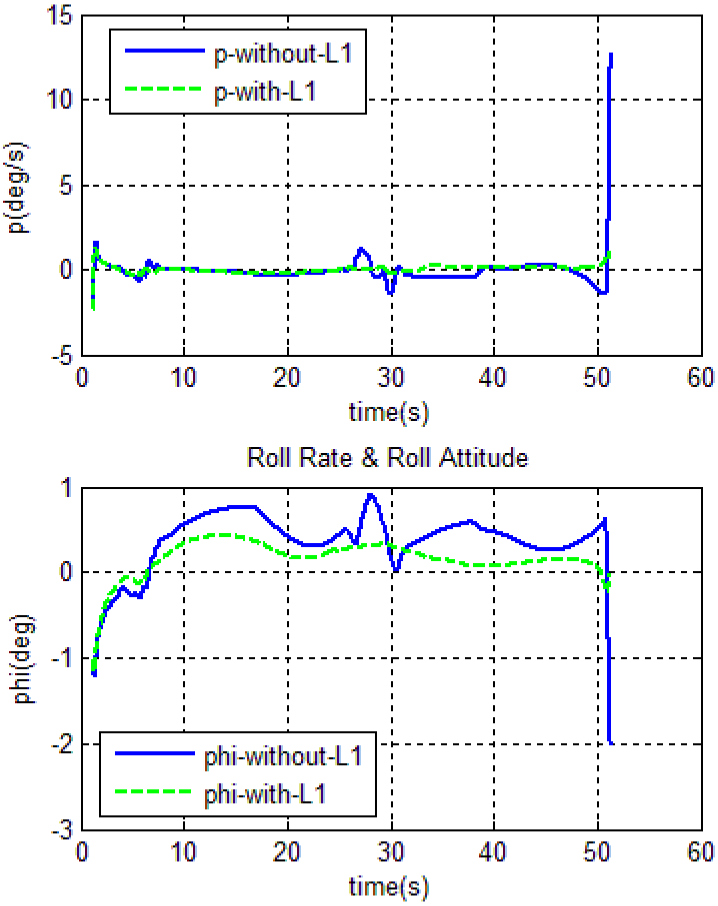

Figure 31 Variation of Roll Rate and Roll Attitude with Time

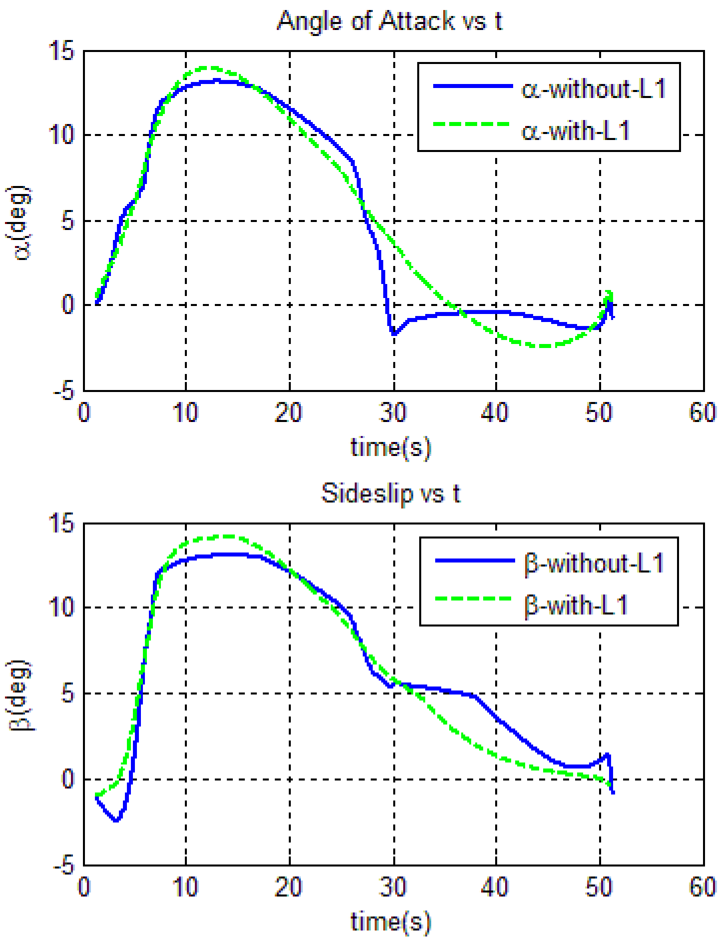

Figure 32 Variation of Angle of Attack and Sideslip with Time

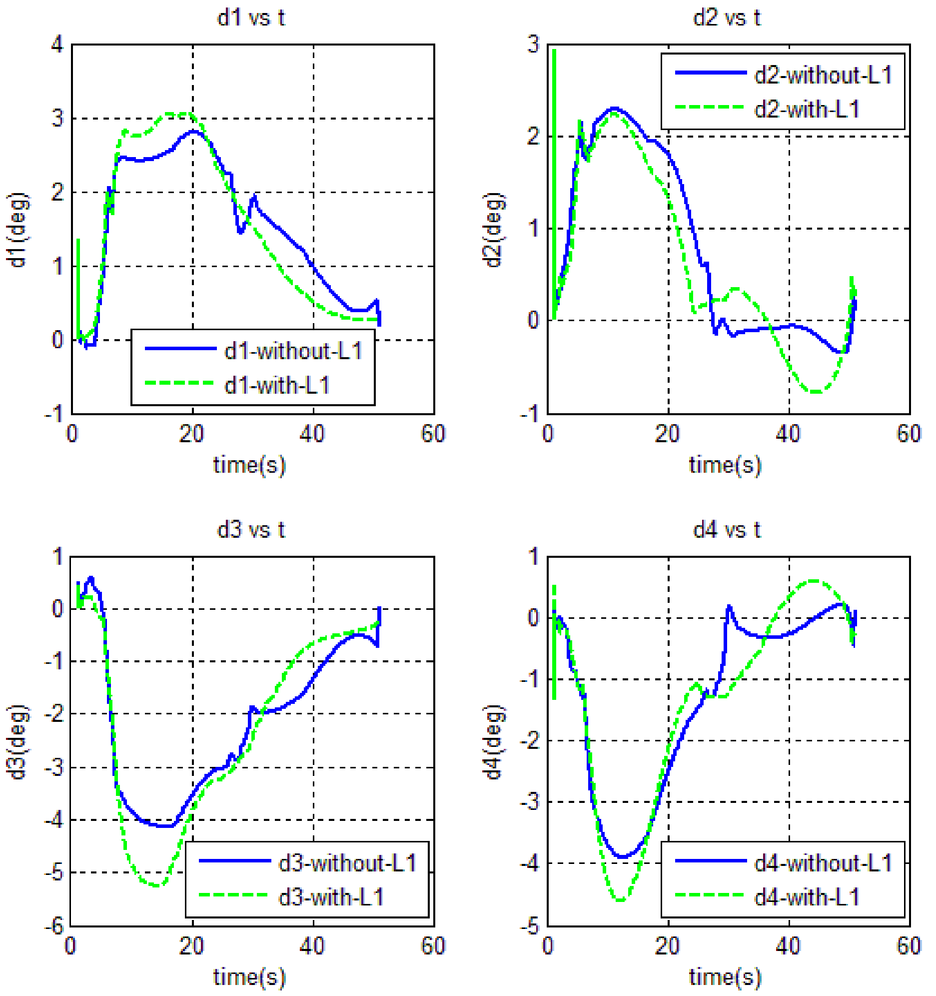

Figure 33 Variation of Control Surface Deflections with Time

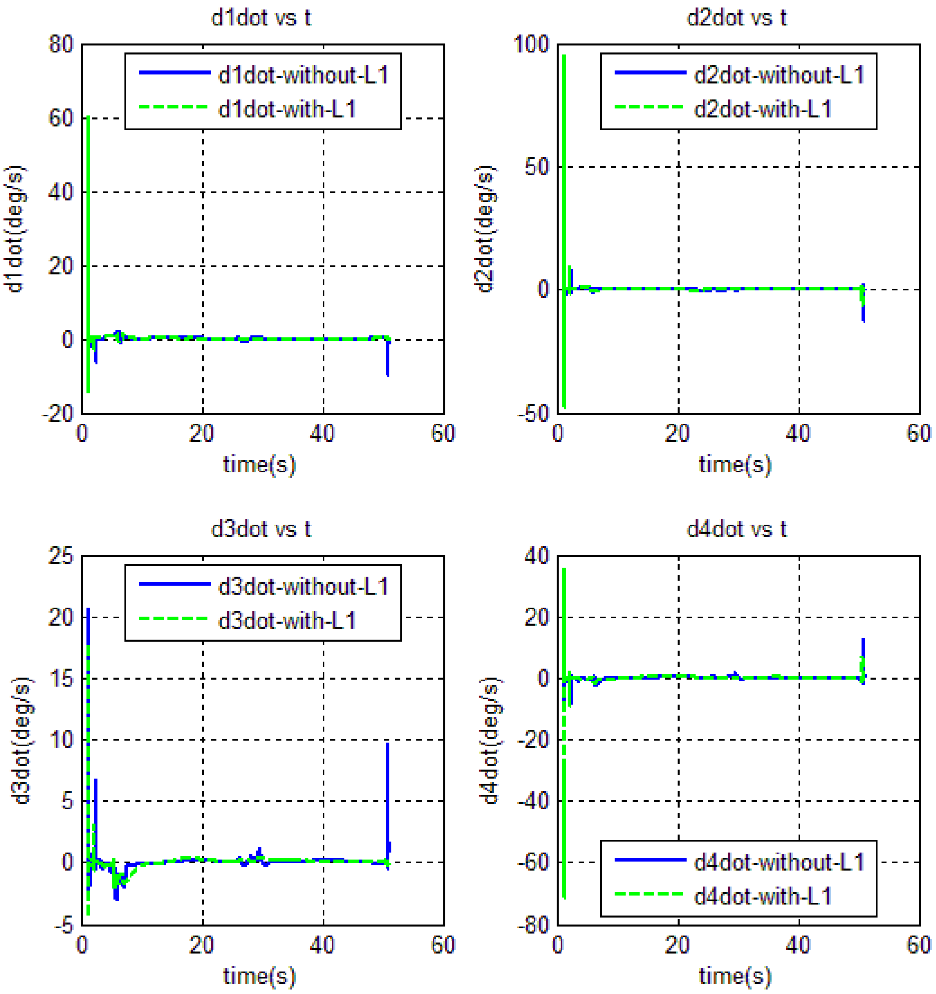

Figure 34 Variation of Control Surface Deflection Rates with Time

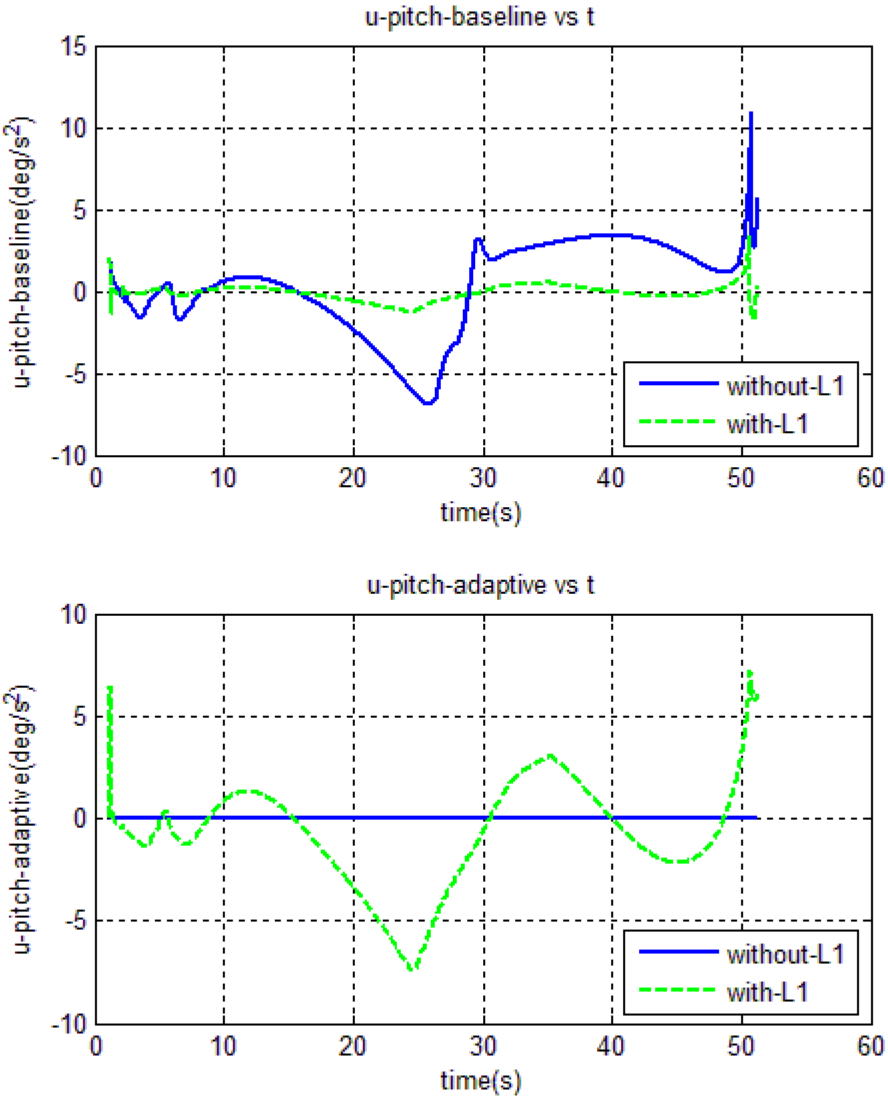

Figure 35 Variation of Pitch Axis Baseline and Adaptive Inputs with Time

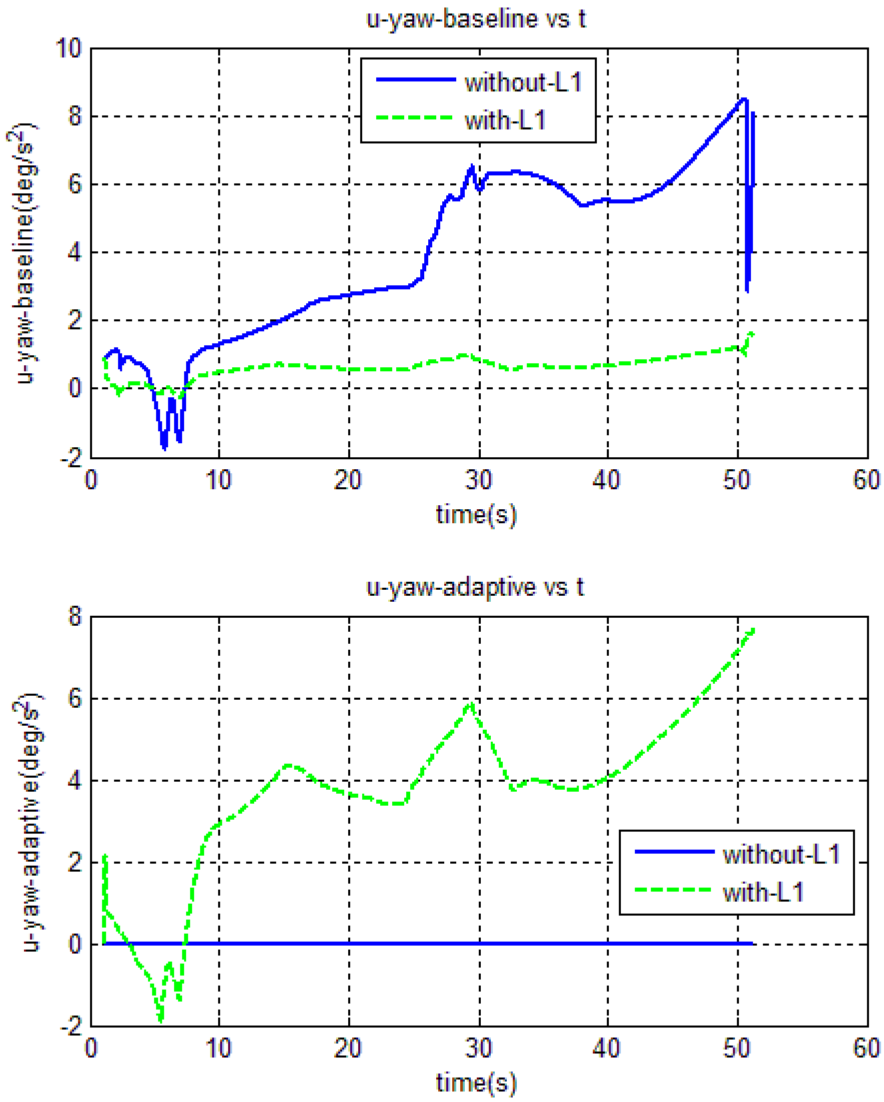

Figure 36 Variation of Yaw Axis Baseline and Adaptive Input with Time

From Figure 29-Figure 36, it is seen that the dynamic inversion based autopilot is successful in controlling the missile to reach its target. From the commanded and realized acceleration point of view, there exist some degradation in performance, the effect of which was compensated by the correcting guidance loop. The baseline autopilot is designed with the aerodynamic data of a single point in the flight envelope which was not a trim condition. During the flight the dynamic conditions of the missile change continuously. Hence, there is a possibility of failure of the stand alone baseline autopilot. It is seen in Figure 29 - Figure 36 that L1 adaptive control augmentation improved the tracking performance of the baseline autopilot. The adaptive control signal works for the compensation of distorting effects which causes the baseline autopilot not being able to correct the error signals. It is seen that the effect of adaptive control input on the control surface deflections is smooth and realizable. With the filtering mechanism introduced in L1 adaptive control high frequency control signals are eliminated. Fast and robust adaptation is provided.

5.5.2 Simulation II: Perturbed Aerodynamics & Increased Input Gain

In the second set of simulations, perturbed aerodynamics and increased input gain cases are examined. For the first simulation the control effectiveness derivatives of the missile are decreased by 50%, and the force and moment coefficients, which are modeled to be functions of Mach number, angle of attack, α, and sideslip, $\beta$are decreased by 50 %. Baseline autopilot with output redefinition design is used.

In the second simulation nominal aerodynamics is used. However the outer acceleration loop gain is increased to 5 times of the design value. Here, the baseline autopilot with two time-scale separation is used.

5.5.2.1 Results for Output Redefinition Method

Release Position:(0, 0, -10660) m, Release Mach: 0.9, Target: (12200, 2300, -1000) m.

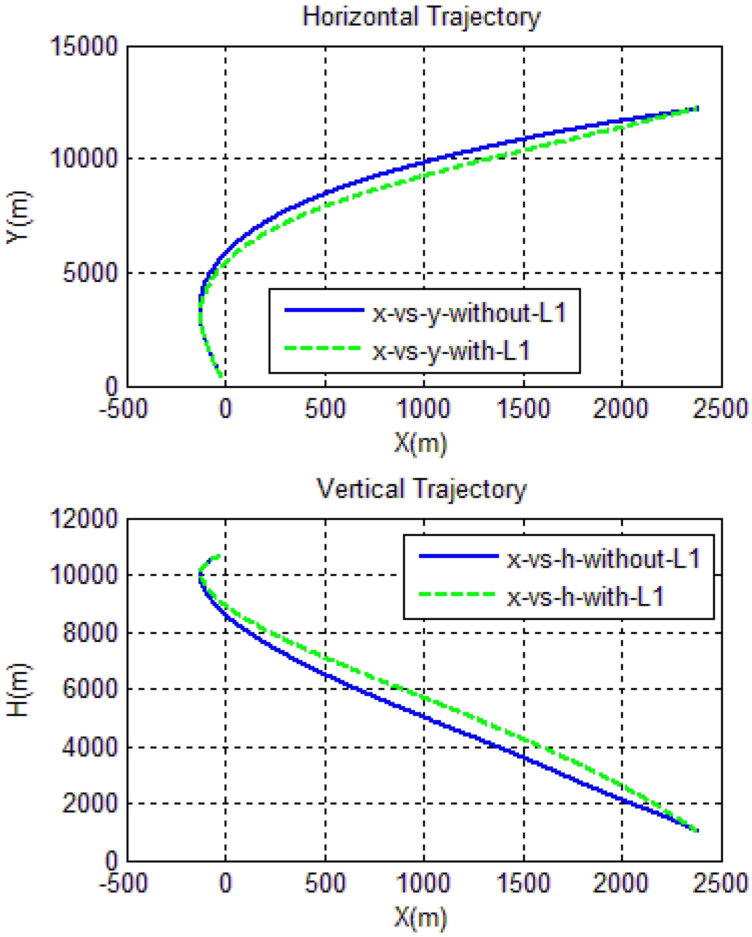

Figure 37 Variation of Trajectory

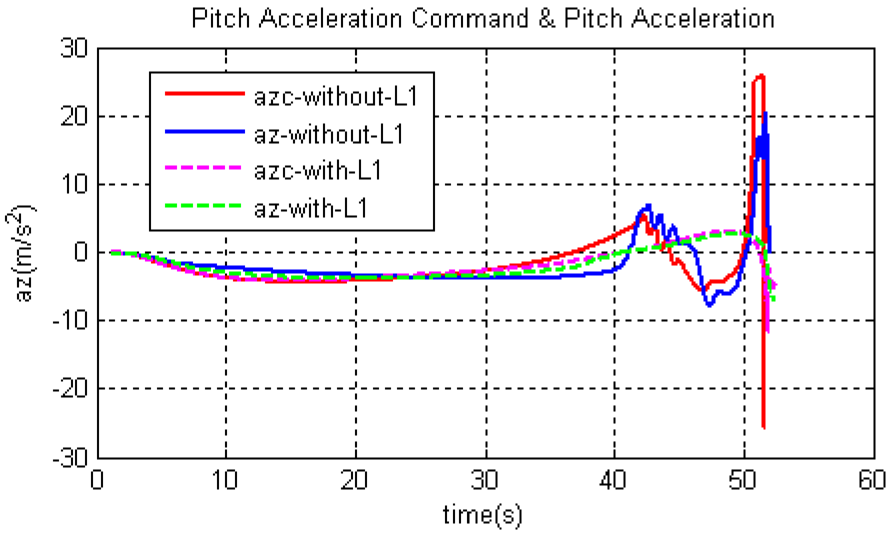

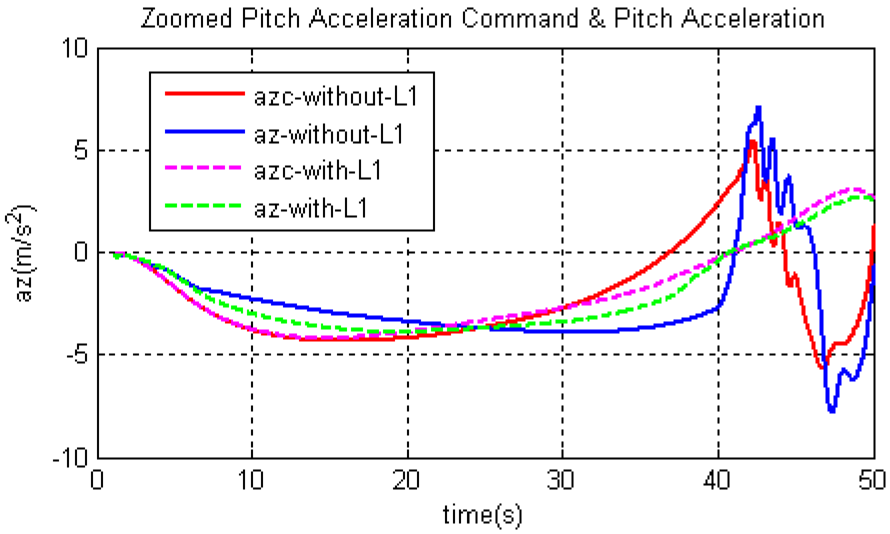

Figure 38 Variation of Pitch Acceleration with Time

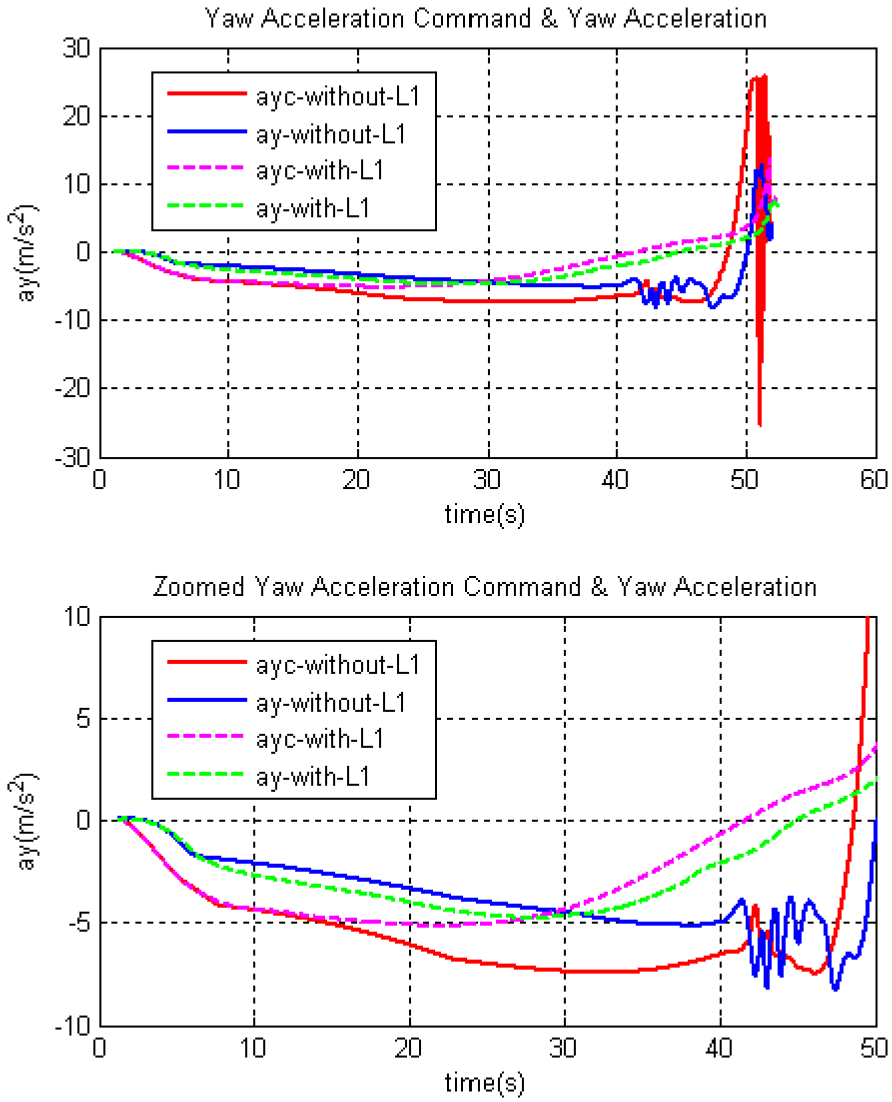

Figure 39 Variation of Yaw Acceleration with Time

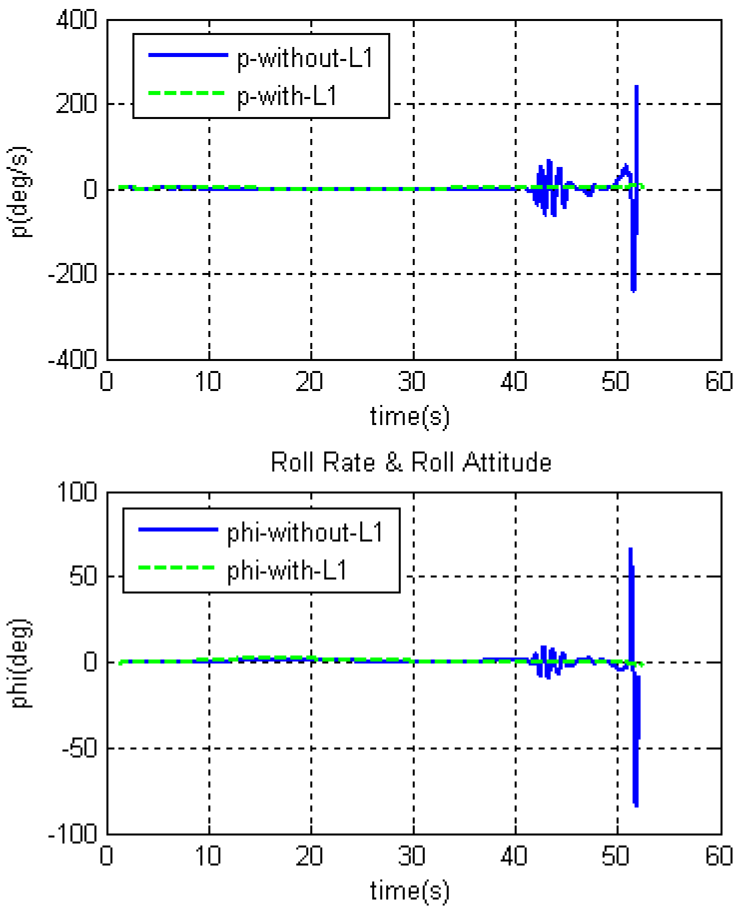

Figure 40 Variation of Roll Rate and Roll Attitude with Time

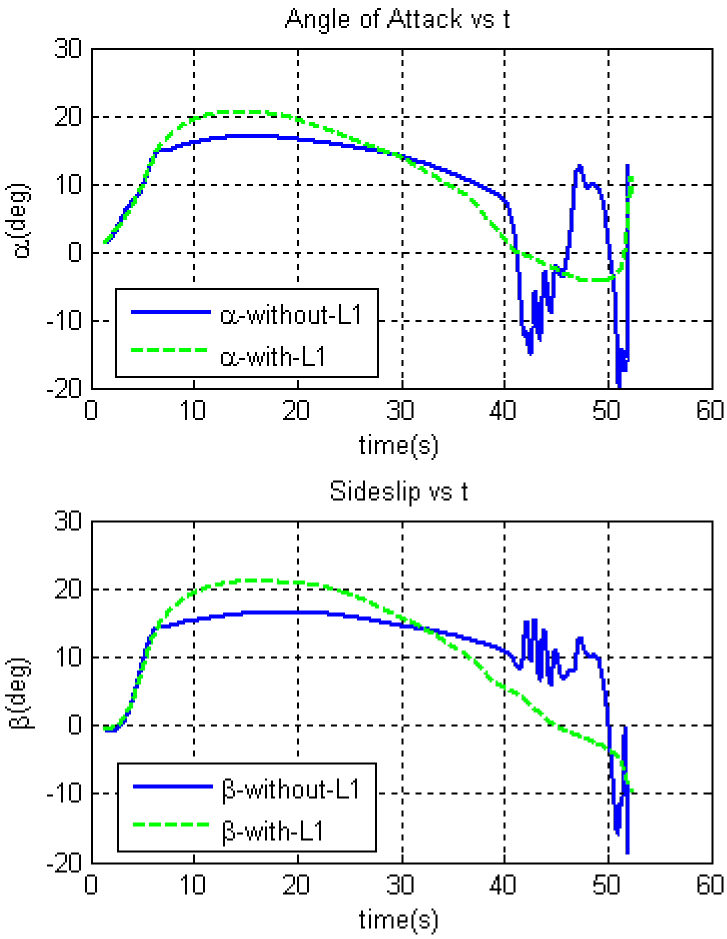

Figure 41 Variation of Angle of Attack and Sideslip with Time

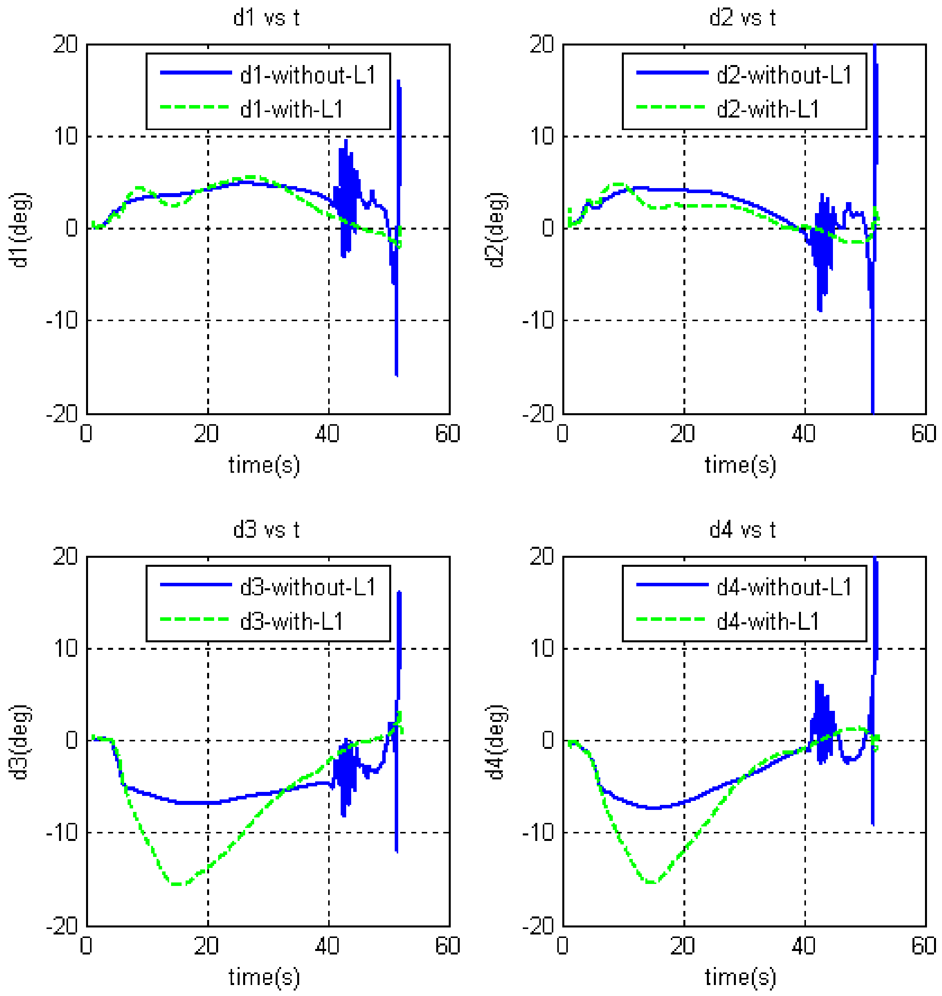

Figure 42 Variation of Control Surface Deflections with Time

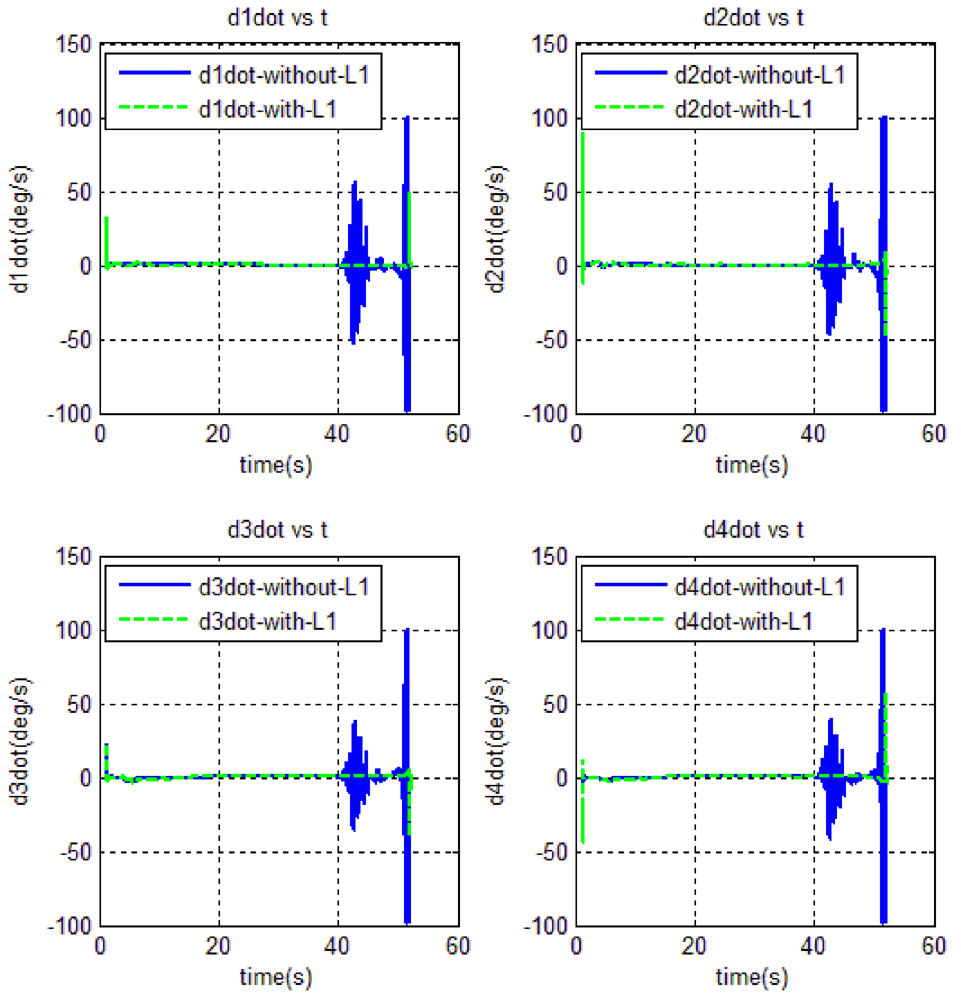

Figure 43 Variation of Control Surface Deflection Rates with Time

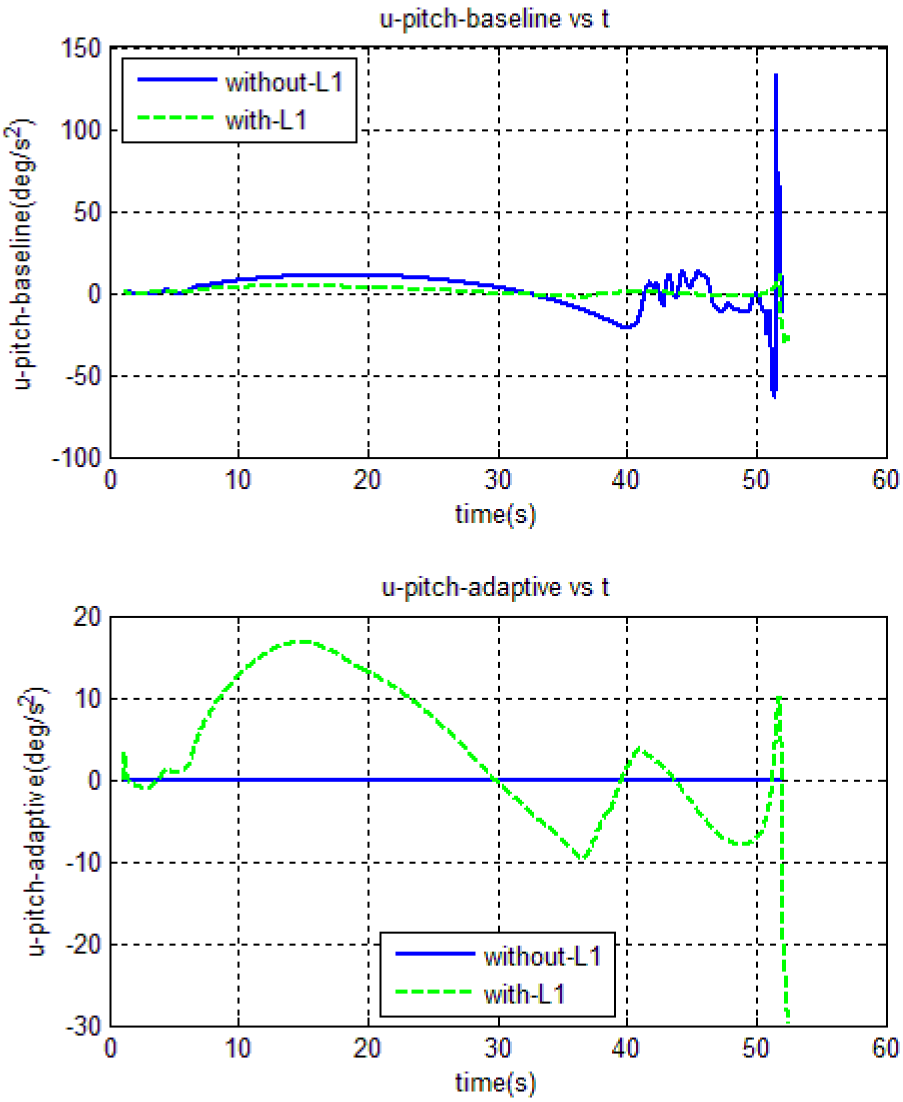

Figure 44 Variation of Pitch Axis Baseline and Adaptive Inputs with Time

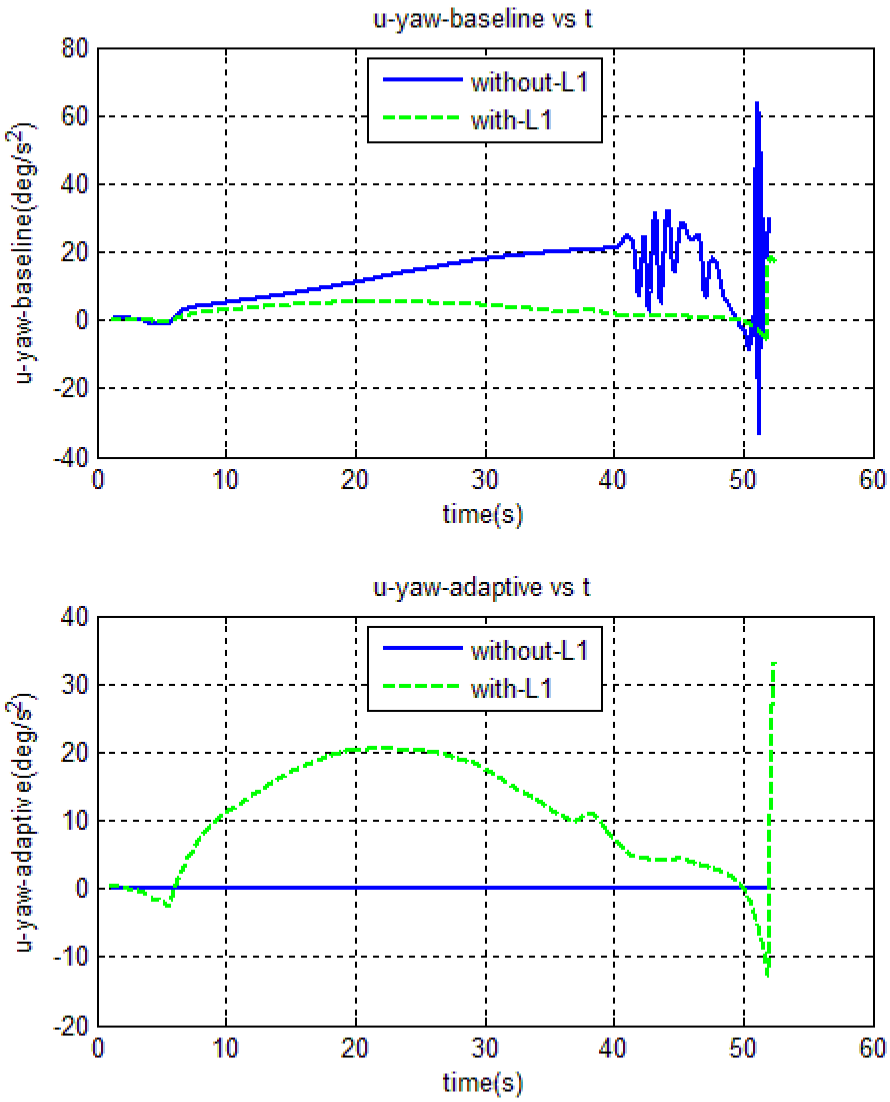

Figure 45 Variation of Yaw Axis Baseline and Adaptive Inputs with Time

5.5.2.2 Results for Two Timescale Separation Method

Release Position:(0, 0, -4570) m, Release Mach: 0.9, Target: (12200, 2300, -1000) m.

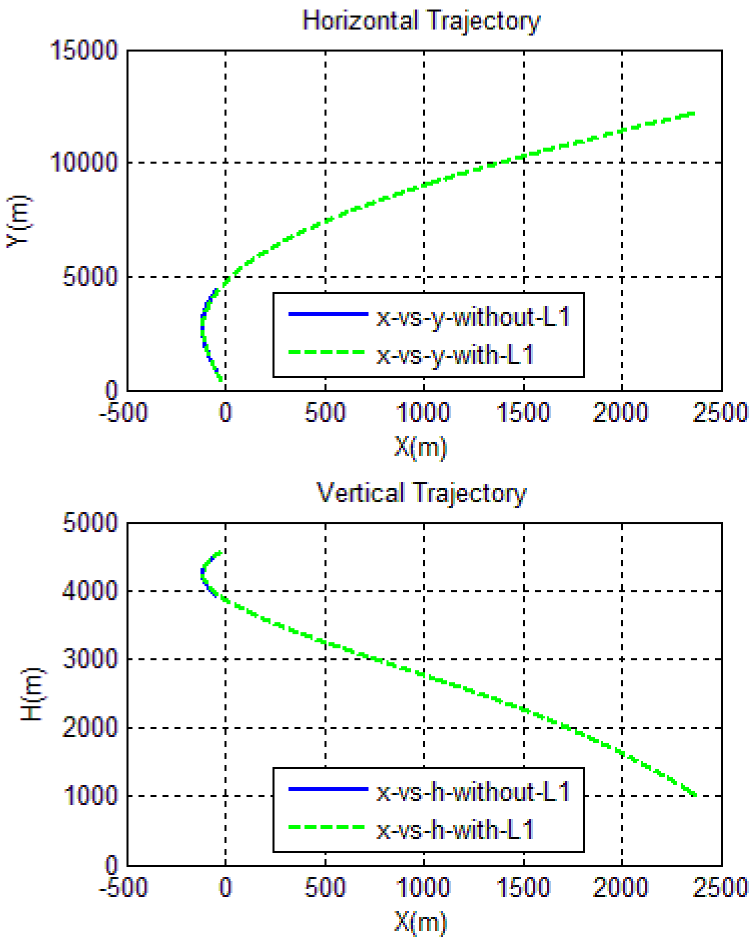

Figure 46 Variation of Trajectory

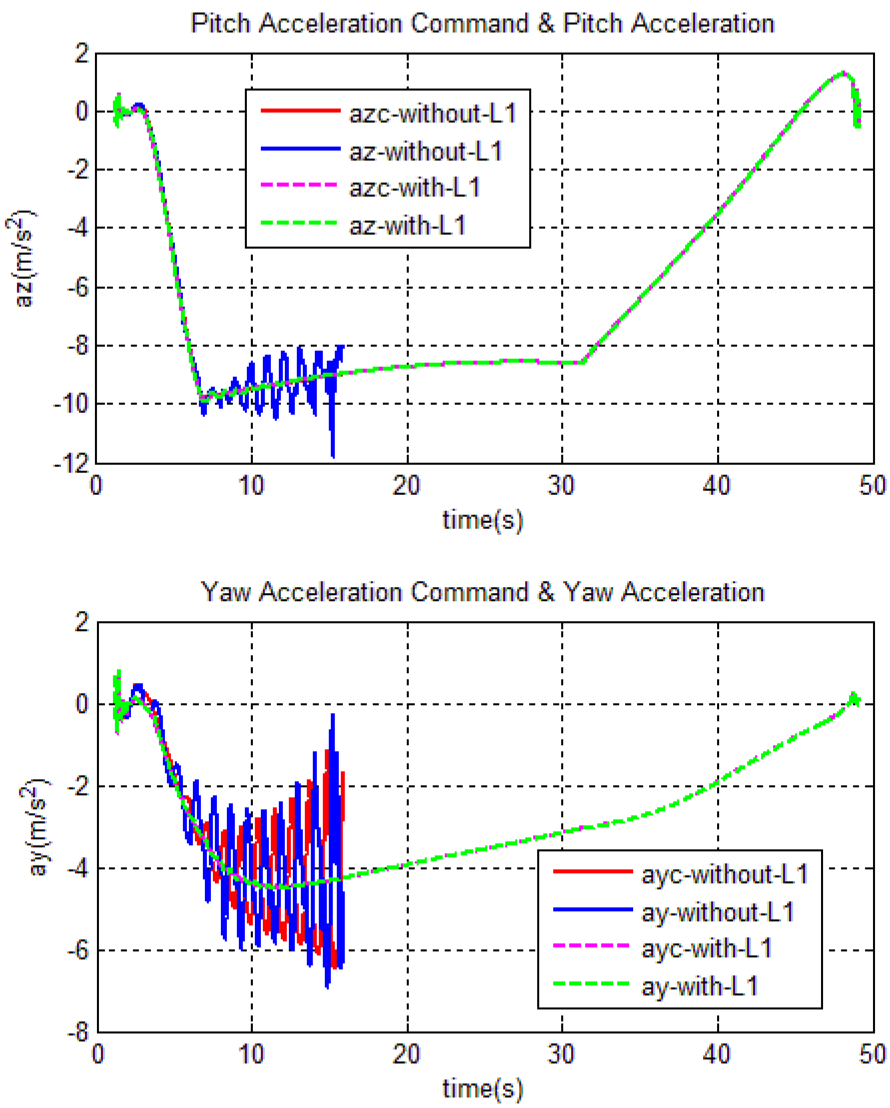

Figure 47 Variation of Pitch and Yaw Axis Acceleration with Time

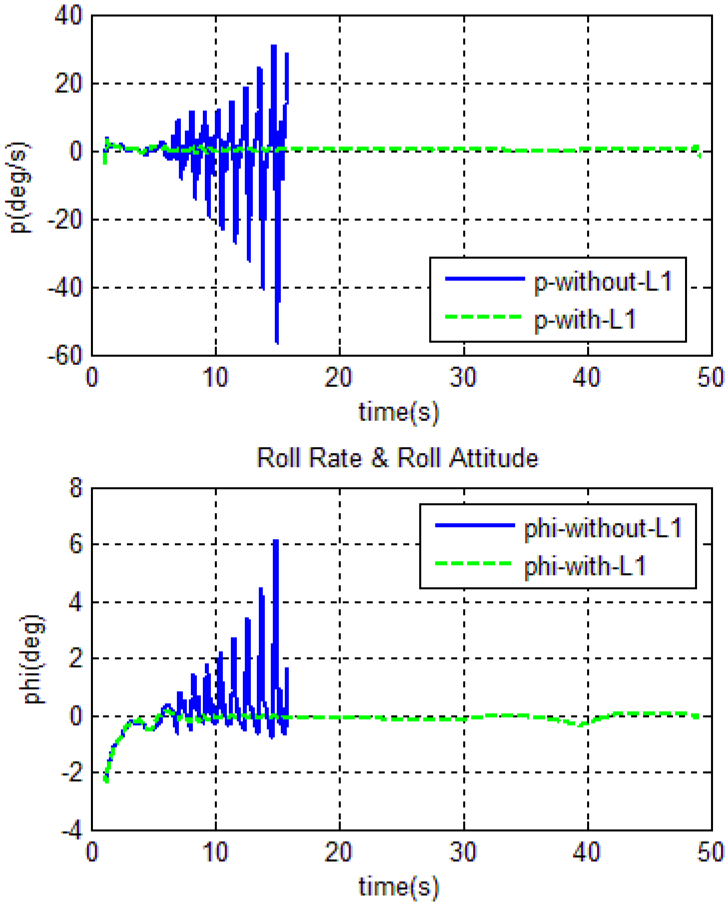

Figure 48 Variation of Roll Rate and Roll Attitude with Time

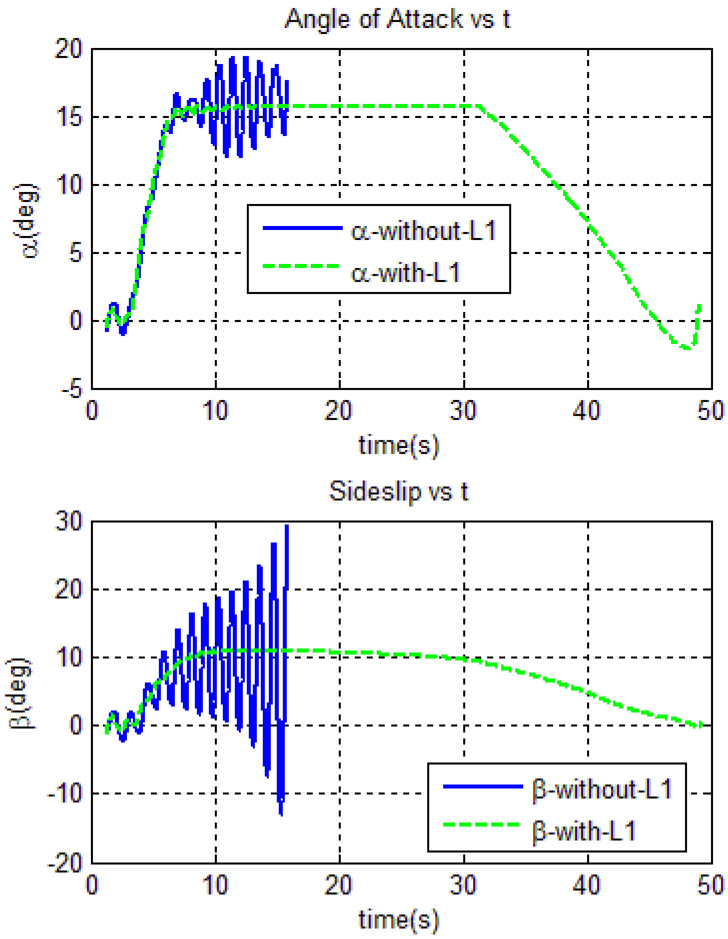

Figure 49 Variation of Angle of Attack and Sideslip with Time

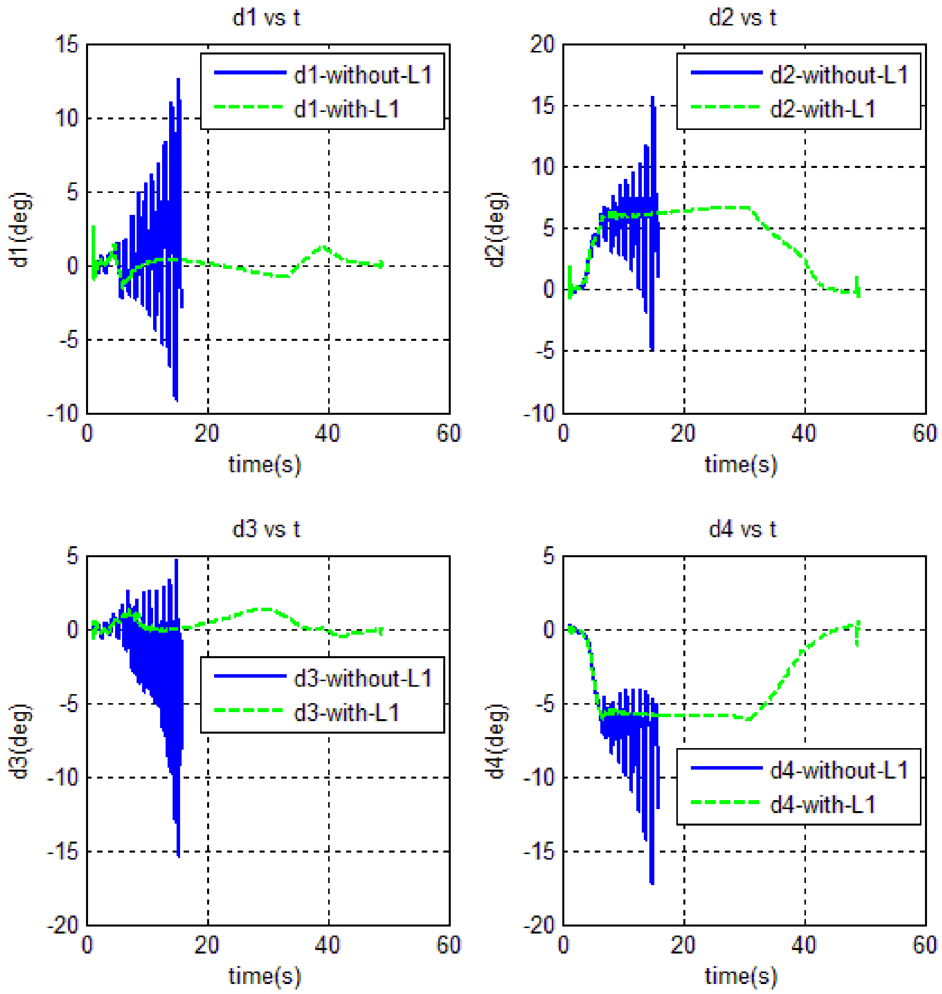

Figure 50 Variation of Control Surface Deflections with Time

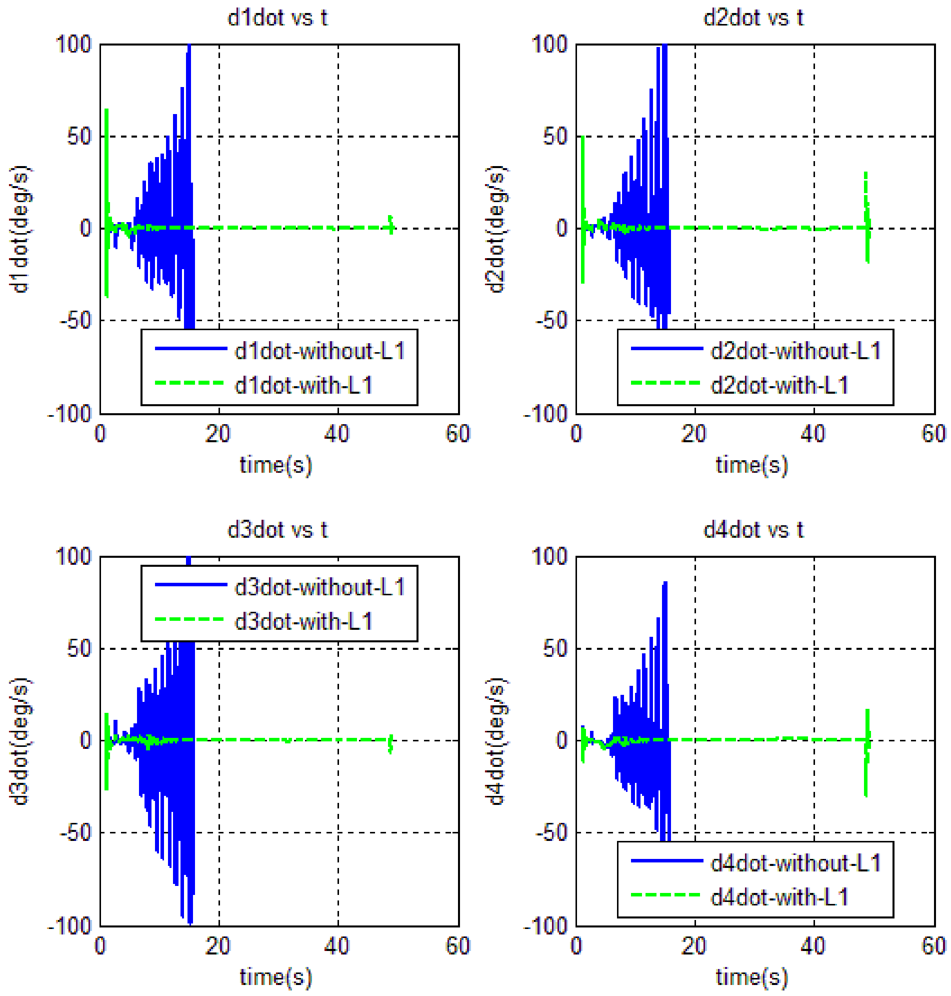

Figure 51 Variation of Control Surface Deflection Rates with Time

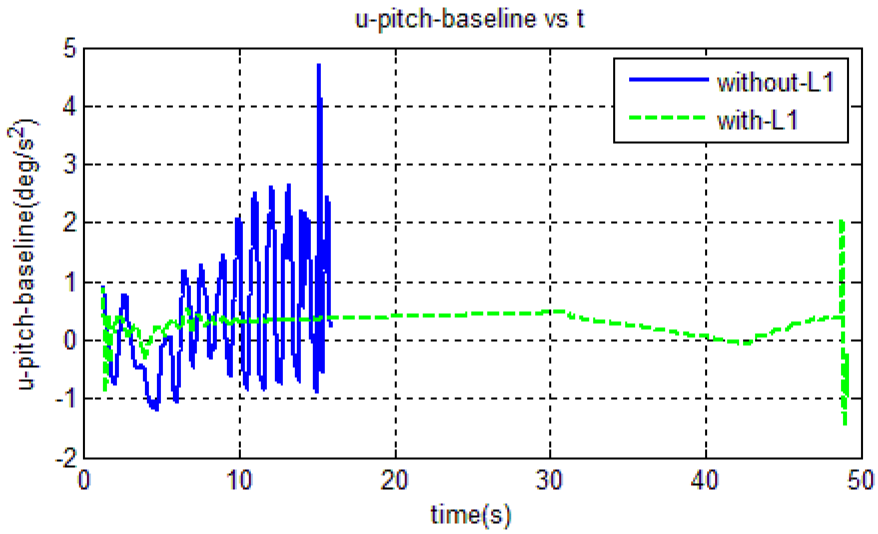

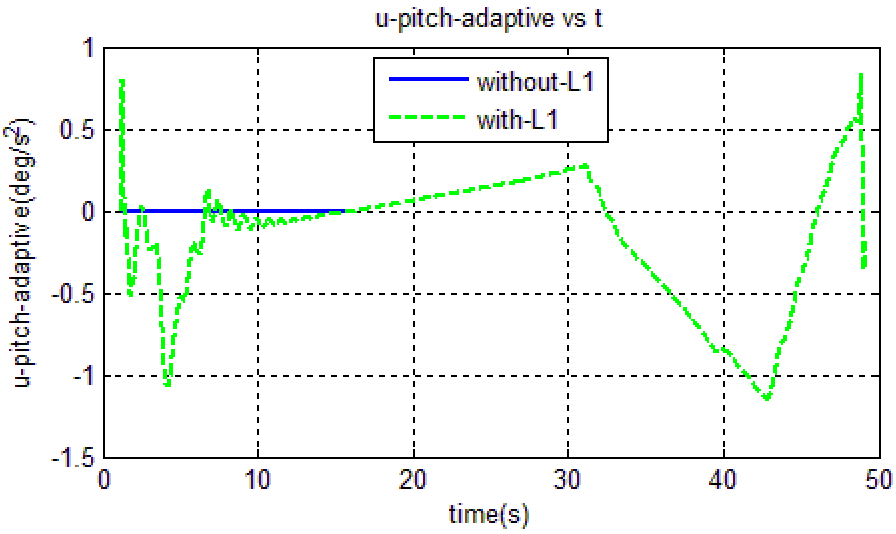

Figure 52 Variation of Pitch Axis Baseline and Adaptive Inputs with Time

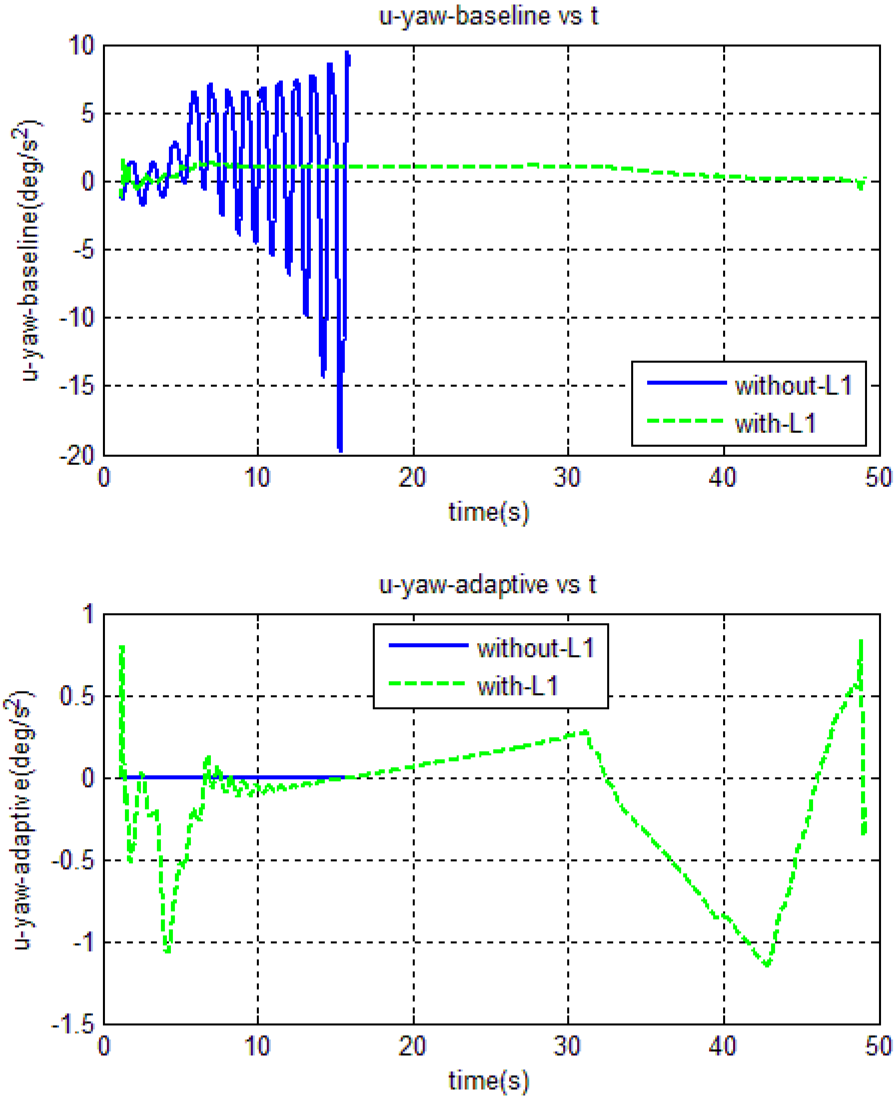

Figure 53 Variation of Yaw Axis Baseline and Adaptive Inputs with Time

From Figure 37- Figure 53, it is seen that dynamic inversion based autopilots show performance degradation in front of aerodynamic perturbations and input gain variation. This was an expected result, since the baseline dynamic inversion autopilots are designed with the aerodynamic data of a single point in the flight envelope. As the missile flies to its target, the velocity, angle of attack, sideslip, altitude and dynamic pressure continuously change. By the help of the correcting guidance loop, dynamic inversion autopilots did well in front of these changes for the nominal aerodynamics case. However, for perturbed aerodynamics or increase in input gain cases, degradation in baseline autopilot performance is much probable. In Figure 37-Figure 45 at the final phase of the flight, oscillations started during the control with baseline autopilot. In this scenario, L1 adaptive control augmentation achieved to recover a smooth, non oscillatory control, and provided adequate tracking of the commanded variables. For the second perturbed simulation in Figure 46-Figure 53, the outer loop gain is increased until the baseline control is unstable. The baseline simulation stops due to exceeding of the sideslip angle, 30 deg. For this scenario, L1 adaptive control augmentation eliminates the destabilizing effects of input gain variation, and provides successful tracking of the commanded variable.

For both of the simulations with L1 adaptive control, the effect of adaptive input signal on the control surface deflections is smooth and realizable. The filtering mechanisation employed in L1 adaptive control forces the adaptive input stay within a realizable bandwidth for the system.

CHAPTER 6

CONCLUSION & RECOMMENDED FUTURE WORK

The motivation of this research was to demonstrate the effects and performance of adaptive control augmentations to baseline controllers which are designed with very limited model data, on a realistic guided missile model. For this purpose, baseline controllers are designed for a missile model with linear and nonlinear control methods. Adaptive control augmentation research has been focused on Model Reference Adaptive Control and L1 Adaptive Control methodologies. Adaptive control augmentation schemes utilizing these methods have been applied to the baseline controllers. Simulations are performed with the linearized models and nonlinear 6 DoF simulation software of the missile. The controllers have been analyzed in the presence of model uncertainties and disturbances.

First, a baseline longitudinal autopilot is designed for the missile by using linear quadratic regulator with projective control method. This design is performed at a single point in the flight envelope. Then, adaptive augmentation of this baseline autopilot with MRAC scheme and L1 adaptive control scheme has been performed. The adaptive augmentations have been constructed to maintain the performance of the baseline controller in the presence of model uncertainties, external disturbances and control failures. A linear simulation environment is formed to test the performance of the controllers. Then, severe model uncertainties have been introduced by which the stability of the baseline closed loop dynamics has been corrupted. The pitching moment coefficient of the missile and pitching moment control derivative is decreased by 75 %. Simulations have been performed with the linearized model of the missile. The simulation results showed that both of the adaptive control augmentation schemes have been successful in re-stabilizing the system with realizable control inputs. In addition to providing satisfactory stability characteristics, the adaptive augmentation schemes is expected to restore the tracking performance of the baseline autopilot without uncertainties. When the tracking performance of MRAC and L1 adaptive control are examined it is seen that both schemes provide satisfactory tracking of the desired reference dynamics. However in particular, transient response characteristics of L1 adaptive control has been better than MRAC. While there are overshoots and oscillations in the transient part of MRAC response, L1 adaptive control achieved smooth and precise tracking. In MRAC architecture the speed of response to uncertainties or failures is mostly dependent on the adaptation rate which appears in the formulation of adaptive parameter estimation formulation. When the adaptation rate is increased, the adaptive controller tries to adapt fastly to the disturbing effect. However, fast adaptation brings adverse effects like oscillations, overshoots, high frequency control signals, etc. On the other hand, when the adaptation rate is lowered, the adaptation may not be effective or too slow to compensate for the disturbing effects. Hence, selection of the adaptation rate is an important issue to be considered about the performance of MRAC architecture. During the design, the best adaptation rate has been found by trial and error. Comparing the control surface deflection rates of MRC and L1 schemes, it is seen that L1 adaptive augmentation produced lower control surface deflection rates than MRAC augmentation. Especially at the beginning of the simulation, when the magnitude of the error signal is high, MRAC augmentation produces a faster control surface deflection rate, which caused the initial oscillatory behaviour. On the other hand, the filtering mechanism used in L1 adaptive control decreases the burden of adaptation rate determination to a trade-off between performance and robustness. L1 adaptive control allows for the use of a low pass filter in the feedback loop of adaptive control signal. The bandwidth of the low pass filter can be adjusted to give better performance or to provide better robustness characteristics. In L1 design, the bandwidth of the low pass filter is selected to be half of the bandwidth of the control actuation system of the missile so that adaptive control signal can be easily realized. By this way, the adaptation rate used in L1 adaptive control can be increased arbitrarily without worrying about high frequency control signal, and the adaptive control signal can shaped to force for the best transient performance that can be realized within the bandwidth of the low pass filter. These properties of L1 adaptive control explain the better performance of L1 adaptive control in transient and steady state tracking. The linear simulations of adaptive control augmentation schemes gave promising results for the adaptive control augmentation of the missile in 6 DoF, nonlinear environment. Hence, autopilots are designed for the control of the missile in roll, pitch and yaw axes. Baseline autopilots are designed with dynamic inversion method, and the adaptive augmentation design is performed with L1 adaptive control method.

The L1 adaptive control augmentation scheme used in the linear application was compensating for system matched uncertainties, unknown input signal and time varying disturbances affecting through the control channel. However, for the nonlinear simulations, an L1 adaptive control augmentation scheme compensating for both matched and unmatched uncertainties is applied to baseline autopilots of the missile. The baseline autopilot design was performed by using the data of the missile at a single point in the flight envelope using dynamic inversion method. Hence, matched and unmatched uncertainties were present in this environment.

The flight simulations demonstrated that, with the nominal aerodynamic model, dynamic inversion autopilots may show slightly degraded performance due to single point design and inexactness of the inversion. Although the guidance loop can compensate for some model uncertainties, it was shown by simulations that L1 adaptive augmentation supports the tracking performance and decreases the magnitude of error states.

The performance of the autopilots with L1 adaptive augmentation is also tested when the aerodynamic model of the missile is perturbed, and when the acceleration loop integrator gain is increased to a destabilizing value. The flight simulations showed that, at certain aerodynamic perturbation degrees, or when the outer loop gain is increased, the baseline dynamic inversion autopilot shows oscillations and experiences a decrease in stability. On the other hand, when these simulations are performed with L1 adaptive augmented autopilot, the missile was able to handle the oscillations and have better stability and tracking performance. In this study, adaptive control augmentation to baseline autopilots was analyzed on a realistic missile model, with high fidelity flight simulation software and found to provide promising results for increasing robustness to system uncertainties and increase the performance of a roughly designed baseline autopilot. It is known that the performance and robustness of most of the conventional autopilot design methods is very much dependent on the model data. And model uncertainties and disturbances are inevitable in real life problems. The analysis performed in this thesis was a demonstration of the applicability and effects of adaptive control augmentation to a realistic missile control problem.

The baseline autopilot architectures and adaptive control augmentation schemes analyzed in this thesis can be applied to other flying platforms, and their performance can be evaluated for these platforms. Within the scope of this thesis the autopilots are tested in front of aerodynamic data perturbation and high input gain cases. As a future study, the performance of these autopilots can be studied in control surface failure, or control actuation system saturation cases. Since the L1 adaptive control augmentation scheme applied in Chapter 5 accounts for matched and unmatched uncertainties in the system, control failure and saturation cases can be analyzed with this scheme.

In this thesis effective control surface deflections in roll, pitch and yaw axes are considered in the control design. However, a flight vehicle may have redundant control surfaces and control allocation may be required to be applied to the system. If the control allocation is not performed in an optimal manner, the critical support of adaptive control augmentation systems to the baseline autopilots may be lost during non-optimal allocations. Analysis of the performance of adaptive control augmentation schemes with optimal control allocation can also be a future work.

The filter design is an important feature of L1 adaptive control. With the filtering mechanization, L1 adaptive control defines the tradeoff between performance and robustness. In the applications of this thesis, simple first order transfer functions are used as low pass filters for L1 control design. However, optimization of the filter design is a recommended future research area. The effects of different filtering schemes on robustness and performance can be analyzed in depth to increase the overall performance of the controller.

The adaptive augmentation scheme studied in this thesis, for the control of missile in 6 DoF, is applied through augmenting the inner loop control signal only. For the two time-scale separation design of dynamic inversion based autopilot, there are two cascade loops on which the adaptive augmentation can be applied. There are examples of cascade adaptive control augmentation in the literature. L1 adaptive control system augmentation system formulation can also be extended for a cascade augmentation scheme and comparison of the performance of this new scheme with the existing one can also be a new research direction.

REFERENCES

[1] McFarland, M. B., D'Souza, C. N., "Missile Flight Control with Dynamic Inversion and Structured Singular Value Synthesis", *AIAA Guidance, Navigation and Control Conference,* AIAA-94-3604-CP, 1994.

[2] M. Tahk, M.M. Briggs, P.K.A. Menon, "Applications of plant inversion via state feedback to missile autopilot design", *Proceedings of the 27th Conference on Decision and Control,* December 1988.

[3] J.Ryu, C. Park, M. Tahk, "Plant inversion control of tail-controlled missiles,", *AIAA Guidance, Navigation and Control Conference,* AIAA-97-3766, 1997.

[4] Snell, S.A., Enns, D. F., Garrad Jr., W.L., "Nonlinear inversion flight control for a supermaneuverable aircraft", *Journal of Guidance,Control and Dynamics*, vol.15, no.4, July-August 1992, pp. 976-984.

[5] McFarland, M. B., Hoque, S. M., "Robustness of a Nonlinear Missile Autopilot Designed Using Dynamic Inversion", *AIAA Guidance, Navigation and Control Conference,* AIAA-2000-3970, 2000.

[6] Schumacher, C., Khargonekar, P. P., "Stability Analysis of a Missile Control System with a Dynamic Inversion Controller", Journal of Guidance, Control, and Dynamics, Vol. 21, No. 3, May-June 1998.

[7] Calise, A. J.,Sharma, M., Corban, J.E., "An adaptive autopilot design for guided munitions," *AIAA Guidance, Navigation and Control Conference,* AIAA-98-4490, 1998.

[8] Kaminer, I., Pascoal, A., Xarsay, E, Cao, C., Hovakimyan, N., Dobrokov, V.,"3D Path Following for small UAVs using Commercial Autopilots augmented by L1 Adaptive Control", AIAA Journal of Guidance, Control, and Dynamics, Vol.33,no 2, pp.550-568, 2010.

[9] Rysdyk, R. T., Calise, A. J., "Adaptive Model Inversion Flight Control for Tilt-Rotor Aircraft", Journal of Guidance, Control and Dynamics, Vol. 22, No. 3, 1999, pp 402-407.

[10] Calise, A. J., Lee, S., Sharma, M., "Development of a Reconfigurable Flight Control Law for the X-36 Tailless Aircraft", Journal of Guidance, Control and Dynamics, Vol. 24, No.5, 2001, pp 896-902.

[11] Leitner, J., Calise, A., Prasad, J. V. R., "Analysis of Adaptive Neural Networks for Helicopter Flight Control", Journal of Guidance, Control and Dynamics, Vol. 20, No. 5, 1997, pp 972-979.

[12] Sharma, M., Calise, A. J., "Neural Network augmentation of Existing Linear Controllers", Journal of Guidance, Control and Dynamics, Vol. 28, No. 1, 2005, pp 12-19.

[13] Sharma,M., Calise, A.J., Corban, J. E., "Application of an adaptive autopilot design to a family of guided munitions," *AIAA Guidance, Navigation and Control Conference*, AIAA-98-4490, 2000.

[14] Steinicke, A., Michalka, G., "Improving Transient Performance of Dynamic Inversion Missile Autopilot by Use of Backstepping", *AIAA Guidance, Navigation and Control Conference,* AIAA-2002-4658, 2002.

[15] McFarland, F. B., Calise, A. J., "Multilayer Neural Networks and Adaptive Nonlinear control of Agile Anti-Air Missiles", AIAA Paper 97-3540, Aug., !997.

[16] Meyer, G., Su, R., “Application of Nonlinear Transformations to Automatic Flight Control”, Automatica, No:1, 20, 1984.

[17] Slotine, J. J. E., Weiping, L., “Applied Nonlinear Control”, Prentice Hall, 1991.

[18] Wise,K.A., Lavretsky, E., Hovakimyan, N., “Adaptive Control of Flight: Theory, Applications, and Open Problems ”, Proceedings of the 2006 American Control Conference, Minneapolis, Minesota, USA, June 14-16,2006.

[19] Cao, C., Hovakimyan, N., “Design and Analysis of a Novel L1 Adaptive Controller, Part I: Control Signal and Asymptotic Stability”, Proceedings of the 2006 American Control Conference, Minneapolis, Minnesota, USA, June 2006.

[20] Cao, C., Hovakimyan, N., “Design and Analysis of a Novel L1 Adaptive Controller, Part II: Guaranteed Transient Performance”, Proceedings of the 2006 American Control Conference, Minneapolis, Minnesota, USA, June 2006.

[21] Cao, C., Hovakimyan, N., “Stability Margins of L1 Adaptive Controller : Part II”, Proceedings of the 2007 American Control Conference, ThC13.4, Newyork, USA, July 2007.

[22] Cao, C., Hovakimyan, N., “L1 Adaptive Output Feedback Controller For Systems with Time-varying Unknown Parameters and Bounded Disturbances”, Proceedings of the 2007 American Control Conference, WeA15.2, Newyork, USA, July 2007.

[23] Wang, J., Patel, V.P., Cao, C., Hovakimyan, N., Lavretsky, E., “L1 Adaptive Neural Network Controller for Autonomous Aerial Refuelling

with Guaranteed Transient Performance”, *AIAA Guidance, Navigation and Control Conference,* AIAA 2006-6206, 2006.

[24] Cao, C., Hovakimyan, N., “Guaranteed Transient Performance with L1 Adaptive Controller for Parametric Strict Feedback Systems”, Proceedings of the 2007 American Control Conference, FrA17.4, Newyork, USA, July 2007.

[25] Cao, C., Hovakimyan, N., “Novel L1 Neural Network Adaptive Control Architecture with Guaranteed Transient Performance”, IEEE Transactions on Neural Networks, Vol. 18, No 4, July 2007.

[26] Cao, C., Hovakimyan, N., “L1 Adaptive Controller for Multi-Input Multi-Output Systems in the Presence of Unmatched Disturbances”, Proceedings of the 2008 American Control Conference, FrA14.4, Washington, USA, June 2008.

[27] Cao, C., Hovakimyan, N., “L1 Adaptive Controller for a Class of Systems with Unknown Nonlinearities: Part I”, Proceedings of the 2008 American Control Conference, FrA14.2, Washington, USA, June 2008.

[28] Dobrokhodov, V., Kitsios, I., Jones, K.D., Xarsay, E., Hovakimyan, N., Cao, C., Lizarraga, M.I., Gregory, I.M., “Flight Validation of a Metrics Driven L1 Adaptive Control”

[29] Beard, R.W., Koebel, N, Cao, C., Hovakimyan, N., Matthews, J., “An L1 Adaptive Pitch Controller for Miniature Air Vehicles”, *AIAA Guidance, Navigation and Control Conference,* AIAA 2006-6777, 2007.

[30] Wang, J., Cao, C., Hovakimyan, N., Hindman, R.E., Ridgely, D.B., “L1 Adaptive Controller for a Missile Longitudinal Autopilot Design”, *AIAA Guidance, Navigation and Control Conference,* AIAA 2008-6282, 2008.

[31] Cao, C., Hovakimyan, N., "L1 Adaptive Output Feedback Controller Non Strictly Positive Real Reference Systems: Aerospace Examples", *AIAA Guidance, Navigation and Control Conference,* AIAA 2008-7288, 2008.

[32] Kharisov, E., Gregory, I., Cao, C., Hovakimyan, N., "L1 Adaptive Control Law for Flexible Space Launch Vehicle and Proposed Plan for Flight Test Validation", *AIAA Guidance, Navigation and Control Conference,* AIAA 2008-7128, 2008.

[33] Cotting, M.C., Cao, C., Hovakimyan, N., Kraus, R.J., Durham, W.C., "Simulator Testing of Longitudinal Flying Qualities with L1 Adaptive Control", *AIAA Atmospheric Flight Mechanics Conference and Exhibit,* AIAA 2008-6551, 2008.

[34] Wise, K.A., Lavretsky, E., Hovakimyan,N., Cao, C., Wang, J. "Verifiable Adaptive Flight Control: UCAV and Aerial Refueling", *AIAA Guidance, Navigation and Control Conference,* AIAA 2008-6658, 2008.

[35] Gregory, I.M., Cao, C., Xarsay,E., Hovakimyan, N., Zou, X., "L1 Adaptive Control Design for NASA AirSTAR Flight Test Vehicle", *AIAA Guidance, Navigation and Control Conference,*AIAA 2009-5738, 2009.

[36] Leman, T., Xarsay, E., Dullerud, G., Hovakimyan, N., Wendel, T., "L1 Adaptive Control Augmentation System for the X-48B Aircraft", *AIAA Guidance, Navigation and Control Conference,* AIAA 2009-5619, 2009.

[37] Cao, C., Hovakimyan, H., "Guaranteed Transient Performance with L1 Adaptive Controller for Systems with Unknown Time-varying Parameters and Bounded Disturbances: Part I", Proceedings of the 2007 American Control Conference, ThC13.3, Newyork, USA, July 2007.

[38] Shahruz, S.M., Behtash, S., "Design of controllers for linear parameter varying systems by gain scheduling technique", Journal of Mathematical Analysis, vol:168, No:1,1992.

[39] Lane, S. H., Stengel, R. F., "Flight Control Using Nonlinear Inverse Dynamics", Automatica, No:24, 1988, pp 471-483.

[40] Bugajski, D., Enns, D., Hendrick, R., "Nonlinear Control Law Design for High Angle of Attack", NASA High Angle of Attack Projects and Techonolgy Conference, 1992.

[41] Wise, K. A., Deylami, F., "Approximating a Linear Quadratic Missile Autopilot Design Using an Output Feedback Projective Control", *AIAA Guidance, Navigation and Control Conference*, AIAA-91-2613-CP.

[42] Khalil, H.K., "Nonlinear Systems", Prentice Hall, NJ, 2002.

[43] Hovakimyan, N., Cao, C., "L1 Adaptive Control Theory", SIAM Advances in Design and control Series, 2010.

[44] Samad,T., "Perspectives in Control Engineering", IEEE Press, 2001.

[45] Sastry, S., Bodson, M., "Adaptive Control (Stability, Convergence and Robustness)", Prentice Hall advanced reference Series, 1998.

[46] Pomet, J. B., Praly, L., "Adaptive Nonlinear Regulation: Estimation from the Lyapunov Theory", IEEE Transactions on Automatic Control, Vol 37, No 6, 1992.

[47] Wise, K.A., Lavretsky, E., Zimmerman, J., Francis Jr, J.H., Dixon, D., Whitehead, B.T., "Adaptive Flight Control of a Sensor Guided Munition", *AIAA Guidance, Navigation and Control Conference*, AIAA-2005-6385.

[48] Harkegard, O., “Modifying L1 Adaptive Control for Augmented Angle of Attack Control”, *AIAA Guidance, Navigation and Control Conference*, AIAA-2009-6071.

[49] Haykin, S., “Neural Networks: a Comprehensive Foundation”, 2nd Edition, Prentice Hall, 1999.

[50] Zhou, K., Doyle, J.C., “Essentials of Robust Control”, Prentice Hall, NJ, 1998.

APPENDIX A

DEFINITIONS OF DIMENSIONAL AERODYNAMIC DERIVATIVES

$$Z_\alpha = \frac{Q_d A_{ref}}{mV} C_{Z_\alpha}$$

$$Z_{\delta_e} = \frac{Q_d A_{ref}}{mV} C_{Z_{\delta_e}}$$

$$M_\alpha = \frac{Q_d A_{ref} d_{ref}}{I_{yy}} C_{m_\alpha}$$

$$M_{\delta_e} = \frac{Q_d A_{ref} d_{ref}}{I_{yy}} C_{m_{\delta_e}}$$

$$M_q = \frac{Q_d A_{ref} d_{ref}}{I_{yy}} C_{m_q}$$

$$Y_\beta = \frac{Q_d A_{ref}}{mV} C_{Y_\beta}$$

$$Y_{\delta_r} = \frac{Q_d A_{ref}}{mV} C_{Y_{\delta_r}}$$

$$N_\beta = \frac{Q_d A_{ref} d_{ref}}{I_{yy}} C_{n_\beta}$$

$$N_{\delta_r} = \frac{Q_d A_{ref} d_{ref}}{I_{zz}} C_{n_{\delta_r}}$$

$$N_r = \frac{Q_d A_{ref} d_{ref}}{I_{zz}} C_{n_r}$$

$$L_p = \frac{Q_d A_{ref} d_{ref}}{I_{xx}} C_{l_p}$$

$$L_{\delta_a} = \frac{Q_d A_{ref} d_{ref}}{I_{xx}} C_{l_{\delta_a}}$$

where Q_d is the dynamic pressure defined as follows:

$Q_d = \frac{1}{2}\rho V^2$, here ρ is the air density, V is the free stream velocity.

A_{ref} is the reference area, d_{ref} is the reference length used in the non-dimensionalization of the aerodynamic forces and moments.

I_{xx}, I_{yy}, I_{zz} are the inertias of the missle about the center of gravity.

APPENDIX B

PROJECTION OPERATOR

Projection operator is a mathematical operator used to keep the adaptive parameters bounded. Projection operator is formulated as follows:

$$Proj(\theta, y) = \begin{cases} y - \dfrac{\nabla f(\theta)\left(\nabla f(\theta)\right)^{\mathrm{T}}}{\|\nabla f(\theta)\|^2} y f(\theta), & \text{if } f(\theta) > 0 \text{ and } y^T \nabla f(\theta) > 0 \\ y, & \text{if not} \end{cases} \tag{156}$$

where the function $f(\theta)$ defines prespecified parameter domain boundary. The parameter domain boundary used in this thesis is expressed as:

$$f(\theta) = \frac{\|\theta\|^2 - \theta_{max}^2}{\varepsilon_0 \theta_{max}^2} \tag{157}$$

θ are the parameters which has the property $\|\theta\| \leq \theta_{max}$, θ_{max} specifies boundary and ε_0 specifies the boundary tolerance.

If $f(\theta) \leq 0 \;\Rightarrow\; \|\theta\| \leq \theta_{max}$, then θ is within bounds.

If $0 < f(\theta) \leq 1 \;\Rightarrow\; \|\theta\| \leq \sqrt{1+\varepsilon_0}\,\theta_{max}$, then θ is within $\left(\sqrt{1+\varepsilon_0}\right)$ percent of bounds.

If $f(\theta) > 1 \;\Rightarrow\; \|\theta\| > \sqrt{1+\varepsilon_0}\,\theta_{max}$, then θ is outside of bounds.

The gradient of $f(\theta)$ is as follows:

$$\nabla f(\theta) = \frac{2\theta}{\varepsilon_0 \theta_{max}^2} \tag{158}$$

In (63)-(65) and (97)-(99), by using the projection operator, the derivative of adaptive parameters is calculated such that the adaptive parameters stay within a pre-specified boundary value.

CURRICULUM VITAE

PERSONAL INFORMATION:

Surname:	TİRYAKİ KUTLUAY
Name:	Kadriye
Date of birth:	28 08.1978
Place of birth:	KIRŞEHİR - TURKEY
Nationality:	Turkish
Permanent address:	Meksika Cad. Defne 3 Sitesi 53/27 Ümitköy Ankara, TURKEY Tel: +90 (312) 236 23 35 Mobile Tel: +90 (532) 684 52 50
Work address:	TÜBİTAK-SAGE Turkish Scientific & Technical Research Council Defense Industries Research & Development Institute P.K. 16, 06261 Mamak – ANKARA / TURKEY Tel: +90 (312) 590 94 32 Fax: +90 (312) 590 91 48-49 E-mail: ktiryaki@sage.tubitak.gov.tr kadriye.tiryaki@gmail.com
Marital status:	Married
Profession:	Aerospace Engineer

EDUCATION:

School	***Years***	***Diploma, Grade and Subject***
Primary School		
Yükseliş College Ankara, TÜRKİYE	1984 – 1989	Primary School Diploma
Secondary & High School		
Yükseliş College Ankara, TÜRKİYE	1989 - 1994	Secondary and High School Diploma
University		
METU Department of Aerospace Eng. Ankara, TÜRKİYE	1994 – 1999	B.Sc.
METU Department of Aerospace Eng. Ankara, TÜRKİYE	2000 - 2002	M.Sc. , “Polynomial Guidance Laws and Dynamic Flight Simulation Studies”
METU Department of Aerospace Eng. Ankara, TÜRKİYE	2004 – 2011	Ph.D. , “Adaptive Control of Guided Missiles”

LANGUAGE SKILLS:

Native Language : Turkish

Other Languages : English

WORK EXPERIENCE:

Organization	Years	Job
TÜBİTAK-SAGE Ankara, TÜRKİYE	2000-2002 2002-2006 2006-	Research Engineer Senior Research Engineer Head Research Engineer